NTNU – Trondheim
Norwegian University of
Science and Technology

A comparison of friction piles bearing capacity based on theoretical and empirical mathematical models

Ermias Hailu Mijena

Report Title: A comparison of friction piles bearing capacity based on theoretical and empirical mathematical models.	Date: July 09, 2012
	Number of pages (including appendices): 116
	Masteroppgave X Projektoppgave
Name: Ermias Hailu Mijena	
Professors in charge/Supervisor: Lars Grande	
Other external professional /Supervisors: Dr. Tewodros Tefera, Frode Oset and Grete Trevdt	

Abstract

One can find in literature lots of different models to predict axial capacity of piles .This study has been carried out to compare some selected empirical (semi-empirical) and theoretical models used in Norway or internationally. The comparisons were made among the various models with respect to the static load test result, which is widely believed to be providing a reliable pile capacity. The study has been undergone based on the data obtained in the bridge project over the Drammen Selva river in the city of Drammen in Norway. In this study, I have included four calculation models, namely the Janbu theoretical models (derived based on plasticity theories and earth pressure approach), the Norwegian Pile Guideline (peleveiledningen (2005)), API RP 2A LRFD (2007), NGI-99 methods. The Norwegian Pile Guideline (2005) is sort of mixed empirical and theoretical approach. The last two are purely empirical.

Recent literature on set up effect were also included in this study and the increase in capacity with time was also accessed in both using a prediction model and static load test result which was performed in various time intervals.

Additionally, a back calculation of parameters was also performed in the study based on the static load test results, for a possible use in design of neighboring piles showing similar soil type and soil parameters. We should be aware that the findings of this study is considered to be of limited nature and should not be generalized.

Key words: pile, bearing capacity, pile load test, analyses

_____

(Signature)

ACKNOWLEDGMENTS

Contents

LIST OF SYMBOLS

γ	unit weight
w	weight of soil
w_w	weight of water
w_s	weight of solid
v_v	volume of void
v_s	volume of solid
D_r	relative density
e_{max}	maximum void ratio
e_n	natural void ratio
e_{min}	minimum void ratio
I_P	plasticity index
w_L	liquid limit
w_P	plastic limit
OCR	overconsolidation ratio
$p_c{'}$	preconsolidation pressure
$p_0{'}$	current overburden pressure
c	cohesion
$\varphi(\Phi)$	friction angle
s_u	undrained shear strength
$\sigma_v{'}$	vertical effective stress
s_t	sensativity
SPT	standard penetration test
CPT	cone penetration test
M	oedometer modulus
G	shear modulus

q_t	corrected cone resistance
q_c	measured cone resistance
q_{net}	net tip resistance
f_t	corrected sleeve friction
f_s	measured sleeve friction
u	pore pressure
N_{KT}	bearing capacity factor
Q_P	pile tip capacity
Q_S	pile skin capacity
Q_u	ultimate pile capacity
Q_a	allowable pile capacity
q_p	unit tip capacity
$f_s(\tau_s)$	unit skin friction capacity
N	SPT blow count
α	adhesion coefficient
p_0'	effective vertical overburden
L	length of pile
$d(B)$	diameter of pile
q'	effective vertical overburden
K	coefficient of lateral earth pressure
δ	friction angle between soil and pile wall
N_q	bearing capacity factor
N_c	bearing capacity factor
τ	shear stress
t	time
r	roughness coefficient
a	attraction

$\beta(\Psi)$	plastification angle
T	dimensionless time factor
c_h	horizontal coefficient of consolidation
U	degree of consolidation
IFR	incremental filling ratio
PLR	plug length ratio
η	hammer efficiency
w_r	ram weight
w_p	pile weight
P_u	ultimate pile capacity
E_h	hammer energy
R_s	static soil resistance
J	a damping constant
V	instantaneous velocity
f_u	tensile stregth
f_c	compressive stregth
f_y	yield stress
r_0	outer pile radius
r_p	radius of the plastic zone
r_i	inner pile radius
G_{50}	shear modulus at 50% of maximum stress
c_u	undrained shear strength

LIST OF FIGURES

LIST OF TABLES

1 INTRODUCTION

1.1 Background

Piles are structural members that transmit the super structure loads to deep soil layers. They are preferred to be used as a foundation material when shallow foundation is not practical to use it. Piles and pile foundations have been in use since prehistoric times [15].The Roman wooden piles are classic example for this. Today piles can be made of wood, concrete or steel.

Pile capacity determination is a difficult thing. A number of different designs practices here in Norway and internationally exist, but seldom have they given the same computed capacity. Especially, determining the skin friction component is not an easy thing since the soil is not intact after the pile is driven and loses its intact engineering property (strength). So far, precise determination of this value has not been possible. Thus today design offices only believe a load test can only give reliable capacity of the pile at the time of test. After installation the design values, i.e. the load carrying capacities of piles are usually verified using different methods such as pile loading test and dynamic analysis.

Scientific approaches to pile design have advanced enormously in recent decades and yet, still the most fundamental aspect of pile design - that of estimating capacity –relies heavily upon empirical correlations [17].

The study focuses on some of selected empirical (semi-empirical) and theoretical mathematical models used here in Norway and internationally. In order to compare the various models, a case study was chosen, which a bridge project with construction was began back in 2002 and completed in 2006 and the bridge is located in the city of Drammen over the Dramen Selva river in Norway. During the investigation of the bridge project, both static and dynamic load tests were performed in order to determine the pile capacity. The load tests were performed on single piles at two chosen axis namely, axis 16 and 25 and both closed-ended steel pipe pile and HP pile were load tested.

The study focuses only on the capacity of single pile under compressive loading condition for the single piles at axis 16 and axis 25. Of course in reality seldom single piles are used, however, the capacity of group piles entirely depends on the capacity of single pile within a group. It should be noted that the pile group capacity is not the intension of this study.

1.2 Scope and objective of the work

The scope of the project work includes

1) Literature survey
The focus is to do intensive literature survey about empirical and theoretical based practices.

2) Analysis and evaluation

The focus is to compare the empirical and theoretical based mathematical models with pile load test and dynamic analysis on the selected case study.

1.3 Outline of the work

This thesis consists of 8 chapters and each chapter is described as follows:

Chapter 2: Presents the different types of piles which exist today and their classification.
Chapter 3: Presents the different soil parameters we use in pile analyses and design and the properties of these parameters.
Chapter 4: Presents the different empirical and theoretical static pile capacity equation. It also presents the effect of time and plugging on pile capacity.
Chapter 5: Presents pile dynamics, static and dynamic load tests on piles.
Chapter 6: Presents a case study which is a case of a bridge project on the Drammen selva river in Drammen, Norway.
Chapter 7: Presents the analysis and results obtained for the case study described in chapter 6.
Chapter 8: It is the last part of the work which presents conclusions and possible future work.

1.4 Methodology

1) Literature review of various methods of predicting pile capacity
2) Single Pile capacity was computed using the various chosen methods
3) Static load test result was chosen as a reference in comparison
4) Comparisons were made between the various empirical and theoretical methods
5) Back calculation of soil data was performed in order to use for neighboring piles showing the same soil type and engineering soil properties.
6) Conclusions

1.5 Delimitation

In real, piles are subjected to different loading conditions, such as axial loads either tension or compression, horizontal loads and bending moments, however, in this study only compressive axial load was considered. Measurement errors are one of the possible forms of error, so there could be a measurement error in engineering soil properties which led to reducing accuracy of the result. Correlations were also considered in the interpretation of CPTU which are also resulting in some sort of error.

2 PILE TYPES

Piles are classified according to three different ways, namely nature of load support, displacement nature and material composition.

2.1 Nature of load support

2.1.1 Friction piles

If the piles do not reach a hard stratum, their load carrying capacity is derived partly from end bearing and partly from the skin friction; these piles are called friction piles.
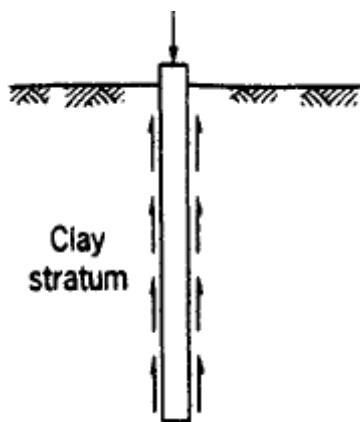
Figure 2.1 Friction pile [2]

2.1.2 End bearing piles

If the piles derive most of their load from end bearing in other words if the piles rest on hard rock or very dense sand or gravelly material, then these piles are called end bearing piles.
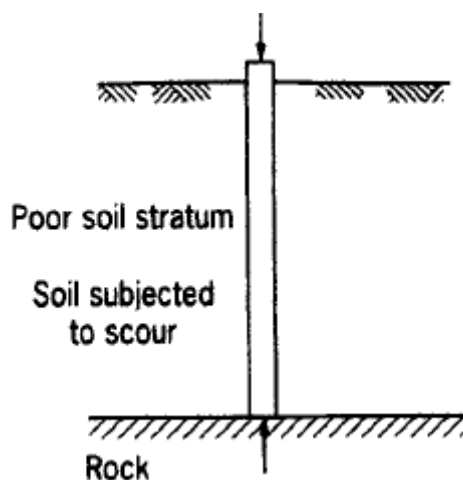
Figure 2.2 End bearing pile [2]

2.2 Displacement nature

2.2.1 Displacement piles

Displacement piles are those piles, which displace the soil radially and vertically during driving. Example: Closed pipe piles.

2.2.2 Partial-displacement piles

Partial-displacement piles are those piles showing behavior intermediate between full-displacement and non-displacement piles. They displace smaller volume of soil. Example: Open end pipe pile, H-piles.

2.2.3 Non-displacement piles

Non-displacement piles are those piles which are casted after boring. They are also called replacement piles. Example: bored piles (Example: Franki piles)

2.3 Material composition

2.3.1 Timber Piles

Timber piles are the oldest form of piles used for foundation purposes. They are normally cheaper compared to steel or concrete piles, but their main problem is they decay in the absence of oxygen and moisture. Timber piles installed in both oxygen and moisture reach sites are well protected from decay. Alternatively, oil born preservatives can also effectively prevent a problem associated with decay. Unlike steel or concrete piles splicing of timber piles is ineffective; however, one can still see timber piles used spliced. Normally the tip has smaller diameter than the butt end to promote easy penetration, but metal driving shoe is used if the pile is driven in hard or gravely soils to avoid breakage of the tip.

Figure 2.3 Timber piles used as foundation material in the city of Trondheim (after Ermias)

2.3.2 Concrete piles

Precast concrete piles: also known as "prefabricated piles" are produced in a casting yard in a location away from the building site or close to the building site if sufficient space is available and great demand of more piles and transported to the construction site. According to Bowles (1996) precast piles using ordinary reinforcement are designed to resist bending stresses during pick up and transport to the site and bending moments from lateral loads and to provide sufficient resistance to vertical loads and any tension forces developed during driving.

Figure 2.4 Concrete piles used as foundation material (after Ermias)

Prestressed piles

In these piles, the longitudinal reinforcement used in reinforced concrete piles are replaced by tensioned steel rods. This longitudinal reinforcement is designed to resist stresses in lifting and handling. Prestressed piles can be either pretensioned or posttensioned.

Cast –in- place piles

Normally formed by drilling a hole in the ground and inserting an open ended casing and the soil in the casing is removed and filled with concrete finally the casing will be removed. Normally of three types: cased, uncased and pedestal types.

2.3.3 Steel Piles

Steel piles are convenient to use in dense soils as they are convenient to drive. They are susceptible for corrosion in order to overcome this copper is added into steel. They are convenient for splicing.

Steel piles are available as available as HP-piles and pipe piles. Pipe piles are further classified as closed ended and open-ended. HP-piles are normally used as end bearing piles since they generate less frictional resistance because of their limited perimeter area. When H-piles or open end pipe piles are used the capacity should be checked both plugged and unplugged condition and the minimum of the two will be taken. Open ended piles and H-piles are considered as small-volume displacement piles since they have small cross sectional area. Pipe piles can also be used filled with concrete.

3 SOIL PARAMETERS FOR PILE ANALYSIS AND DESIGN

Soil investigations generally proceed through following four phases [15]:

1) Preliminary Soil Investigations
2) Detailed Soil Investigations
3) Construction Verification
4) Post Construction Monitoring

3.1 Scope, objectives and extent of the soil investigation

The objectives of foundations soil investigation are to determine the extent, thickness, and properties of the soils and rocks and the ground water levels at a site [15]. It is carried out in a way soil stratigraphy is described in detail with sufficient test pits.

The extent of the investigation depends on the following factors:

➢ Character of the soil
➢ Available information from previous experience
➢ The degree of variation of the soils around the site
➢ The importance of the structure

3.2 Various soil investigation and testing methods

One way of performing soil investigation is by soil boring this can be accomplished by retrieving sample for laboratory testing which in turn result in possible conclusion of the stratigraphy and soil parameters.

3.2.1 Boring techniques

Here some of the different boring techniques used in different part of the world

- Auger boring
- Wash boring
- Rotary drilling
- Percussion drilling

3.2.2 Soil sampling and laboratory testing

In Scandinavia, the piston sampler with diameter 54mm is widely used to retrieve a sample for a possible laboratory testing program. Depending on the type of test we accomplish we retrieve either a disturbed or undisturbed sample.

Laboratory testing is carried out to classify the soils and to provide soil parameter for design.

The following are some of the properties of soils determined in the laboratory.

Unit weight (γ)

Basically calculated as dividing the total weight of soil by volume of soil.

$$\gamma = \frac{w}{v} = \frac{w_w + w_s}{v_v + v_s}$$

(3-1)

Relative density (D_r)

It is an important parameter defining cohesionless soils. Basically defined as:

$$Dr = \frac{e_{max} - e_n}{e_{max} - e_{min}} \text{ Or,}$$

(3-2)

$$D_r = (\frac{\gamma_n - \gamma_{min}}{\gamma_{max} - \gamma_{min}})(\frac{\gamma_{max}}{\gamma_n})$$

(3-3)

Water content (w)

The natural water content (w_n) is determined from disturbed soil sample. The sample is weighed first and then oven dried and weighed again from this procedure the water content can be determined.

Atterberg limits

The liquid limit and plastic limit is routinely determined for cohesive soils and using these values, plasticity index is determined.

$$I_p = w_L - w_p$$

(3-4)

Overconsolidation

A soil is called normally consolidated if the current stress level is the largest in the history of the soil. While the soil is over consolidated if the soil is exposed to a stress larger than the present stress in its history.

$$OCR = \frac{p'_c}{p'_o}$$

(3-5)

p'_c = preconsolidation pressure

p'_o = current overburden pressure

A normally consolidated soil has OCR =1 and overconsolidated soil has OCR >1.

3.2.3 Field testing

The following field testing methods are commonly used in various parts of the world

Standard penetration test (SPT)

The main goal of this test is to determine SPT N value, and the SPT N value is empirically related to many engineering properties of soils. In literatures, one can find different engineering properties of soils correlated with SPT N value.

The test is performed by attaching a split spoon sampler to the bottom of the core barrel and lowered into the desired position at the bottom of the borehole, and then the sampler is driven into the ground by a drop hammer weighing 68Kg falling from a height of 76cm. The number of blow required to drive the sampler three successive 150mm increments is registered. The first increment (0-150mm) is not included in the N value as it is believed to be disturbed by the drilling. The N value is the number of blows required to assist the last two increments (150mm-450mm). Finally, the N value should be corrected to the standard energy.

Cone penetration test (CPT)

The CPT is one of the in-situ tests commonly used in Norway. It was first discovered in the Netherlands. It is available as Dutch cone, electric cone, electric piezo, electric piezo/friction and seismic cone. Continuous measurement is taken for both the soil resistance and the sleeve friction by putting the cone at the end of serious rods. Penetration rate is 2cm/sec. Nearly 95% of offshore investigation is carried out using the CPT.

The following parameters can be determined from the CPTU:

- Undrained shear strength, s_u
- The soil unit weight
- Pre-consolidation pressure, p_c
- Friction angle, ϕ
- Deformation modulus, M, G
- Coefficient of consolidation, c_c

Corrected cone resistance and sleeve friction can be obtained by correcting the tip resistance and sleeve friction for pore pressure acting on the geometry.

$$q_t = q_c + (1-a)u_2 \qquad\qquad (3\text{-}6)$$

Where

q_t = corrected cone resistance

q_c = measured cone resistance

a = net area ratio

u_2 = pore pressure at u_2 position.

And,

$$f_t = f_s - (\pi d_2 t_2 u_2 + \pi d_3 t_3 u_3)/(\pi d_c h_s) \qquad (3\text{-}7)$$
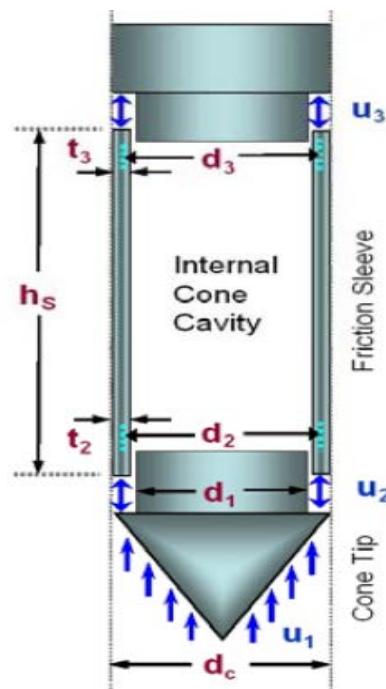
Figure 3.1 Cone penetration test

The Undrained shear strength is determined from the CPT as:

$$s_u = (q_t - \sigma_{vo})/N_{Kt} \qquad (3\text{-}8)$$

Where

σ_{vo} = in-situ vertical overburden pressure

N_{Kt} = Bearing capacity factor

Using theory of expanding cavities;

$$s_u = \Delta u_2 / N_{\Delta u} \qquad (3\text{-}9)$$

Where

Δu_2 = excess pore pressure at the u_2 position

$N_{\Delta u}$ = bearing capacity factor

 Vane shear test

The vane shear test is commonly used field test for the interpretation of undrained shear strength and sensitivity of cohesive soils. The blade has a height-to-diameter ratio of 2. The test is performed by inserting the vane into the soil and applying the torque for about 5 to 10 minutes and the required torque to cause shearing is measured and the undrained strength is calculated using equation

$$S_{uv} = \frac{6T}{7\pi D^3}$$ (3-10)

Where

T is the measured torque

D is the diameter of the vane

It is common to continue the vane rotation for 10 to 12 revolutions after rupture for the soil to be substantially remoulded, a rest period of 1 to 2 min is taken, and then a second torque reading is made to obtain the remolded strength.

The ratio of undisturbed strength to the remolded strength gives the sensitivity of the soil. Sensative clays have very low remolded strength. For example: quick clay

Bjerrum (1973) suggested correction factor for effect of anisotropy of the soil and rate of loading in undrained shear strength [2].
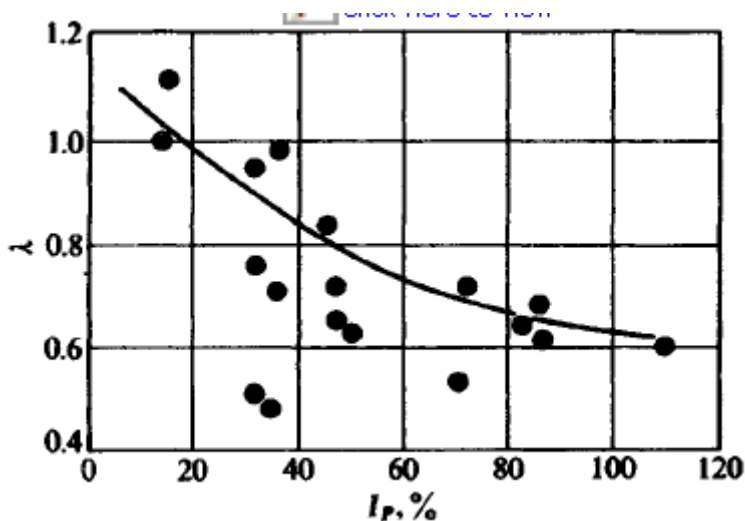
Figure 3.2 Bjerrum's correction factor for vane shear test
 [After Bjerrum's (1972) and Ladd et al. (1977) [2]]

Aas (1986) suggested a correction factor μ which includes effects of aging and OCR which relates s_{uv} to s_{uLAB}.

Where

$$s_{uLAB} = \frac{(s_{uA} + s_{uD} + s_{up})}{3}$$

(3-11)
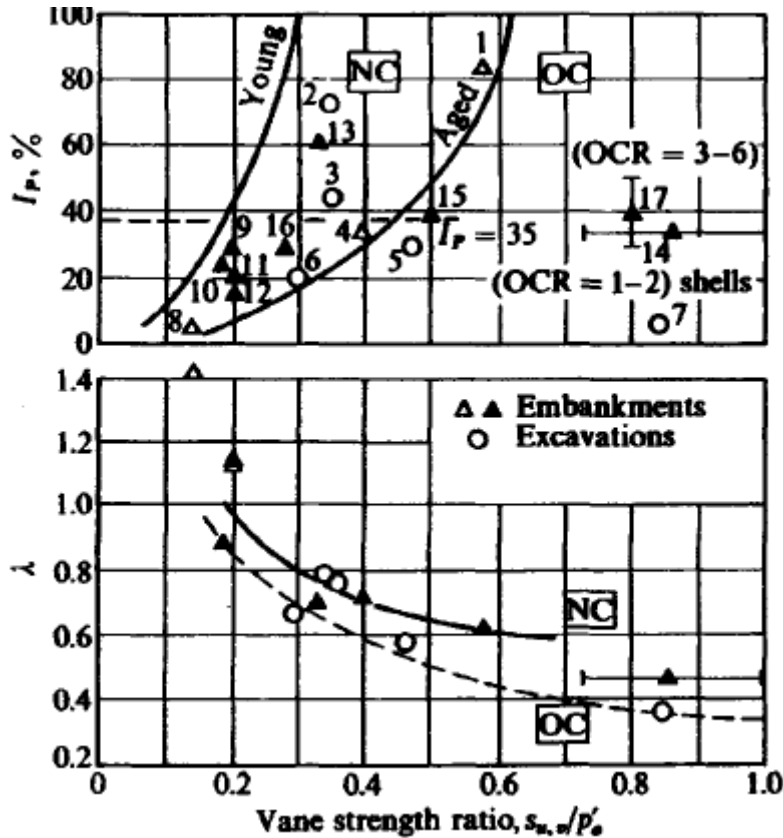
Figure 3.3 Reinterpretation of Bjerrum chart by Aas et al. [2]

❖ In addition to these, the measured results can be affected by rate effects, in-situ stress level, and damage to vane and rod system.

3.2.4 Groundwater level measurement

It is a critical factor in foundation design and sufficient attention should be given during all stages of soil investigation [15]. It gives information on the existence of normal, perched, hydrostatic, or artesian levels and variation of these levels over the site and with time [15].

Ground water level is measured first at a depth where it encountered and at a depth it stabilizes itself.

Ground water is measured by installing either of the following piezometers.

➤ Open stand pipe piezometer
➤ Porous element piezometer
➤ Electric piezometer

3.3 Design parameters

3.3.1 Strength parameters

The strength parameters needed are cohesion (c) and angle of internal friction (ϕ). They are determined from laboratory tests on undisturbed sample using the triaxial apparatus. Basically there are three types of triaxial test:

1) Unconsolidated undrained (UU) tests.
2) Consolidated undrained (CU) tests.
3) Consolidated drained (CD) tests.

We can also determine the c and ϕ using direct shear or direct simple shear apparatus.

Undrained shear strength (s_u)

Can be determined from unconfined compressive tests, triaxial test, fall cone test, vane shear test or CPT.

For normally consolidated soils, s_u can be estimated as according to Skempton and Henkel (1953) [2].

$$s_u = \sigma'_v (0.1 + 0.004 PI) \tag{3-12}$$

According to Bjerrum and Simons (1960)

$$\frac{s_u}{p_0'} = 0.45 (I_P)^{0.5} \qquad I_P > 0.5 \tag{3-13}$$

$$\frac{s_u}{p_0'} = 0.18 (I_L)^{0.5} \qquad I_L > 0.5 \tag{3-14}$$

Sensativity

Sensativity is the ratio of undisturbed strength to the remolded strength.

$$s_t = \frac{\text{Undisturbed strength}}{\text{Remolded stregh}}$$

Thixotropy

Thixotropy is the regain of strength from remolded state with time. Driven piles in soft clay deposite often have very little load carrying capacity until a combination of aging/cementation (thixotropy) and dissipation of excess pore pressure (consolidation) occurs [2].

3.3.2 Soil pile adhesion

It is quite difficult to determine. A back calculation of static load test on a prototype foundation can only give a reliable result. It is affected by factors such as consistency of the soil, method of installation of the pile, material which the pile is made from, and the time after installation.

3.3.3 Elastic soil parameters

The most common elastic soil parameter in the design of pile is the modulus of elasticity, E_s [14].

4 STATIC PILE CAPACITY

Generally, we determine the capacity of a pile in two alternative ways i.e.

1) Testing e.g. static load test and dynamic load test
2) Calculation e.g. static design equations based on laboratory and field investigations and pile driving formula

Sufficient emphasis should be given to the accuracy in the estimation of pile capacity, this will lead us to not only to safer structure but also to economic savings. It should be noted that the term capacity in this thesis refers to capacity of the bearing soil and it is not the structural strength of the pile itself.

The ultimate axial load carrying capacity of piles should be determined by the equation:

$$Q_{u=}Q_p + Q_s = q_p A_p + f_s A_s$$

(4-1)

And design load capacity, in other words allowable bearing capacity is given as

$$Q_a = \frac{Q_u}{FS}$$

(4-2)

Where

$$eeA \quad \pi \quad A \quad \pi$$
$$= \quad r^2 \quad = \quad r^2$$

Q_u = Ultimate pile capacity

Q_a = Allowable pile capacity

q_p = Unit pile tip resistance

f_s = Unit skin friction capacity

A_p = The pile tip area

A_s = The pile side area

FS = Factor of safety

The following Parameters affect the capacity of piles

1) **Pile characteristics**

   - Geometry (diameter, wall thickness, penetration ratio)

- Tip detail (weather it is open-ended or closed-ended; driving shoe)
- Material, roughness

2) Loading condition

- Weather subjected to tension or compression load
- Weather subjected to static or cyclic load
- Weather vertical load alone or in combination with horizontal load or moments
- Time between driving and loading

3) Installation

- Rate of penetration
- Continuity of penetration
- Installation methods, i.e. driving, jacking or vibration
- Mode of penetration, i.e. weather it is plugged or not

4) Soil characteristics

- Soil stratigraphy
- In situ stress state
- Stress history in other words over consolidation ratio (OCR)
- Undrained shear strength
- Plasticity Index (IP)
- Sensitivity
- Relative density
- Cone resistance value, q_c
- Pile soil interface friction angle,

4.1 Empirical Methods

4.1.1 Method based on Cone penetration test (CPT)

Since invented, the cone penetration test has been used to estimate pile capacity. Over the years, a number of other empirical methods have been developed to estimate the capacities of pile, for instance the schmertmann method (schmertmann 1978), the Dutch method (de Ruiter and Beringen 1979) and some more others too.

The unit tip bearing capacity of the pile (q_p) is evaluated from the tip resistance (q_c) profile and the unit skin friction of the pile (f_s) is evaluated from either the sleeve friction (f_s) profile or the cone tip resistance (q_c) profile.

Almeida et al. (1996)

The unit shaft friction is computed from [13]:

$$q_s = q_{net}/k_1$$

(4-3)

Where $q_{net} = q_t - \sigma'_{vo}$

$$k_1 = 10.5 + 13.3 \log(q_{net}/\sigma'_{vo})$$

The unit point resistance is computed from:

$$q_p = q_{net}/k_2$$

(4-4)

Where $k_2 = N_{Kt}/9$

$N_{Kt} = $ Empirical cone factor

$$= q_{net}/s_u$$

4.1.2 Method based on Standard penetration test (SPT)

From the standard penetration test (SPT) data, Meyerhof (1956, 1976) proposed for the pile tip resistance as [2]:

$$P_{pu} = A_p (40N) \frac{L_b}{B} \leq A_p (380N)$$

(4-5)

Where N= statistical average of the SPT N_{55} numbers in a zone of about $8B$ above to $3B$ below the pile point

B = width or diameter of pile point
L_b = pile penetration depth into point bearing stratum

Meyerhof (1976, 1983) also proposed an empirical relation for driven piles for the unit skin friction and expressed using the following relation

$$Q_{su} = 2N_{cor}A_s$$

(4-6)

Where

$$Q_{su} = \text{Ultimate skin friction in } KPa$$
$$N_{cor} = \text{corrected SPT N value}$$
$$A_s = \text{Skin friction contact area}$$

4.1.3 Axial pile capacity in clay using various pile design practices

Pile skin capacity

Basically, there are three commonly used methods of calculating the skin resistance for cohesive soils. These are called the alpha, lambda, and beta methods. The beta method is also used for cohesionless soils.

The α method

It is called as a total stress approach used in the estimation of the skin friction along the shaft of piles embedded in clay.

Tomlinson (1957) initially proposed effective stress based general equation for the skin friction

$$fs = \alpha c + p_0 ' K \tan \delta \qquad (4\text{-}7)$$

Later this equation is used simply as

$$fs = \alpha s_u \qquad (4\text{-}8)$$

Where α = adhesion factor from Figure 4.1
s_u = Undrained shear strength for the point of interest
p'_0 = average effective vertical stress
K = lateral earth pressure coefficient
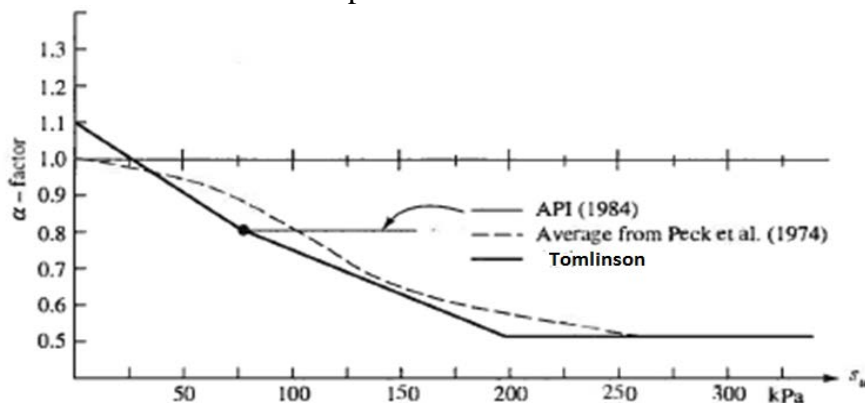
Figure 4.1 Relationship between the adhesion factor and undrained shear strength [2]

The λ method

Vijayvergiya and Focht (1972) proposed an effective stress based method based on back calculated 47 load test results performed on pipe piles with varying diameters to incorporate the skin friction resistance with both undrained strength (s_u) and vertical effective stress (p'_0). The method starts with the assumption that the displaced soil particle during pile installation causes a passive horizontal pressure at any depth along the pile.

$$f_s = \lambda(p'_0 + 2s_u)$$

(4-9)

Where s_u = undrained shear strength

   p'_0 = average effective vertical stress

   λ = coefficient obtained from Fig.3.1, is pile length-dependent
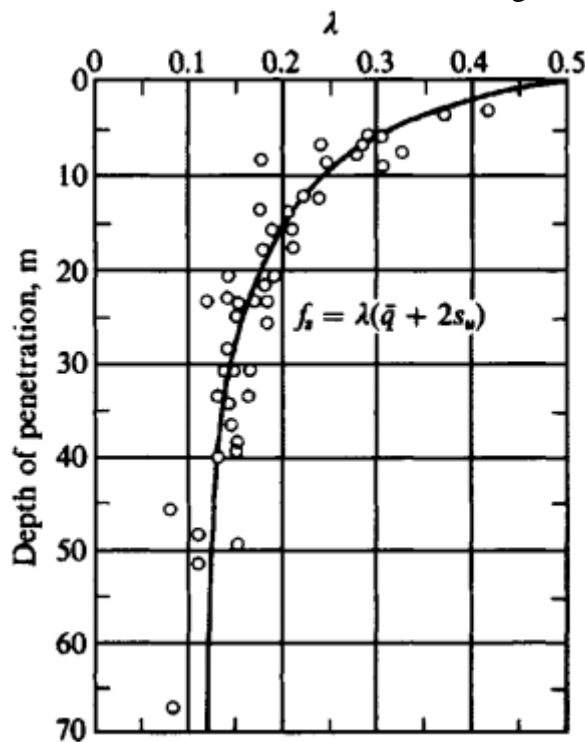
Figure 4.2 The dependent of λ coefficient on pile penetration. Data plotted and depth converted to meters by author from Vijayvergiya and Focht (1972) [2]

The λ coefficient above was obtained from back calculation of a large number of data and best-fit analysis of the plot. It is clear that the λ term in the equation above includes both the effects of α and $K \tan \delta$ [2].

The β method

Surprisingly, Burland (1973) developed an effective stress based method from load tests on bored piles, but has gained wide spread acceptance in designing driven piles. The equation looks like of the form:

$$f_s = K p'_0 \tan \delta \qquad (4\text{-}10)$$

Taking $\beta = K \tan \delta$, the equation for the skin resistance can be rewritten as

$$f_s = \beta \bar{q} \qquad (4\text{-}11)$$

p'_0 = average effective vertical stress

This method is recommended only for cohesionless soils.

Meyerhof (1976) extended Burland's approach for overconsolidated clay.

$$\beta_{OC} = (1 \pm 0.5)\beta_{NC}\sqrt{OCR}$$

a) **Norwegian Pile Guideline (Peleveiledningen) (1991): section 1**

According to the guideline, the unit skin friction for cohesive soils along the pile shaft relates with the undrained shear strength through the following expression.

$$f_s = \alpha s_u \qquad (4\text{-}12)$$

Where $\quad\quad\quad\quad \alpha =$ an empirical factor

$\quad\quad\quad\quad\quad\quad$ Fun $(\dfrac{L}{d}, \dfrac{s_u}{p_0'})$; see Fig.4.3

$\quad\quad\quad L =$ pile length
$\quad\quad\quad d =$ width or diameter of pile
$\quad\quad\quad s_u =$ average undrained shear strength along the pile

$\quad\quad\quad p_o' =$ average effective vertical stress along the pile
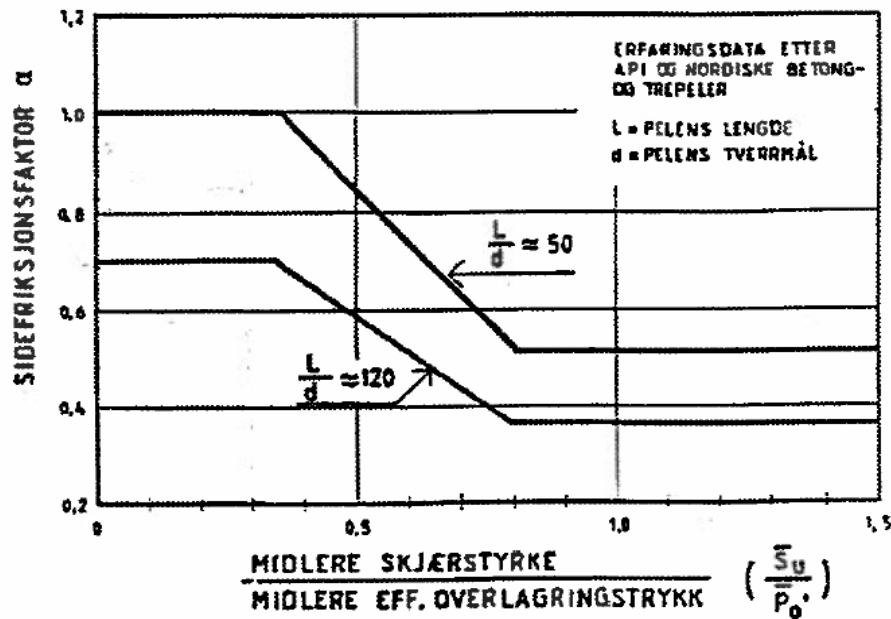
Figure 4.3 Side friction according to peleveiledningen 1991 (after Gunnar Aas) [13]

b) Norwegian Pile Guideline (Peleveiledningen) (1991): section 2

This method is based on the work of Flaate and Selnes (1977), and recommends the average skin friction along the pile as:

$$f_s = \beta \times \bar{p}_0 \tag{4-13}$$

Where
$$\beta = (0.4 \pm 0.1) \times \frac{L+20}{2L+20} OCR^{0.5}$$

L = pile length

$\bar{p}_0$ = average effective vertical overburden along the pile

OCR = over consolidation ratio (average)

c) Norwegian Pile Guideline (Peleveiledningen) (2005)

The updated version of the Norwegian Pile Guideline was printed in 2005 and recommends the skin friction for clay in the same way as that of the NGI-99 (refer category 4.1.3f)

d) API PR2A LRFD (1987, 2007)

According to the API RP 2A (1987, 2007), the unit skin friction for cohesive soils along the pile shaft relates with the undrained shear strength through the following expression.

$$f_s = \alpha s_u \tag{4-14}$$

Where α = an empirical factor,

s_u = average undrained shear strength along the pile

The factor, α, can be computed by the equations:

$$\alpha = 0.5\psi^{-0.5} \qquad \psi \leq 1.0$$

$$\alpha = 0.5\psi^{-0.25} \qquad \psi > 0$$

With the constrain that, $\alpha \leq 1$,

$$\psi = \frac{c}{p'_0} \quad \text{for the point in question.}$$

p'_0 = effective vertical stress at the point in question

e) NGI/API 1992

NGI modified the API method for side friction from back calculating some load tests (e.g. Tilbrook Grange tests). It appears that API (1987) lies somewhat on the low (conservative) side of the test results for $\frac{s_u}{\sigma'_{vo}}$ greater than about 0.7. It is therefore proposed that for $\frac{s_u}{\sigma'_{vo}} > 0.7$ API (87) could be upgraded as shown in the dashed line in Fig.4.4. [13]

The proposed new relationship is:

$$\alpha = 0.5(\frac{s_u}{\sigma'_{vo}})^{-0.5} \ for \ \frac{s_u}{\sigma'_{vo}} < 0.7 \qquad\qquad (4\text{-}15)$$

$$\alpha = 0.56(\frac{s_u}{\sigma'_{vo}})^{-0.2} \ for \ \frac{s_u}{\sigma'_{vo}} > 0.7 \qquad\qquad (4\text{-}16)$$
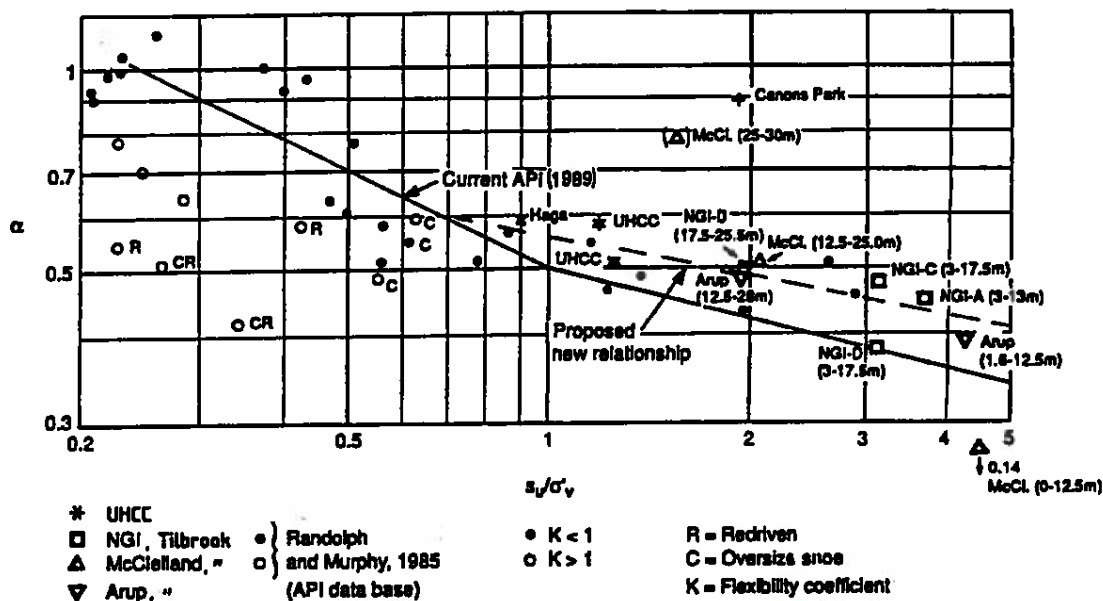
Figure 4.4 Comparison between $\alpha - \frac{s_u}{\sigma'_{vo}}$ *relationsfrom new tests and load test data from API data base [13]*

f) NGI-99

Karlsrud et al. (1992) suggested that API (1987) do not predict the low skin friction values measured in NC clays of low plasticity and later confirmed by full-scale load tests in Drammen, Norway, Tvedt & Fredriksen (2003) and in sandpoint, Idaho, Fellenius et al (2004) [4]. In 1993 Norwegian Geotechnical Institute led a research program described as Karlsrud et al. (1993) at 3 test sites namely, Onsøy test site with normally consolidated medium plastic clay deposit, pentre test site with normally consolidated silty clay deposit and lierstrand test site with a silty clay deposit. Both open ended and closed ended piles were driven at the test sites with depth ranging from 15 to 37.5m and based on the load test results at these sites Karlsrud et al. (2005) come up with a new design method called NGI-99.

"Results observed from pile load tests indicate that piles driven closed-ended in stiff clays have higher skin friction than open-ended piles. The NGI-99 method includes a factor that reflects this observation. However, there is considerable scatter and uncertainty when it comes to the precise effect of plasticity upon the skin friction in soft clays. Further pile load tests in soft clays of medium and low plasticity are highly desirable" [4]
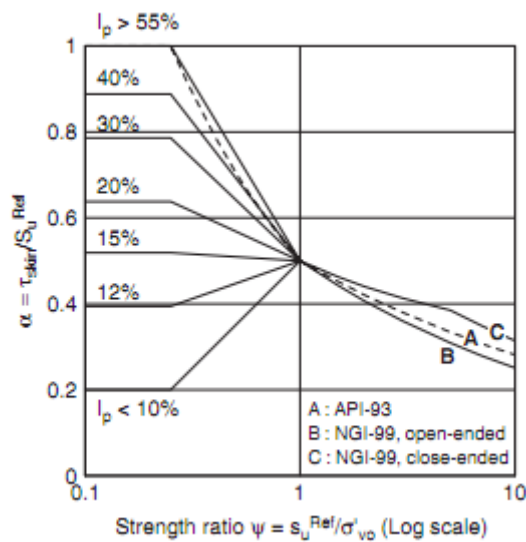
Figure 4.5 Comparison between NGI-99 and API-87 α -values [4]
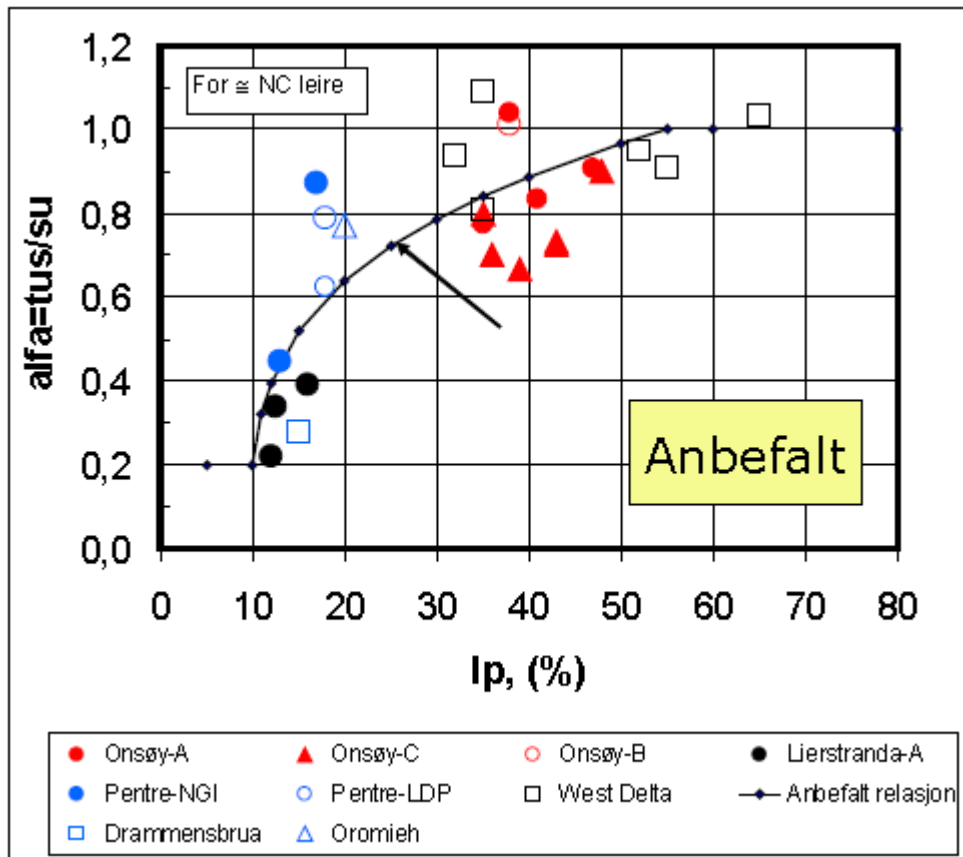
Figure 4.6 Normalized side friction for piles installed in normally consolidated clay [12]

4.1.4   Axial capacity in sand using the various pile design practices

a) Norwegian Pile Guideline (Peleveiledningen) (1991)

Recommend the drained bearing capacity of skin friction for the whole pile length based on the average characteristics specific side friction along the pile as [13]:

$$f_s = \beta \, \bar{p}_o \tag{4-17}$$

Where $\qquad\qquad$ β = empirical side friction factor

$\qquad\qquad\qquad\qquad$ L = pile length

$\qquad\qquad\qquad\qquad$ d = width or diameter of pile

$\qquad\qquad\qquad\qquad$ $\bar{p}_0$ = average effective vertical overburden along the pile.

The characteristic specific tip resistance (q_p):

$$q_p = N_q P_p' \tag{4-18}$$

Where N_q = bearing capacity factor

$P_p{}'$ = effective vertical overburden pressure at pile tip.
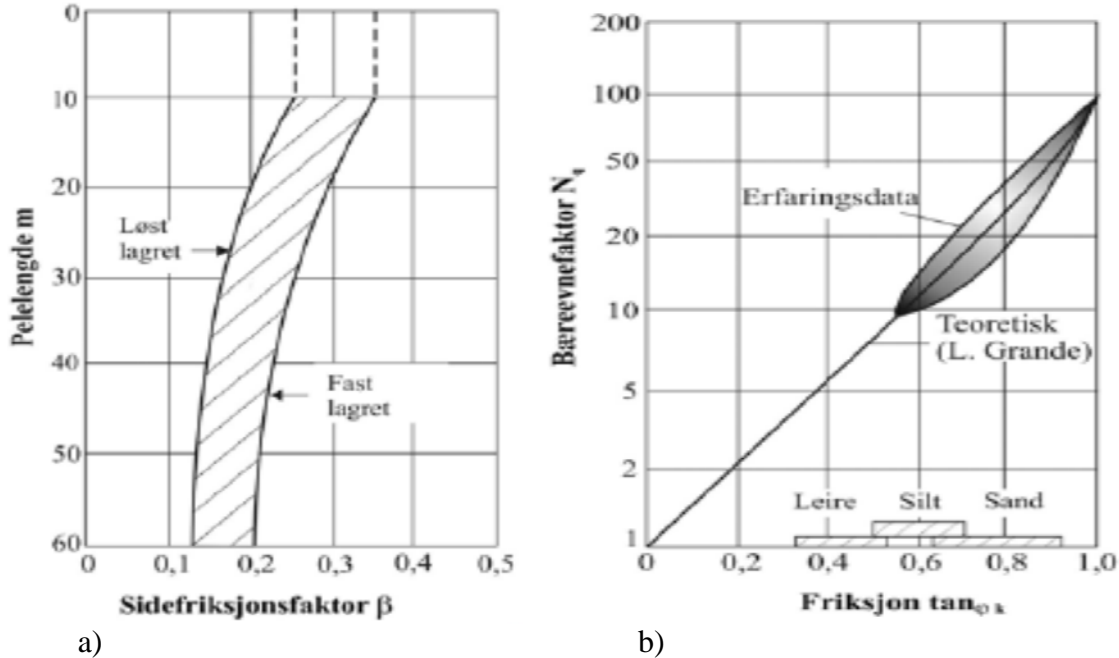
Figure 4.7 Side friction factor and bearing capacity factor in sand according to Peleveiledningen 1991 [12]

b) Norwegian Pile Guideline (Peleveiledningen) (2005)

The updated version of the Norwegian Pile Guideline was printed in 2005 and the recommended skin friction and pile tip capacity for sand is the same as that of the 1991 version (refer section 4.1.4a).

c) API RP2A LRFD (1987, 2007)

For piles in cohesionless soils, the API RP 2A (1987, 2007) relates the local shaft friction, f_s to the vertical effective stress using the equation

$$f_s = KP_o{}'\tan\delta$$

(4-19)

Where

K = coefficient of lateral earth pressure

$P_o{}'$ = effective vertical stress at the point in question

δ = interface friction angle between the soil and the pile shaft

In case of open-ended piles API RP 2A (1987, 2007) recommends $K = 1$ for piles designed as plugged condition and $K = 0.8$ for piles designed as unplugged and the interface friction angle δ is used from the Fig. 4.8 provided that other data is not available and it varies from 15^0 to 35^0. Although Equation (4-19) indicates f_s increases indefinitely and linearly with depth, the API RP 2A (1987) sets a limiting maximum value.

Density	Soil Description	Soil-Pile Friction Angle, δ Degrees	Limiting Skin Friction Values kips/ft² (kPa)	N_q	Limiting Unit End Bearing Values kips/ft² (MPa)
Very Loose	Sand	15	1.0 (47.8)	8	40 (1.9)
Loose	Sand-Silt**				
Medium	Silt				
Loose	Sand	20	1.4 (67.0)	12	60 (2.9)
Medium	Sand-Silt**				
Dense	Silt				
Medium	Sand	25	1.7 (81.3)	20	100 (4.8)
Dense	Sand-Silt**				
Dense	Sand	30	2.0 (95.7)	40	200 (9.6)
Very Dense	Sand-Silt**				
Dense	Gravel	35	2.4 (114.8)	50	250 (12.0)
Very Dense	Sand				

*The parameters listed in this table are intended as guidelines only. Where detailed information such as in situ cone tests, strength tests on high quality samples, model tests, or pile driving performance is available, other values may be justified.
**Sand-Silt includes those soils with significant fractions of both sand and silt. Strength values generally increase with increasing sand fractions and decrease with increasing silt fractions.

Figure 4.8 Recommended parameters according to API RP 2A (1987,2007) for piles in cohesionless siliceous soil [7]

In order to avoid over-estimating, the API introduced limiting friction for long piles installed in cohesionless soils.

For piles in cohesionless soils, the unit end bearing is calculated by the equation:

$$q_p = P_o N_q \qquad (4\text{-}20)$$

Where

P'_0 = effective overburden pressure at the pile tip.

N_q = dimensionless bearing capacity factor.

Recommended values of N_q from Fig. 3.7
For pipe piles:

$$Q = \text{minimum of: } (Q_{P-Full} + Q_{f-outside}; Q_{P-Annulus} + Q_{f-outside} + Q_{f-inside})$$
$$\text{(Plugged or unplugged capacity)}$$
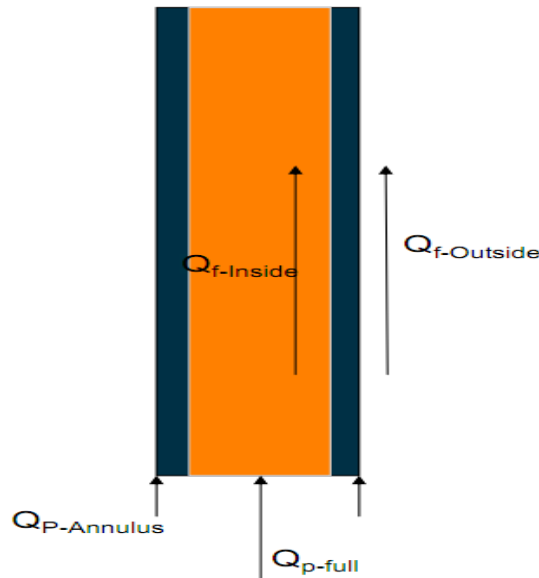
Figure 4.9 Forces on open ended pile

d) NGI-99

NGI-99 method for sand requires input of relative density which can be correlated with field tests, such as CPT, SPT, PMT or the observed pile driving resistance.

The measured SPT N-value is corrected using expression (4-21) and the cone tip resistance is calculated using expression (4-22) and then the relative density is calculated using the computed cone tip resistance and using expression (4-23). The relative density is the main input parameter in the NGI-99 method in computing the skin friction.

$$N^{SPT}_{corr} = N^{SPT}_{meas}.0.77\log_{10}(1915KPa/\sigma'_{vo}) \tag{4-21}$$

$$q_c = 2.8.N^{SPT}_{corr}.\sigma_{atm} \tag{4-22}$$

$$D_r = 0.4.\ln\left\{ q_c / \left[22.(\sigma'_{vo}.\sigma_{atm})^{0.5} \right] \right\} \tag{4-23}$$

The local unit skin friction on a driven pile in sand τ_{skin} is given by:

$$\tau_{\sin}(z) = \frac{z}{z_{tip}} . \sigma_{atm} . F_{Dr} . F_{sig} . F_{tip} . F_{load} . F_{mat}$$

(4-24)

$$\tau_{skin}(z) > 0.1.\sigma'_{vo}$$

z = depth below the ground surface

z_{tip} = pile tip depth

σ_{atm} = atmospheric reference pressure = 100KPa

$$F_{Dr} = 2.1.(D_r - 0.1)^{1.7}$$
$$F_{sig} = (\frac{\sigma'_{vo}}{\sigma_{atm}})^{0.25}$$
F_{tip} = 1.0 for a pile driven open-ended, 1.6 for a close-ended pile

F_{load} = 1.0 for tension, 1.3 for compression

F_{mat} = 1.0 for steel and 1.2 for concrete

The point resistance acting against a pile driven close-ended is given by:

$$\sigma_{tip} = 0.8.\frac{q_c}{(1 + Dr^2)}$$

The plugged tip resistance of an open-ended pile is calculated as:

$$\sigma_{tip} = 0.7.\frac{q_c}{(1 + 3.Dr^2)}$$

4.2 Theoretical method

The theoretical methods presented in this study comply with the Norwegian University of Science and Technology (NTNU) way of teaching.

4.2.1 Short term capacity

a) Shaft friction

Based on the earth pressure approach the shaft friction is estimated from

$$\tau_s = r\tau_c = r\frac{s_u}{FS}$$

(4-25)

Where:

r is a combination of roughness ratio and remolding caused by the pile driving following reconsolidation.

$\dfrac{S_u}{FS}$ = mobilized undrained shear strength in depth z.
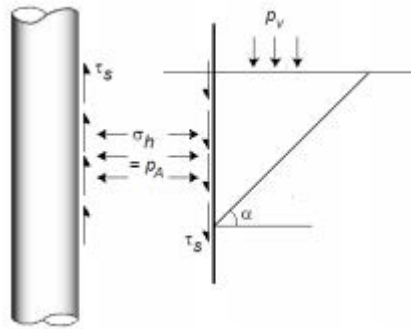
Figure 4.10 Side friction derivation using earth pressure concept (after Lars Janbu)

b) Point bearing

By assuming a bearing capacity failure as shown in figure the point bearing is estimated from

$$\sigma_{pn} = N_c \tau_c = N_c \frac{S_u}{FS} \qquad (4\text{-}26)$$

Where

$\sigma_{pn} = \sigma_p - P_p$ = net tip resistance

N_c is approximately equals to 9
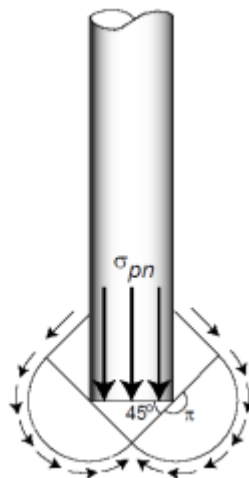
Figure 4.11 Point bearing (after Lars Grande)

4.2.2 Long term capacity

a) Shaft friction

Janbu (1976) by using an earth pressure approach for long term drained condition he developed an expression for computing the skin capacity as shown below

$$P'_a + a = K_A(p' + a)$$

$$\tau_s = r.\tan\rho.K_A(p' + a)$$ (4-27)

$$\tau_s = s_v(p' + a)$$

$$s_v = r.\tan\rho.K_A$$

Where

r = mobilized roughness ratio along the pile (negative for piles in compression)

$\tan\rho$ = mobilized friction in the soil (negative for active earth pressure)

K_A = classical earth pressure coefficient, active state, negative roughness, plane shear surface.

S_v = shear ratio

p' = Effective overburden in depth z

a = attraction = $c.\cot\varphi$

$$S_v = \frac{r\tan\rho}{(\sqrt{1 + \tan^2\rho} - \tan\rho.\sqrt{1 + r})^2}$$

It should be noted that K_A (not K_P) is used in the equation 3-26 to be conservative
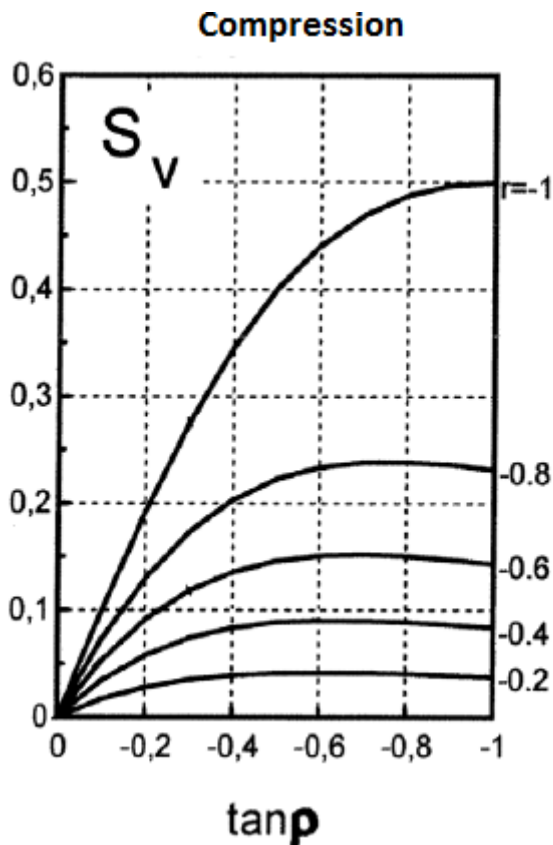
Figure 4.12 S_v vs. $\tan \rho$ chart for compressive pile (after Janbu)

b) Negative shaft friction

When a pile is driven and loaded into a newly placed fill placed on compressible soil, initially the pile load is carried by adhesion of the compressible soil later when consolidation starts the compressible soil will down drag relative to the pile. This downward movement of soil will develop a skin friction between the pile and the surrounding soil and is termed as negative skin friction. To reduce the skin friction pre-boring or filling the annulus with bentonite can be used as a remedial measure.

$$\tau_{sn} = s_{vn}(p'+a) \quad \text{Where } n \text{ denotes negative shaft friction} \tag{4-28}$$

$$S_{vn} = r\tan\rho.K_A = r\tan\rho.\frac{(1+f_\omega^{\,2})N}{1+f_\omega^{\,2}}.e^{2.\omega.\tan\rho}$$

$$\tan\rho \quad f_\omega = \frac{\tan\omega}{\tan_{\alpha_c}} = \frac{1}{r}(1-\sqrt{1-r2})$$

$$\tan_{\alpha_c} = \sqrt{1+\tan^2{}_\rho} + \tan\rho$$

(Roughness should be positive and $\tan\rho$ should be negative)
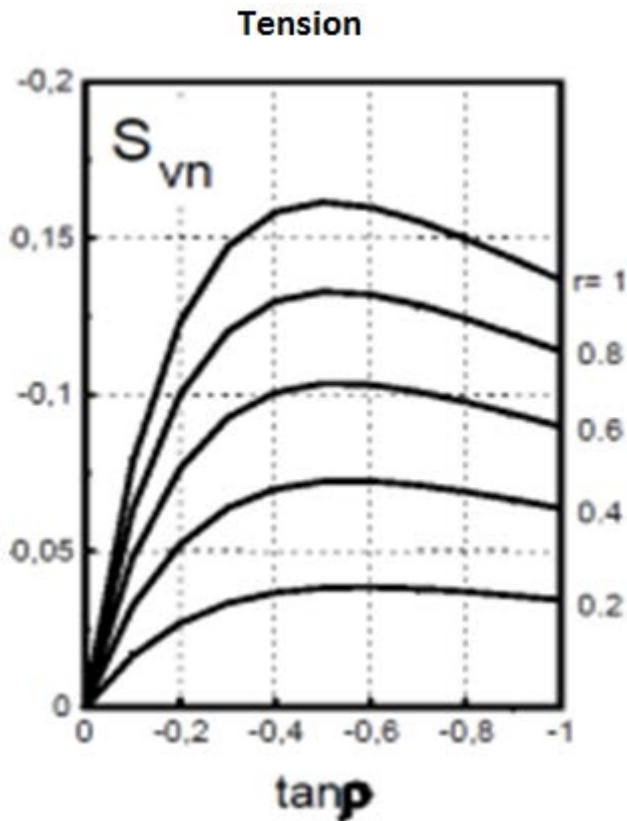
Figure 4.13 S_v vs. $\tan \rho$ chart for piles with negative skin friction (after Janbu)

c) Point bearing

The point bearing is estimated from

$$\sigma_{pn} = (N_q - 1)(p'_p + a + \bar{\gamma} d_o B_o)$$

$$d_0 B_0 \ll D$$

$$(4\text{-}29)$$

$$\sigma_{pn} = (N_q - 1)(p'_p + a)$$

Where:

$\sigma_{pn} = \sigma'_p - p'_p =$ Net effective point resistance

$N_q = N_+ . e^{(\pi - 2\beta) \tan \rho} =$ Bearing capacity ratio for vertical loading ($r = 0$)

β is angle of plastification

$p'_p =$ Effective vertical overburden at point level

$B = B_o$ Width or diameter of the pile

$D =$ Penetration depth of the pile

$\beta = 15^0$, for loose soils and $\beta = 0^0$, for dense soils.
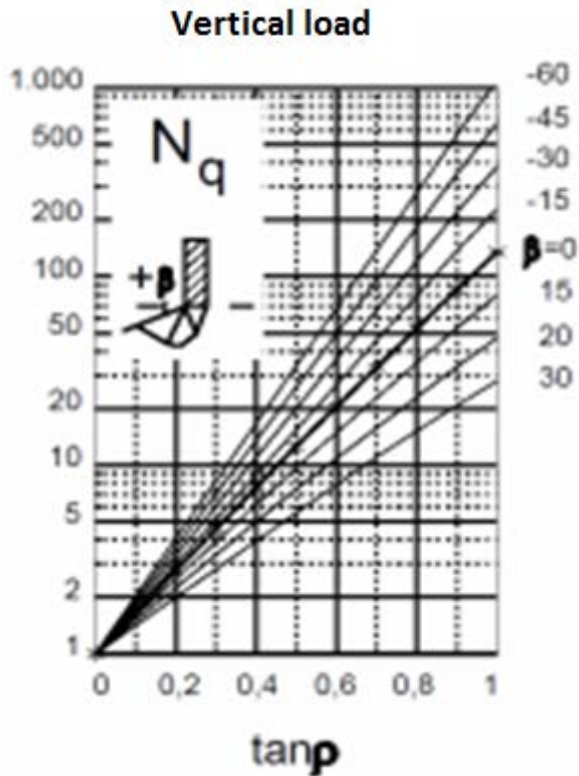
Figure 4.14 Nq vs $\tan \rho$ chart for different plastification angles (after Lars Grande)
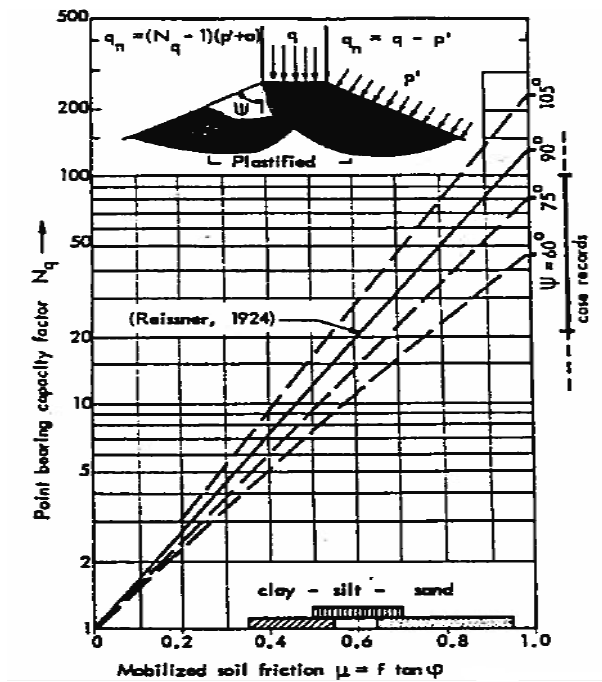
Figure 4.15 point bearing capacity factor Nq vs $\tan \rho$ chart (after Janbu (1991))

4.3 Effect of time on pile capacity

Interval between installation of a pile and application of the load is an important thing to be known. When a displacement pile is driven, it displaces a volume of soil equal to volume of the pile, thus applies very high normal and shear stress in the surrounding soil causing buildup of excess pore pressure. The time between installation and loading of a pile sometimes might not be enough for the excess pore pressure to dissipate.

Randolph (2003) noted that any scientific approach to determining the shaft resistance of a displacement pile should consider the complex stress-strain history experienced, which includes; the initial in situ condition, pile installation, equalization and loading (see Figure 4.16)
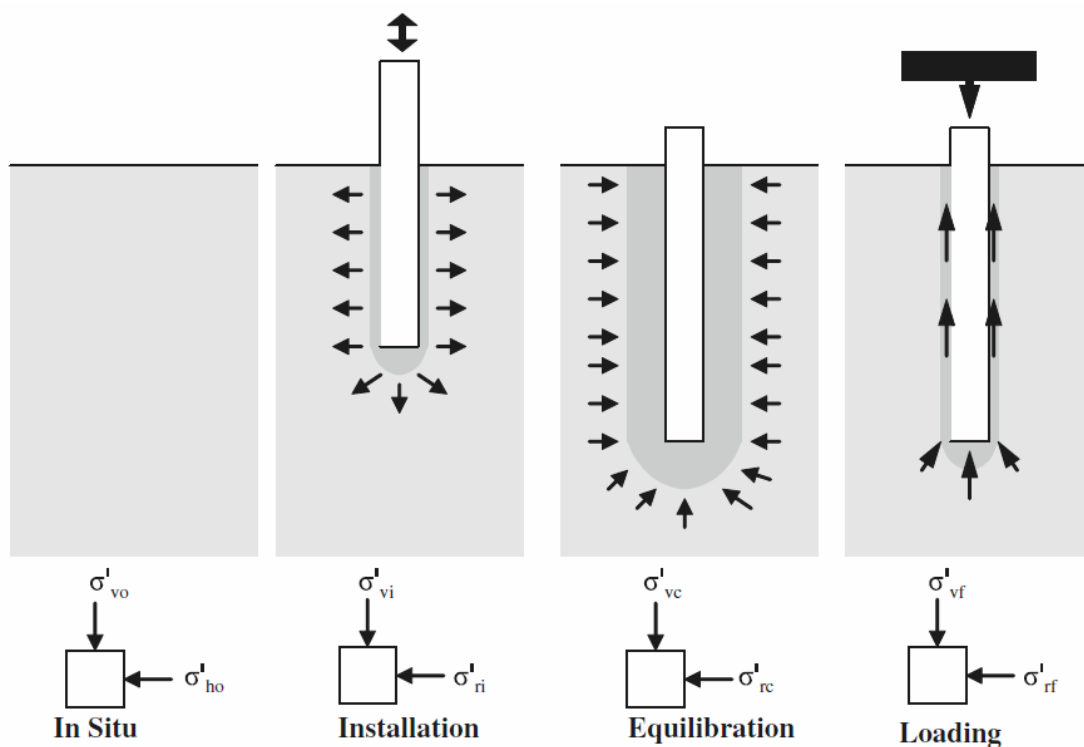
Figure 4.16 Changes in pile stress regime over time [16]

Increase in pile capacity after installation is referred to us a pile set up while a decrease is termed as relaxation. This phenomenon is observed in both clay and sand soils. In sand due to their high permeability, the dissipation of excess pore pressure may take only hours, to days causing only a short term setup, but substantial long term setup are caused due to aging which is described as a particle rearrangement around the pile shaft.

Taking into consideration of this phenomenon will lead us to a more economical design. The basic mechanism of set up in sand and clay is quite different. In clay dissipation of excess pore pressure generated due to soil remolding during the installation of the pile will increase

the radial effective stress of the soil which in turn increases the effective stress of the soil; consequently, the axial capacity of the pile will increase. In clay the dissipation of excess pore pressure will take months even years. In clay even after dissipation of excess pore water pressure, additional set up may occur at constant effective stress due to aging.

Chow believes the increase in shaft friction is unlikely from aging of sand or corrosion of steel piles, and he believes it is likely caused by relaxation of soil arched around the shaft, thereby increasing the radial stress at the interface [1].

Terzaghi and Peck noted that the carrying capacity decreases during the first two or three days after driving, this is due to it is probable, but not certain , that the high initial bearing capacity is due to a temporary state of stress that develops in the sand surrounding the point of the pile during driving [1].

The simplest way of modeling rate of pore pressure dissipation is using the radial consolidation theory and using this theory the time factor is given by the expression

$$T = \frac{t.c_h}{r_0{}^2}$$
(4-30)

Where

T = dimensionless time factor

c_h = horizontal coefficient of consolidation

t = consolidation time

r_0 = outer pile radius

Using cavity expansion model based on the assumption of an ideal isotropic linear-elastic – perfectly-plastic (EP) type soil model the plasticized radius can be expressed in the following form [24]:

$$\frac{r_p}{r_0} = \sqrt{\frac{G_{50}}{c_u}} \cdot \sqrt{\frac{r_0{}^2 - r_i{}^2}{r_0{}^2}}$$
(4-31)

Where

r_p = radius of the plastic zone

r_i = inner pile radius

G_{50} = shear modulus at 50% of maximum stress

c_u = undrained shear strength
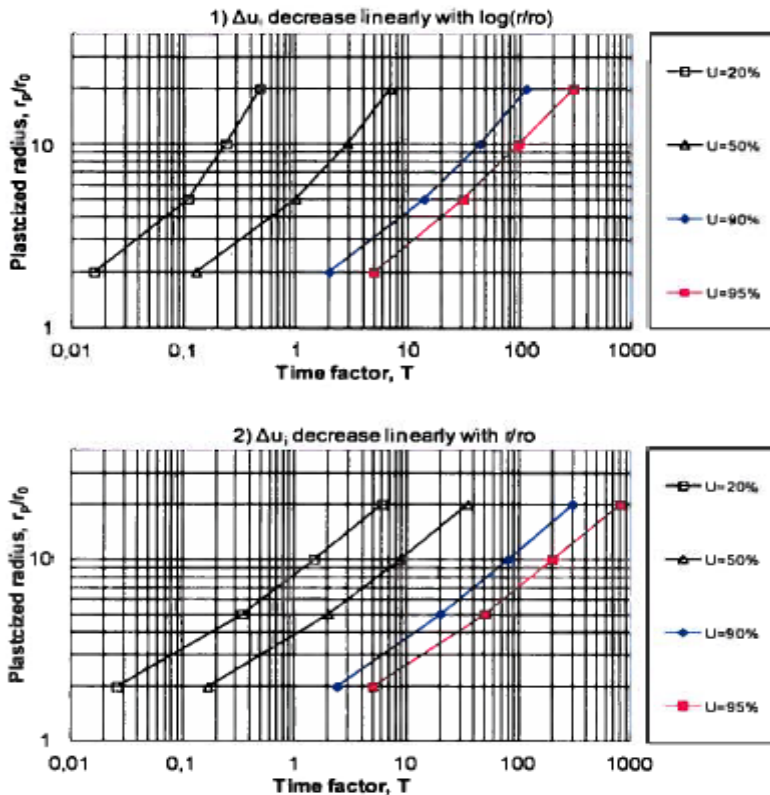
Figure 4.17 Time factors vs. degree of consolidation from linear radial consolidation theory of 1) Δu_i decreases linearly with log $(^r/_{r_0})$, 2) Δu_i decreases linearly with $(^r/_{r_0})$ (based on analytical results presented by Levadoux, 1982 and Chin, 1986) [24]
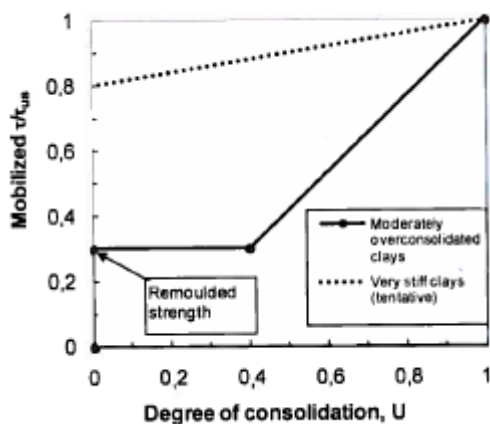
Figure 4.18 Proposed build-up of shaft friction during the re-consolidation phase [24]

Skov and Denver (1988) a semi-logarithmic empirical relation to describe the time dependent increase in capacity which is of the form

$$Q(t) = Q_0 . \left[1 + \Delta_{10} . \log_{10}(\frac{t}{t_0}) \right]$$

(4-32)

$Q_0 = $ The reference capacity at a reference time t_0

Δ_{10} Value is dimensionless capacity increase for a ten -fold time increase also called set-up factor

According to Skov and Denver (1988) the value of Δ_{10} for piles in sand and clay are 0.2 and 0.6 respectively corresponding to reference time t_0 assumed 0.5 and 1 days respectively.

NGI-05 method proposed by Karlsrud et al. (2005) assumes the increase in pile capacity after the end of re- consolidation can be expressed with the following expression:

$$Q(t) = Q(100) . \left[1 + \Delta_{10} . \log_{10}(\frac{t}{100}) \right]$$

(4-33)

Where t is time in days after pile installation

$\qquad$ $Q(t)$ is the capacity after t days and

$\qquad$ $Q(100)$ is the reference capacity after 100 days

$$\Delta_{10} = 0.1 + 0.4.(1 - I_P/50).OCR^{-0.8}$$

$$0.1 < \Delta_{10} < 0.5$$

Where I_P and OCR are average values along the pile shaft.

This approach assumes that at both time t and time equals 100 days, full dissipation has taken place. The Δ_{10} value is dimensionless capacity increase for a ten -fold time increase:

4.4 Effect of plugging on pile capacity

It is customary to see open –ended piles to be used as a foundation in both onshore and offshore structures. The way how pile penetrates significantly controls the way how the pile behave during and after installation. When an open-ended pile is driven into the ground, there is a possible formation of soil plug inside the pile which prevents additional soil from entering the pile. So the plugging effect will affect the bearing capacity of the pile.

In case of API RP 2A (1993), the bearing capacity of open ended pile can be estimated either in a fully plugged mode or unplugged mode the lesser of the two values will be taken as the capacity of the pile.
Expressing it using an equation

The ultimate capacity is the lesser of

$$Q_{unplugged} = \Sigma f_{so}.A_o + \Sigma f_{si.}A_i + q_p.A_p \qquad (4\text{-}34)$$

$$Q_{plugged} = \Sigma f_{so}.A_o + q_p.A_p \qquad (4\text{-}35)$$

f_{so} – Unit skin friction outside the pile

f_{si} – Unit skin friction inside the pile

A_o – Outside shaft area

A_i – Inside shaft area

q_p – Unit end bearing capacity

Alternatively, in literature one can find design methods based on incremental filling ratio (IFR). The degree of soil plugging is adequately quantified using the IFR (Paikowsky et al. 1989; Paik and Lee 1993) [23]. The IFR is defined as

$$IFR = \frac{\Delta L}{\Delta D} * 100\% \qquad (4\text{-}36)$$

Where IFR = increment of soil plug length corresponding to a small increment of pile penetration depth. $IFR = 0$ for fully plugged mode and $IFR = 100\%$ for unplugged/fully coring mode. A partially plugged condition will have a value between 0 and 100%.

Alternative to the IFR Plug length ratio (PLR) can also correlated to the pile capacity in open-ended piles. PLR is defined as the ratio of soil plug length to pile penetration [23].

$$PLR = \frac{L}{D} \qquad (4\text{-}37)$$
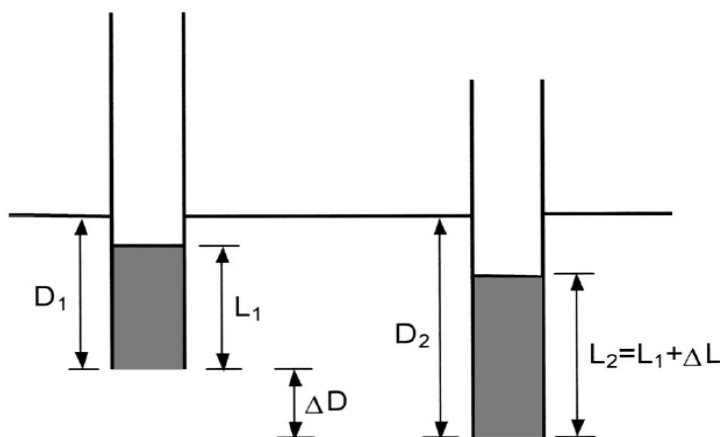
Figure 4.19 Definition incremental filling ratio and plug length ratio [23]

4.5 Build-up/ drop-off in bearing capacity in layered soils

The end- bearing capacity of piles resting close to weak layer underlying a strong layer and the other way around a strong layer underlying a weak layer shows a build-up of resistance and drop-off resistance at a distance x from the interface.
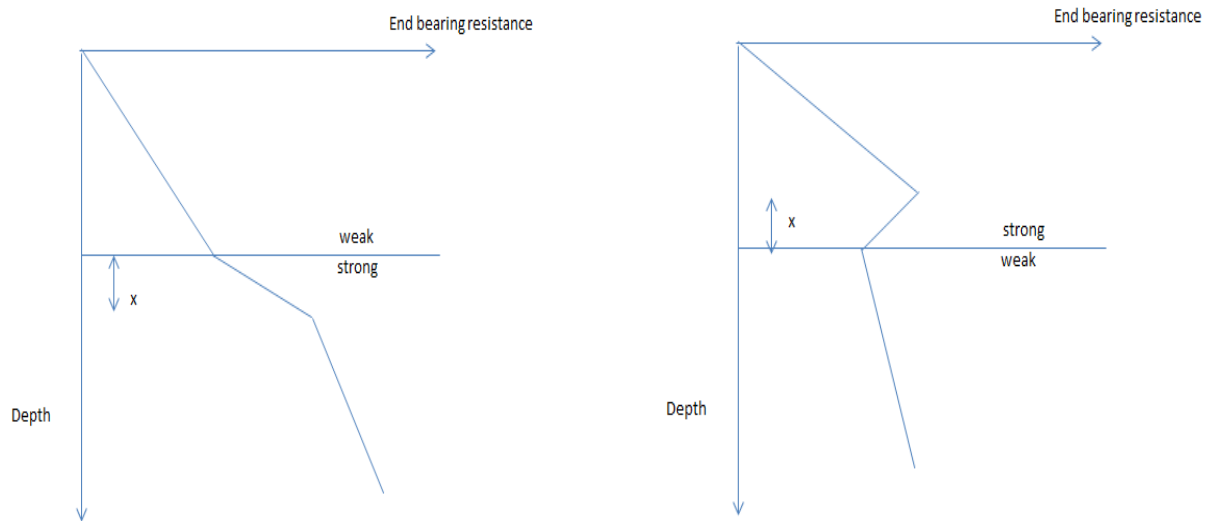
Figure 4.20 Build-up/drop-off in end-bearing resistance in layered soils (after Kraft, 1990)

According to Meyerhof (1976) the build-up of end-resistance as a pile penetrates a strong layer underlying a weak layers takes place at a distance $10D$ where D is the diameter of the pile, and Kraft (1990) based on the results of load tests come to the conclusion that the transition zone varies from $5D$ to $15D$, and he also commented the decrease is the result of

- Difference in strength between the layers decreases
- Overburden stress increases
- Density of the sand increases

Kraft recommended using $x = 5D$ when the weak and strong layers are sands of different density.

5 PILE DYNAMICS AND PILE LOAD TESTS

"The development of the wave equation analysis from the pre-computer era of the fifties (Smith 1960) to the advent of a computer version in the mid-seventies was a quantum leap in the foundation engineering. For the first time, a design could consider the entire pile driving system, such as wave propagation characteristics, velocity dependent aspects (damping), soil deformation characteristics, soil resistance (total as well as its distribution of resistance along the pile shaft and between the pile shaft and the pile toe), hammer behavior, and hammer cushion and pile cushion characteristics" [25].

5.1 Pile installation

Piles are normally inserted into the ground using a hammer resting on the pile cap and there are different types of hammer exist today the simplest of them is the drop hammer, which is used for small projects and inaccessible conditions. The main disadvantage of using a drop hammer is the difficulty of controlling the drop height.

Single acting hammer: they are also called compressed air hammers. The hammers are lifted up using steam or air pressure and drop using gravity. They operate at a rate up to 60 strokes per minute. They deliver slow blow rate, but still better blow rate than the drop hammers.

Double acting hammers: These hammers use steam or compressed air both to lift the ram and drop it. Their ram weight generally ranging from 90kg-2300kg and rate of driving 300 blows per minute for light types. They are mainly used for sheet pile driving. According to Tomlinson (1995) one specific example of this hammer type is Vulcan 400C, with a ram mass of 18140kg and energy of 15660m/kg and driving rate of 100 blows per minute.

Diesel hammer: This hammers work in a mechanism when the ram falls the air and the fuel compress and becomes hot this impact atomizes the diesel and result in explosion this explosion aids the hammer to drive the pile and to lift the ram as well. This hammer works pretty well in hard soils. They are easily moved from place to place and their fuel consumption is low.

Jetting: High pressure water at pile point is sometimes used to assist driving. This method is normally used in sand or sandy gravel soils.

Vibratory drivers: This method is best suited for driving sheet piles or bearing piles in sandy or gravelly soils. They have little use in stiff clays

According to Bowles (1996) the three principal advantages of the vibratory drivers are the following.

1. Reduced driving vibrations
2. Reduced noise
3. Great speed of penetration-penetration rate up to 50mm/sec is possible.

Figure 5.1Concrete pile driving in the city of Oslo (after Ermias)

5.2 Pile driving formulas

The principles behind the various dynamic formulas we come across in different literature were derived by using the basic principle of Newtonian principle of impact between rigid bodies.

Pile dynamic formulas only represent conditions at the time of driving and they do not take into account the long term capacity, settlement, effects of remolding and negative skin frictions [2].

Hiley (1930) developed an equation expressed by the following expression [2]:

$$Q_u = \left[\frac{\eta W_r h}{s + \frac{1}{2}(k_1 + k_2 + k_3)} \right] \left[\frac{W_r + n^2 W_p}{W_r + W_p} \right] \qquad (5\text{-}1)$$

Energy in = work +impact loss +cap loss+ pile loss+ soil loss

The Hiley formula is the basis for the various pile driving formulas which exists in the literature. They are simplified form of Hiley formula by adopting various assumptions [2]

Janbu et al. proposed a pile-driving formula which assists in predicting the necessary hammer energy to install the pile to the desired depth or alternatively, to estimate the pile capacity based on the behavior of the pile during driving, taking into account various input parameters. Janbu's idealized energy diagram resembles the one at Figure 5.2.
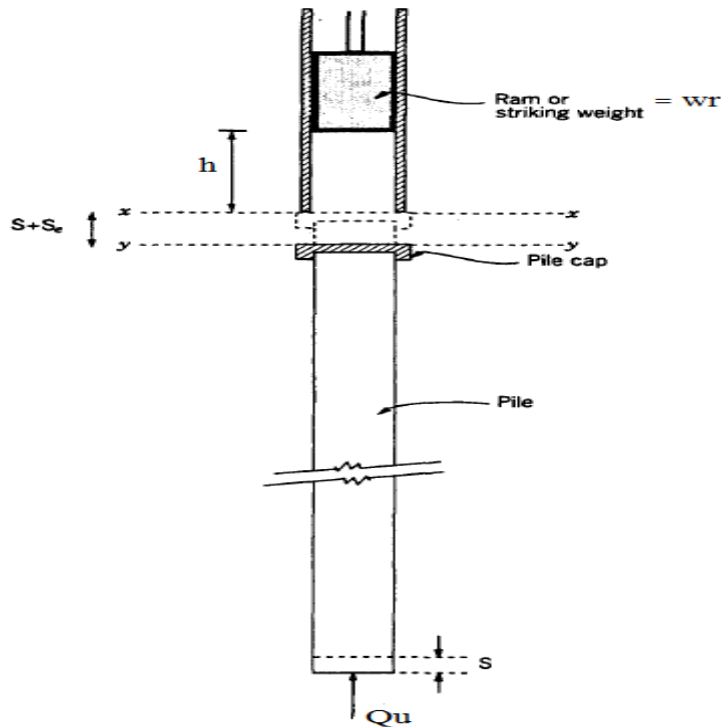
Figure 5.2 Basic concept behind derivation of pile driving formula [15]

$$\eta w_r h = Q_u . s + \frac{1}{2} Q_u \delta_e \qquad (5\text{-}2)$$

where

$$\delta_e = \frac{Q_u . L_e}{EA}$$

Danish formula [2] [Olsen and Flaate (1967)] (Recommend Factor of safety=3 - 6)

$$Q_u = \frac{\eta E_h}{s + C_1} \qquad (5\text{-}3)$$

$$C_1 = \sqrt{\frac{\eta E_h L}{2AE}}$$

The symbols used in the pile driving formulas are defined as below:

A = pile cross-sectional area
E = modulus of elasticity
η = hammer efficiency

g = acceleration of gravity

h = height of all of ram

k_1 = elastic compression of cap block and pile cap and is a form of $\dfrac{Q_u L}{AE}$

k_2 = elastic compression of pile and is a form of $\dfrac{Q_u L}{AE}$

k_3 = elastic compression of soil, also termed quake for wave equation analysis.

L = pile length

m = mass (weight/g)

Q_u = ultimate pile capacity

s = amount of point penetration per blow

W_p = weight of pile including weight of the pile cap, all or part of the soil "plug," driving shoe, and cap block (also include anvil for double acting steam hammers)

W_r = weight of ram (for double acting hammers include weight of casing)

E_h = hammer energy

5.3 Wave equation analysis

This method was first put into practice by Smith (1962). Smith proposed an idealization of hammer-pile-soil system capable of representing the passage of the stress wave down the pile. The pile is modeled as a rigid mass which able to act in both tension and compression. The time element (Δt) should be chosen as sufficiently small for the stress wave to propagate element length (ΔL).

According to Tomlinson (1995), Smith expressed the instantaneous soil resistance force, R, acting on an adjacent rigid mass as

$$R = R_s(1 + JV)$$

(5-4)

Where

R_s = static soil resistance

J = a damping constant

V = instantaneous velocity of the adjacent mass.
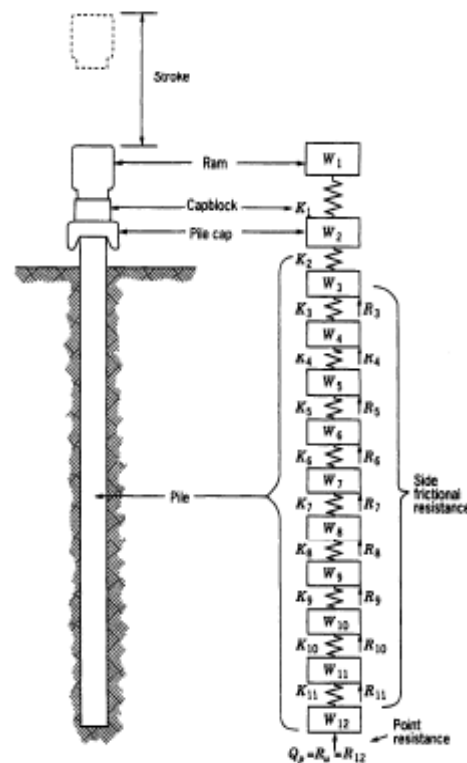
Figure 5.3 Wave equation analyses: Method or representation of pile and other parts of modell. a) Actual, b) as represented (after Smith, 1962) [15]

The wave equation is used often for contractors to determine the drivability with available equipment before project bidding and it is also used for determining the driving stresses. But it has little use in predicting the pile capacity [2].

The analysis requires assumption of certain soil parameters or used in conjunction with dynamic monitoring. Dynamic monitoring consists connecting a gauge below the pile head and recording the force and acceleration induced in the pile by the hammer impact. The force and acceleration measurements are recorded by a data acquisition unit called the Pile Driving Analyzer, PDA.

"The PDA data are usually presented in the form of PDA "wave traces", which show the measured force and velocity developments drawn against time. The case method uses the data recorded by the PDA in the form of wave traces and determines the pile capacity. However the capacity determined is the capacity at the time of testing. The capacity may be smaller than a capacity measured by a static loading test tested after development of set-up." [25].

"The two traces from the PDA, force and velocity are mutually independent variables. By taking one trace, lets us say the velocity trace in a wave equation analysis program called CAPWAP the force trace will be obtained. The shape of this force trace normally depends on hammer input, input dynamic soil parameters. By adjusting these parameters we should obtain a good match between measured and calculated force. Ultimately after, after a few iterations, the calculated force agrees well with the measured force. Finally the both the side capacity and total capacity will be obtained" [25].

"The capacity obtained by CAPWAP program is usually close to the capacity obtained from a static loading test. This doesn't mean that the capacity is exactly the same. Even the capacity obtained by the static loading test varies with in 20% by the definition of the failure load." [25].

5.4 Pile Load Tests

The uncertainties in the sub surface soil properties in computation of capacity, uncertainties in using pile driving formulas and uncertainties using the wave equation lead us to perform a full-scale field load test. The load test is believed to be the most reliable method of computing the pile capacity.

There are two broad types of pile load tests, namely the static pile load test and dynamic pile load test, but since the static load tests are traditionally used and perceived to show the long term sustained loading condition they are usually preferred to be used.

5.4.1 Static pile load test

Despite the facts that load tests are the most time consuming and expensive to perform, they are the most accurate way of determining the ultimate compressive and tensile load capacities. Load tests are performed on piles to confirm results obtained by various methods such as laboratory testing methods, field investigations based methods, dynamic analysis based methods. Static load test involves assembling of a full- size prototype foundation then slowly loads it to failure. Practically load tests are performed on either on a test pile or a working pile. By definition, test piles are preliminary piles and during testing they are tested until failure and help to confirm the pile design. In the contrary, a working pile is one of the actual piles used and is tested until two times the design capacity. The test procedure is alike in both cases.

There are two ways of measuring the settlement. Namely, pile butt movement measurement and incremental strain measurement. The incremental strain measurement is used to address the distribution of load transfer from the pile to the soil and it can be optional.

Static loads were applied and maintained using a hydraulic jack and were measured with a load cell. Reaction to the jack load is provided by a steel frame that is attached to an array of steel H-piles located at least 3m away from the test pile.

Pile head deflections were measured relative to a fixed reference beam using dial gauges. Telltale measurements were made in reference to the pile head or the reference beam using dial gauges. Pile head and telltale deflection data were recorded for each loading increment.

5.4.2 Testing methods

One thing which makes static load test difficult is the output i.e. the load-displacement curve is rate dependent. We have load controlled tests or displacement controlled tests. The load controlled tests are further divided into quick ML test and slow ML test. In load controlled tests we apply vertical loads and observe the vertical displacement and in displacement-controlled tests the displacement is fixed and the load to maintain this displacement is measured. Both tests yield load vs. displacement curves.

There should be sufficient time lapse between driving and testing for excess pore pressure to dissipate in both cohesionless and cohesive soils. Cohesionless soils dissipate the excess pore pressure quite faster.

The following [15] are some of the commonly used testing methods

1) Slow maintained load test (SM test)
2) Quick maintained load test (QM test)
3) Constant rate of penetration test (CRP test)
4) Swedish cyclic test (SC)

Figure 5.4 Typical pile load set up using adjacent piles in group for reaction (after Frode Oset)

Figure 5.5 Typical pile load set up using adjacent piles in group for reaction (after Frode Oset)

5.4.3 Interpretation of the load test

A considerable amount of information can be obtained from pile load test, particularly with instrumented piles. It is difficult to deduce the failure load of a pile while the pile has not been loaded to failure. The data obtained from the load test is plotted with the load in the x-axis and the settlement in the y-axis and interpretation varies from method to method to be used. Some define a failure load as the load at which settlement continues to increase without further increase in load.

1) **Old definition theory**

   Defines the failure load as the load causing a settlement of 10% of pile diameter.

2) **Brinch Hansen's 90% criterion**

   It is a trial and error based method and defines the failure load as the load that gives twice the movement of the pile head as compared to movement obtained by 90% of

the design load. The method is best applicable for CRP test method regardless of the soil type.
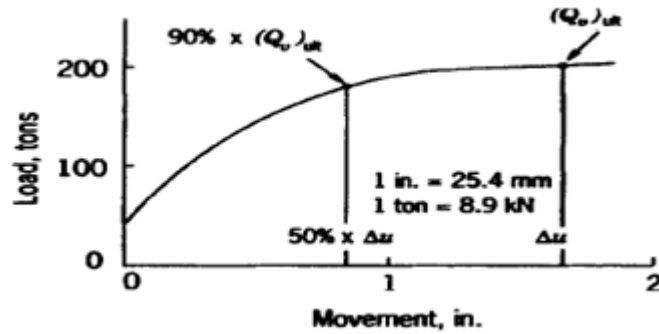
Figure 5.6 Load test interpretation using Brinch Hansen's 90% criterion [15]

3) Brinch Hansen's 80% criterion

In this method, each movement is divided with its corresponding load and is plotted against the movement. The failure load and the failure movement are then given by:

$$Q_u = \frac{1}{2\sqrt{C_1 C_2}} \tag{5-5}$$

$$\Delta_u = \frac{C_2}{C_1}$$
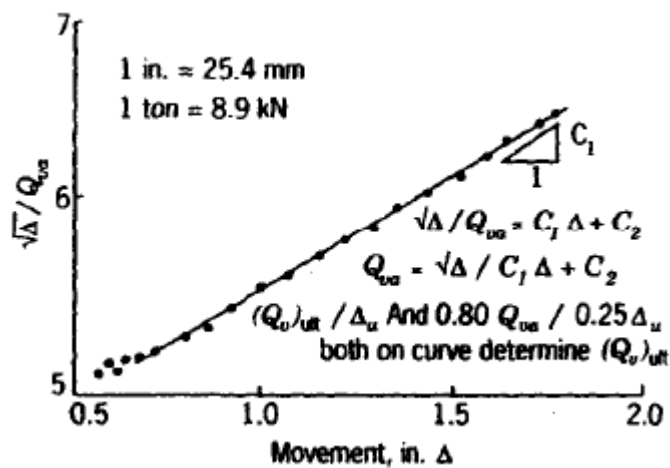
Figure 5.7 Load test interpretation using Brinch Hansen's 80% criterion [15]

4) Davisson offset limit method

This method is widely practiced in North America and defines the failure load as the load corresponding to a movement equal to the elastic compression of the pile (PL/AE) plus 0.15in (4mm) plus D/120 of the pile, where D is the diameter of the pile. The method is best applicable for QM load test method.
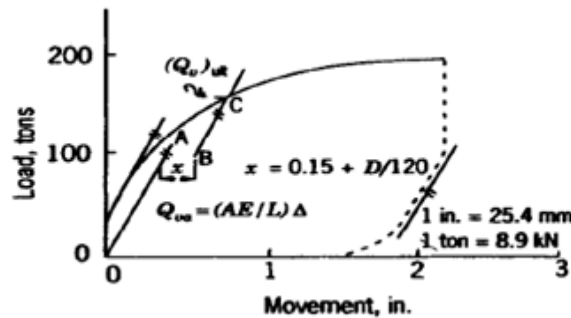
Figure 5.8 Load test interpretation using Davisson's offset limit method [15]

5) Chin-Kondner Method

In this method, each movement is divided with its corresponding load and is plotted against the movement. The plotted points will fall in straight line, except a few variations at the beginning, from the plot the inverse slope of the line is Chin- kondner ultimate load value.
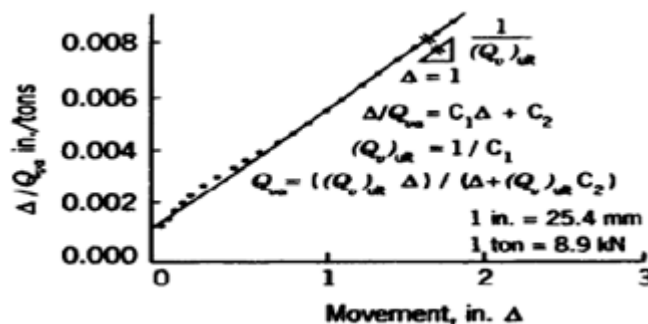
Figure 5.9 Load test interpretation using Chin-Kondner method [15]

6) De Beer's method

In this method, load and movement will be plotted on a double logarithmic chart and the values will then fall on two approximate straight lines one before failure and the other after failure load. De Beer called the intersection a yield load.
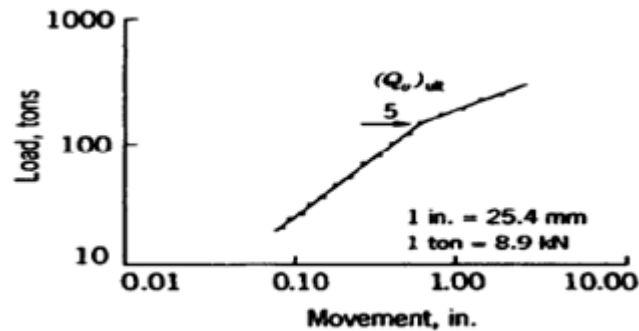
Figure 5.10 Load test interpretation using De Beer's method [15]

5.5 Pile driving stresses

To avoid material failure piles should be sized sufficiently [2]. The axial stress in the pile should be less than the strength of the pile material. The ultimate capacity can be found from the pile driving formulas or the wave equation. Dividing this capacity by the cross-sectional area will give us driving stress.

The following are recommended limits of the driving stresses [2]:

Wooden piles: $\sigma_{max} \leq f_u$
Concrete piles: $\sigma_{max} \leq 0.6 f_c$
Steel piles: $\sigma_{max} \leq 0.8 f_y$

Where

f_u is the tensile strength of the wood

f_c is the unconfined compressive strength of concrete

f_y is the tensile yield stress of steel

$$\sigma_{max} = \frac{Q_u}{A_P}$$

Where

Q_u is ultimate capacity of the pile

A_P is the cross sectional area of the pile.

6 CASE STUDY

6.1 Background of the study

The site of this study is located in the city of Drammen. The city of Drammen is located in the west of Oslo. It has a population of 60,000. The city was once said to be the ugliest place in Norway. This is due to the 2km E-18 highway crossing the Drammen selva river creating an ugly view. The bridge is known to be Norway's longest bridge built so far.

Figure 6.1: The bridge site (after Grete Trevdt)

The existing bridge is a box girder bridge which was built in the mid seventeenth and comprise of a 2 lane road. The length of the existing bridge is 1892m and consists of 41 spans ranging from 37-60m. The maximum clearance to the water is 11m, box height of 2.5m and constructed span by span by the use of movable shuttering system (MSS).

The existing bridge is supported by a rectangular shaped pier/column resting on a pile group. During the construction time, concrete piles or a combination of concrete/timber piles were used. Regarding the soil, it varies from soft clay, clay, quick sand, and sand to glacial deposits.

The traffic congestion over the existing 2 lane bridge connecting Oslo to the surrounding areas led Norwegian public roads administration (NPRA) to come up with a solution to increase the lane from 2 to 4, but there was a challenge from the locals, who are not even happy with the existence of the old bridge because they felt it made the city look ugly, but consulting company Dr. IngA. Aas- Jakobsen proposed aesthetically good alternative and the problem with the locals were settled.

During the pre- study to expand the existing bridge from 2 to 4 lanes; four solutions were proposed. The solutions were; building a twin bridge, a new bridge outside of the city, an immersed tunnel and a rock tunnel. Finally, based on the cost assessment, the last three options were rejected. The twin bridge cost as half as the other options proposed.

In April 2002, NPRA awarded the contract to consulting group consisting of Dr. IngA. Aas Jakobsen as a main consultant and with Vianova As, Geovita AS, Arkitektskap As, Grindaker As and Electronova As as subcontractors. The foundation work was awarded to a contractor company called NCC and the superstructure work was awarded to Skanska construction. The CPTU was performed by a Swedish company called statens geotekniska institute.

During the construction of the new bridge, a movable shuttering system (MSS) was used to carry the separate spans, and a total of 41 foundations were planned of which 11 of them located under water while the rest 30 located on land. The new bridge will have 42 spans varying from 20m to 60m and a circular pier column of diameter 2m.

There has been a challenge in the piling close to the existing pile foundation, but due to highly skilled workers and careful follow up of the foundation work, the work was successfully completed. The new bridge has a clearance of 0.5m from the existing bridge.

The construction for the new bridge commenced in Dec. 2004 and open to the public in Dec. 2006. The construction cost for the project is nearly NOK 874m/Euro 100m. An estimated number of 22000 vehicles use the bridge every day.
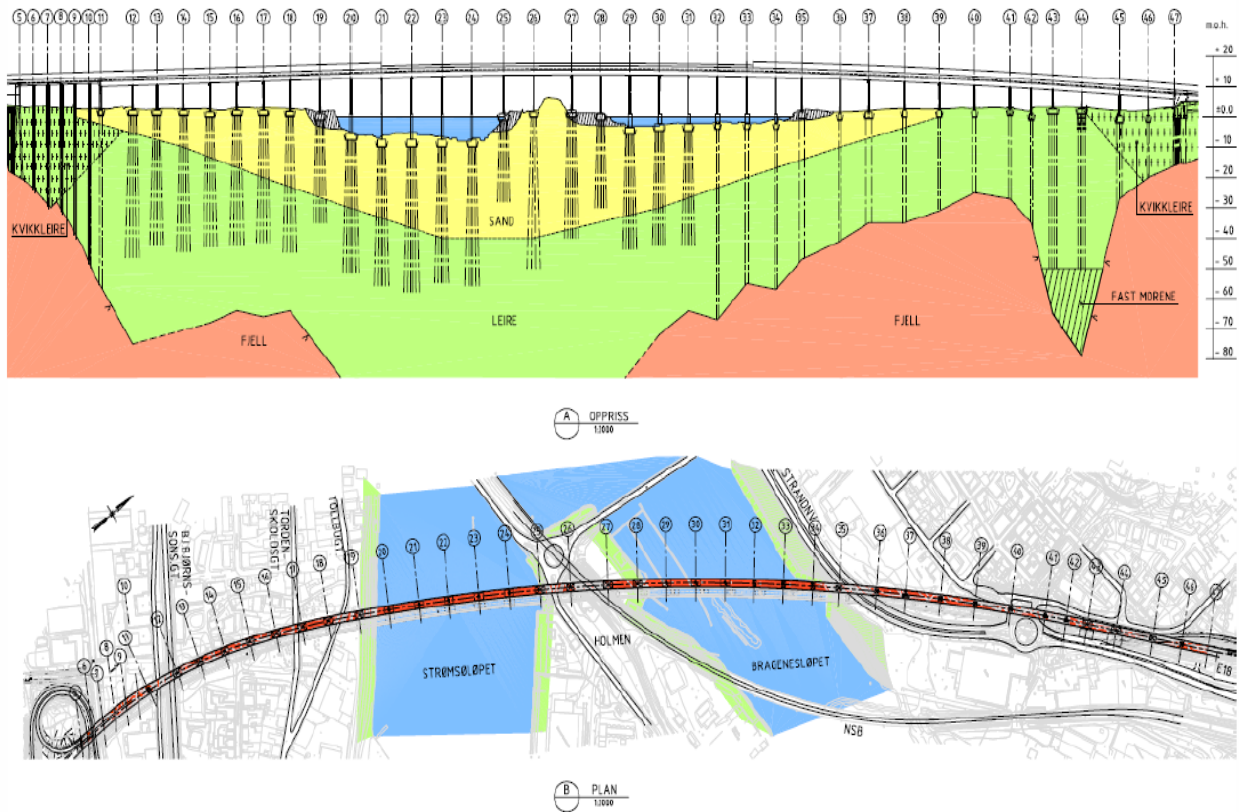
Figure 6.2 section and plan view of the new bridge project (after Grete Trevdt)

Figure 6.3 The old and new bridge side by side after completion of the new bridge (after Grete Trevdt)

The project had two phases, the first phase is construction of the new bridge alongside the existing bridge and the second phase is upgrading the pier of the existing bridge from rectangular to circular cross section due to esthetic reason.

Figure 6.4 The old and the new bridge side by side after the pier of the old bridge upgraded to a circular cross section (after Grete Trevdt)

6.2 Soil condition of the area

The soil condition of the area is mainly sands underlying clay and the clay resting on the bed rock. It is clearly seen that, there are some quick clay areas especially at location close to the bridge abutment, but fortunately the bed rock at this location is close to the surface so end bearing piles were installed which led to economic savings and safe design. Moraines were also observed between axis 42 and 46 below the clay stratum. After the completion of the design process as can be seen in figure 6.2, some of the piles were positioned totally in sand serving as friction piles and some others penetrating both the sand and clay soil and resting on the clay serving as friction piles. We can also observe from figure 6.2, some piles were resting on bed rock serving as end bearing piles.

6.3 Soil Parameters

In the project site, various geotechnical testing programs, such as rotary sounding tests, cone penetration tests were taken place. The soil sampling was taken place with a piston sampler with diameter of 54mm.Various laboratory tests, such as index tests, shear strength tests (triaxial, DSS), stiffness and consolidation tests (oedometer) were also taken place. From the

geotechnical report various useful soil parameters specifically, for axis 16 and 25 were collected to proceed to the pile capacity analysis.

6.3.1 Soil parameters at axis 16

The soil investigation report at axis 16 shows that, the soil until the depth of 15.5m is sandy soil from this depth downwards the soil is clay until the start of the bedrock at approximately 60m. Since the bed rock at this axis is found at a deeper depth, using friction pile was found to be a cost effective solution. The soil properties for the clay and the sand are summarized in table 6.1 and table 6.2 respectively. Regarding the sandy soil, the parameters (γ, φ, D_r) are found from interpretation of the CPTU and $\delta = \varphi - 5^0$ according to the API's recommendation. Parameters $(OCR, w_L, w_P, I_P, S_t)$ for the clay were found from interpretation of the laboratory tests and (γ, s_u) were found from interpretation of the CPTU.

Table 6.1 soil parameters for the clay at axis 16

Depth (m)	Unit weight $(\gamma\ (KN/m3)$	Undrained shear strength $(s_u(KPa))$	Overconsolidation ratio (OCR)	Liquid limit (w_L)	Plastic limit (w_p)	Plasticity index (I_P)	Sensativity (s_t)
15.5	19	40	1	46	28	18	7
17	19	43	1	52	28	24	8
30	19	105	1	-	-	-	3
33	19	105	1	-	-	-	5
35	19	80	1	-	-	-	6

Table 6.2 soil parameters for the sand at axis 16

Depth (m)	Unit weight $(\gamma(\frac{KN}{m3}))$	Friction angle $(\varphi(°))$	Relative density (D_r)	Soil-pile friction angle $(\delta(°))$
7.5	18	35	0.44	30
11	18	35	0.39	30
15.5	18	35	0.35	30

Cone penetration test

Cone penetration test was also performed during the investigation stages. Obviously, the cone penetration test has various uses, such as determination of stratigraphy, in-situ state of stress, stress history, strength parameters, deformation characteristics, flow and consolidation characteristics, in-situ pore pressure and so on and so forth.

Cone penetration test at axis 16

During the investigation stage at axis 16, taking measured data using the CPTU was started at a depth 1.7m and was stopped at 66.67m. The groundwater water was observed at the depth of 2.8m below the surface and the CPTU has a cone factor (a) =0.7. Table 6.3 shows some the results obtained from the CPTU at axis 16.

Table 6.3 CPTU results at axis 16

Depth (m)	Density (ton/m3)	Soil type
0-1.70m	1.8	Sand/dry crust
1.70-15.50m	1.8	Sand
15.50-30.00m	1.9	Clay NC
30.00-67.00m	1.9	Clay NC

6.3.2 Soil parameters at axis 25

The soil investigation report at axis 25 shows that, the soil until an approximate depth of 30m is sandy soil. The sand at axis 25 has similar geotechnical soil properties as that of the sand at axis 16. The bed rock start depth at this axis cannot be seen from the geotechnical report, but as can be seen in Figure 6.2 it is pretty much deep, so this led to decision to use a friction pile as economical alternative. The soil properties for the sand are summarized in table 6.4. Regarding the sandy soil, the parameters (γ, φ, D_r) are found using interpretation of the CPTU and $\delta = \varphi - 5^0$ according to the API's recommendation.

Table 6.4 soil parameters for the sand at axis 25

Depth (m)	Unit weight (γ)	Friction angle (φ)	Relative density (D_r)	Soil-pile friction angle (δ)
15	18	35	0.52	30
25	18	35	0.44	30

Cone penetration test at axis 25

During the investigation stage at axis 16, taking measured data using the CPTU was started at a depth 3m and was stopped at 27.36m. The groundwater water was observed at the depth of 1.5m below the surface and the CPTU has a cone factor (a) =0.7. Based on the results obtained from the CPTU, the soil was classified according to the table 6.5. Table 6.5 shows some of the results obtained from the CPTU at axis 25.

Table 6.5 CPTU results at axis 25

Depth	Density (ton/m3)	Soil type
0-3m	1.8	Predrilled
3-11m	1.75	Sand
11-15m	1.8	Sand
15-17m	1.9	Sand
17-27.4m	1.8	Sand

6.4 Pile parameters

Two piles were used during the load testing. The first is steel pipe pile (P1) with dimension of ($\emptyset813 * 12.5$) and the second pile is HP pile (P2) with dimension of ($HP\ 400 * 122$).

6.5 Load tests

During the pre-investigation of the new bridge project, after long discussion time, it was decided to perform load tests using both closed-ended steel pipe pile (P1) and HP pile (P2) at two chosen axises, namely axis 16 and axis 25 (see figure 6.2). During the testing process, both static and dynamic (PDA, CAPWAP) load tests were performed. The tests were carried out with the piles driven to various depths and at various time intervals, with the maximum time lapse of 4 months between driving and testing to capture the increase in capacity. The load test arrangements can be seen at figure 6.5 and figure 6.6.
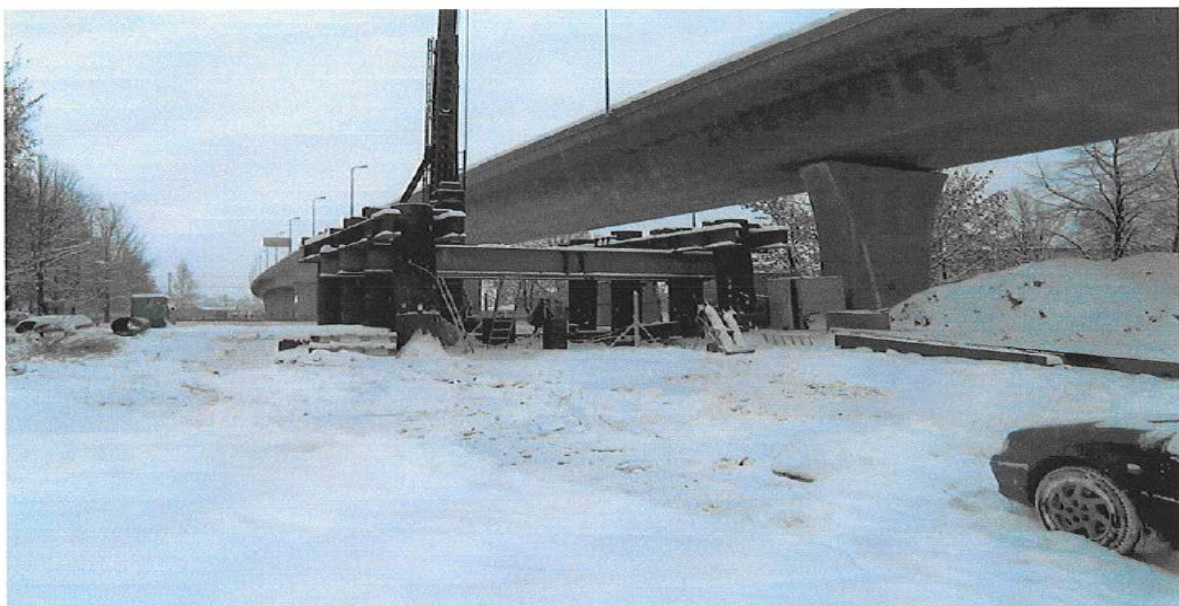
Figure 6.5 Static load test at axis 16 (after Grete Trevdt)

Figure 6.6 Static load test at axis 25 (after Grete Trevdt)

7 ANALYSES AND RESULTS

7.1 Results of the analyses

In this section, three empirical (semi-empirical) and one theoretical method were chosen. The methods chosen were Norwegian Pile Guideline (Peleveiledningen) (2005), Janbu theoretical, API RP 2A LRFD (2007) and NGI-99. Using these methods both the skin friction and tip resistance component over a varying depth were analyzed for both the closed-ended steel pipe pile (P1) and HP pile (P2).

7.1.1 Results of the analyses using empirical and theoretical methods for axis 16P1

In this section, ultimate pile capacity computation was made for the closed-ended steel pipe pile, over depths at 7.5m, 11m, 15.5m, 30m, 33m, and 35m. These depths were actually chosen based on the layering condition, the results of the soil data and considering punching through effect. For instance, 15,5m is the depth at sand-clay interface and 7.5m is the depth at $10D$ from the sand-clay interface to include punching through effect. Table 7.1 shows the results obtained using the selected methods. (Refer appendix A for the analyses).

Table 7.1 Pile capacity results using the various empirical and theoretical methods for axis 16P1

Length (m)	Norwegian Pile Guideline 2005			Janbu method			API RP 2A LRFD 2007			NGI-99		
	$Q_s(KN)$	$Q_p(KN)$	$Q_u(KN)$	$Q_s(KN)$	$Q_p(KN)$	$Q_u(KN)$	$Q_s(KN)$	$Q_p(KN)$	$Q_u(KN)$	$Q_s(KN)$	$Q_p(KN)$	$Q_u(KN)$
7.5	328	792	1120	348	1276	1624	574	1760	2334	563	1676	2239
11	605	1044	1649	662	1682	2344	1092	2320	3412	688	1736	2424
15.5	1022	1368 / 180	2390 / 1202	1192	2204 / 180	3396 / 1372	1967	3040 / 180	5007 / 2147	786	1782 / 180	2568 / 966
17	1118	194	1312	1331	194	1525	2122	194	2316	882	194	1076
30	1926	473	2399	2737	473	3210	3898	473	4371	1690	473	2163
33	2417	473	2890	3370	473	3843	4690	473	5163	2181	473	2654
35	2666	360	3026	3692	360	4052	5092	360	5452	2430	360	2790

When we look at the results in table 7.1, we can see that the tip resistance computed in the clay stratum i.e. below the sand-clay interface (15.5m) is the same in all cases, this is due to all the methods were computed using $q_p = 9s_u$ and when we look at the point bearing capacity in the sand layer i.e. a layer above 15.5m, the capacity computed using the Norwegian Pile Guideline (2005) is the most conservative estimate while the capacity

computed using the API RP 2A LRFD (2007) method is the highest compared with all the other methods, this is due to the API RP 2A LRFD (2007) method overestimates N_q value at higher φ.

Table 7.2 bearing capacity factor N_q computed using Janbu, Norwegian Pile Guideline (2005) and API RP 2A LRFD (2007) method

φ	N_q (Janbu)	N_q (Norwegian Pile Guideline (2005))	N_q (API RP 2A LRFD (2007))
30^0	$\Psi(60^0)10$	11	20
35^0	$\Psi(70^0)20$	18	40
40^0	$\Psi(80^0)48$	38	50

Looking at table 7.2, which is a more general case, the values tell us that the Norwegian Pile Guideline (2005) method gives quite a conservative N_q value and the API RP 2A LRFD (2007) method delivered a higher N_q value and the Janbu method lies somewhat in the middle of the two methods.

Concerning the skin friction capacity in the sand layer, the API RP 2A LRFD (2007) and NGI-99 method gave a higher value compared with Janbu and Norwegian Pile Guideline (2005), this is due to the β value in the Norwegian Pile Guideline (2005) and s_v value in the Janbu are smaller as compared with $ktan\delta$ value in the API RP 2A LRFD (2007). When we look at the skin friction in the clay, the Janbu and API RP 2A LRFD (2007) delivered a higher capacity compared with the NGI-99 and Norwegian Pile Guideline (2005), this is due to lesser α value in the case of Norwegian Pile Guideline (2005) and NGI-99 as compared with r in Janbu and α value in the API RP 2A LRFD (2007).

Overall, when we look at the ultimate pile capacity at a depth of 35m, the Norwegian Pile Guideline (2005) and the NGI-99 method gave a conservative estimate compared with the Janbu and the API RP 2A LRFD (2007) method.

7.1.2 Results of the analyses using empirical and theoretical methods for axis 16P2

The same computation was made at axis 16 in the case of HP pile. In this section, analysis using NGI-99 method was not performed for the reason that the NGI-99 method was introduced for steel pipe pile or concrete pile. There is no proposal from NGI yet to come for the HP pile case. The results obtained using the selected methods were briefly reported in table 7.3. (Refer appendix A for the analyses).

Table 7.3 Pile capacity results using the various empirical and theoretical methods for axis 16P2

Length (m)	Norwegian Pile Guideline 2005			Janbu method			API RP 2A LRFD 2007			NGI-99		
	$Q_s(KN)$	$Q_p(KN)$	$Q_u(KN)$	$Q_s(KN)$	$Q_p(KN)$	$Q_u(KN)$	$Q_s(KN)$	$Q_p(KN)$	$Q_u(KN)$	$Q_s(KN)$	$Q_p(KN)$	$Q_u(KN)$
7.5	204	215	419	217	347	564	402	54	456	_	_	_
11	380	284	664	416	458	874	765	71	836	_	_	_
15.5	654	372 49	1026 703	763	599 49	1362 812	1023	94 49	1117 1072	_	_	_
17	716	53	769	853	53	906	1103	53	1156	_	_	_
30	1254	129	1383	1788	129	1917	2027	129	2156	_	_	_
33	1580	129	1709	2209	129	2338	2439	129	2568	_	_	_
35	1755	98	1853	2437	98	2535	2648	98	2746	_	_	_

When we look at the results reported in table 7.3, the ultimate capacity obtained using the Norwegian Pile Guideline (2005) and Janbu until the depth of 15.5m is pretty close and beyond 15.5m the Norwegian Pile Guideline (2005) is quite conservative. The API RP 2A LRFD (2007) delivered the highest capacity throughout all the depth compared with the others.

Overall, when we look at the ultimate pile capacity at a depth of 35m the capacity obtained using the Norwegian Pile Guideline (2005) is the most conservative compared with the other methods.

7.1.3 Results of the analyses using empirical and theoretical methods for axis 25P1

The ultimate pile capacity analysis at depths 15m and 25m were done using the four selected methods for the closed-ended steel pipe pile case. Table 7.4 shows the results obtained by the four selected methods. (Refer appendix B for the analyses).

Table 7.4 Pile capacity results using the various empirical and theoretical methods for axis 25P1

Length (m)	Norwegian Pile Guideline 2005			Janbu method			API RP 2A LRFD 2007			NGI-99		
	$Q_s(KN)$	$Q_p(KN)$	$Q_u(KN)$	$Q_s(KN)$	$Q_p(KN)$	$Q_u(KN)$	$Q_s(KN)$	$Q_p(KN)$	$Q_u(KN)$	$Q_s(KN)$	$Q_p(KN)$	$Q_u(KN)$
15	840	1215	2055	672	1958	2630	1616	2700	4316	1750	2204	3954
25	1799	1935	3734	1295	3118	4412	4155	4300	8455	2232	2346	4578

When we look at the results reported in table 7.4, the skin friction capacity computed using Norwegian Pile Guideline (2005) and Janbu delivered a conservative value as compared with the API RP 2A LRFD (2007) and NGI-99 methods, this is due to the β in the Norwegian Pile Guideline (2005) and the s_v in the Janbu method are smaller than the $ktan\delta$ in the case of API and and looking at the tip resistance value again, the Norwegian Pile Guideline (2005) and Janbu delivered a conservative estimate than the NGI-99 and API RP 2A LRFD (2007) , this is simply due to the Norwegian Pile Guideline (2005) and Janbu gives smaller N_q value as compared with the API RP 2A LRFD (2007). The tip resistance value obtained using the API RP 2A LRFD (2007) method is much more than all the other methods, this is due to the API RP 2A LRFD (2007) method overestimates N_q value at higher φ.

Overall, looking at the ultimate pile capacity at a depth of 25m, the Norwegian Pile Guideline (2005) delivered the most conservative estimate due to conservative estimate of β value in the skin friction and N_q value in the tip resistance.

7.1.4 Results of the analyses using empirical and theoretical methods for axis 25P2

The ultimate pile capacity analysis at depths 15m and 25m were done using the selected methods for the HP pile case. Table 7.5 shows the results obtained by the selected methods. (Refer appendix B for the analyses).

Table 7.5 Pile capacity results using the various empirical and theoretical methods for axis 25P2

Length (m)	Norwegian Pile Guideline 2005			Janbu method			API RP 2A LRFD 2007			NGI-99		
	$Q_s(KN)$	$Q_p(KN)$	$Q_u(KN)$	$Q_s(KN)$	$Q_p(KN)$	$Q_u(KN)$	$Q_s(KN)$	$Q_p(KN)$	$Q_u(KN)$	$Q_s(KN)$	$Q_p(KN)$	$Q_u(KN)$
15	543	330	873	434	532	966	1132	83	1215	–	–	–
25	1183	526	1709	852	848	1700	2910	132	3042	–	–	–

When we look at the results reported in table 7.5, the tip resistance value obtained using Norwegian Pile Guideline (2005) < Janbu < API RP 2A LRFD (2007), this is due to the N_q values obtained by each methods (see table 7.2) and in the skin friction case Norwegian Pile Guideline (2005) < Janbu < API RP 2A LRFD (2007), this is due to the same reason as explained above in section 7.1.3.

Overall, the ultimate pile capacity obtained at a depth of 25m, using Norwegian Pile Guideline (2005) is the most conservative as compared with all the other methods.

7.2 Interpretation of the load test

The load-movement plot obtained from the load test is the bases for computing pile capacity and since there is no unique plunging point the failure should be determined according to either of the various methods explained in section 5.4.3.

According to the Norwegian practice, generally Hansen's 90% criterion ($Q_{u,\ 90\%}$) is generally used, but the ultimate capacity should not be greater than $Q_{u,\ D/10}$ (ϕ 813 steel pipe pile) or $Q_{u,\ D/5}$ (HP 400*122). Moreover, the ultimate capacity should not be greater than $0.93 Q_{u,\ failure}$.

When piles are partly in clay with a "peak" on the load displacement curve with maximum value between 20 & 40mm vertical deformation, the ultimate capacity is defined as 93% of the "peak" value.

The symbols above are defined as below:

$Q_{u,\ 90\%}$ is the ultimate bearing capacity interpreted by Hansen's 90% criterion

$Q_{u,\ failure}$ is the ultimate bearing capacity at large displacements

$Q_{u,\ D/10}$ is the ultimate bearing capacity defined as the applied load at vertical deformation of

$\frac{1}{10}$ of pile diameter

$Q_{u,\ D/5}$ is the ultimate bearing capacity defined as the applied load at vertical deformation of

$\frac{1}{5}$ of pile diameter

$Q_{u,\ 120}$ is the ultimate bearing capacity defined as the applied load at vertical deformation of

120mm

$Q_{u,\ chosen}$ is the chosen ultimate bearing capacity

$D_{steel\ pipe\ pile} = 813mm$

$D_{HP-pile} = 400mm$ (Equivalent diameter)

The various load-displacement plots in section 7.2.1, section 7.2.2, section 7.2.3 and section 7.2.4, shows the results obtained from the static load test, PDA and CAPWAP analysis.

7.2.1 Interpretation of the load test at axis 16 P1

Static load tests, using the closed-ended steel pipe pile, were performed at axis 16 at depths 11m, 17m and 35m. The main purpose of testing at varying depth is to determine the necessary pile length for the bridge structure during panning. At 11m and 17m the load tests were performed 1 day after driving while at a depth of 35m static load tests were performed at varying time to capture the increase in capacity due to time. The selected times were 1day, 14 days and 4 months after driving.

The following plots of diagrams were obtained from the static load tests and dynamic analyses (PDA and CAPWAP). The ultimate pile capacity obtained from the static load tests are presented in a tabular form in table 7.6.

Figure 7.1 Load-movement plot at axis 16 using steel pipe pile of 11m length measured one day after driving

Figure 7.2 Load-movement plot at axis 16 using steel pipe pile of 17m length measured one day after driving

Figure 7.3 Load-movement plot at axis 16 using steel pipe pile of 35m length measured one day after driving

Figure 7.4 Load-movement plot at axis 16 using steel pipe pile of 35m length measured 14 days after driving

Figure 7.5 Load-movement plot at axis 16 using steel pipe pile of 35m length measured 4 months after driving

Table 7.6 Ultimate pile capacity from the static load test for axis 16P1

Length (m)	Time after driving, or the last load testing	$Q_{u, D/10}$ (KN)	$Q_{u, 90\%}$ (KN)	$Q_{u, 120}$ (KN)	$0.93Q_{u, failure}$ (KN)	$Q_{u, chosen}$ (KN)	Note
11	1 Day	1200	-	1375	1479	1200	
17	1 Day	1260	1255	1300	1300	1255	
35	1 Day	1400	1400	1500	1488	1400	
35	15 Days	2100	-	2125	2000	2000	
35	4 Months	2900	-	2700	2418	2837	$Q_{u, chosen}$ $= 0.93Q_{peak}$

7.2.2 Interpretation of the load test at axis 16 P2

In the case of HP pile case, the static load tests were performed at depths 11, 17 and 35m from the ground surface. In a similar manner to that of axis 16P1, the static load tests at a depth of 11 and 17m were performed one day after installation of the pile and while at the depth of 35m load tests were performed 1 day, 14 days and 4 months after installation.

The following plots of diagrams were obtained from the static load tests and dynamic analyses (PDA and CAPWAP). The ultimate pile capacity obtained from the static load tests are presented in a tabular form in table 7.7.
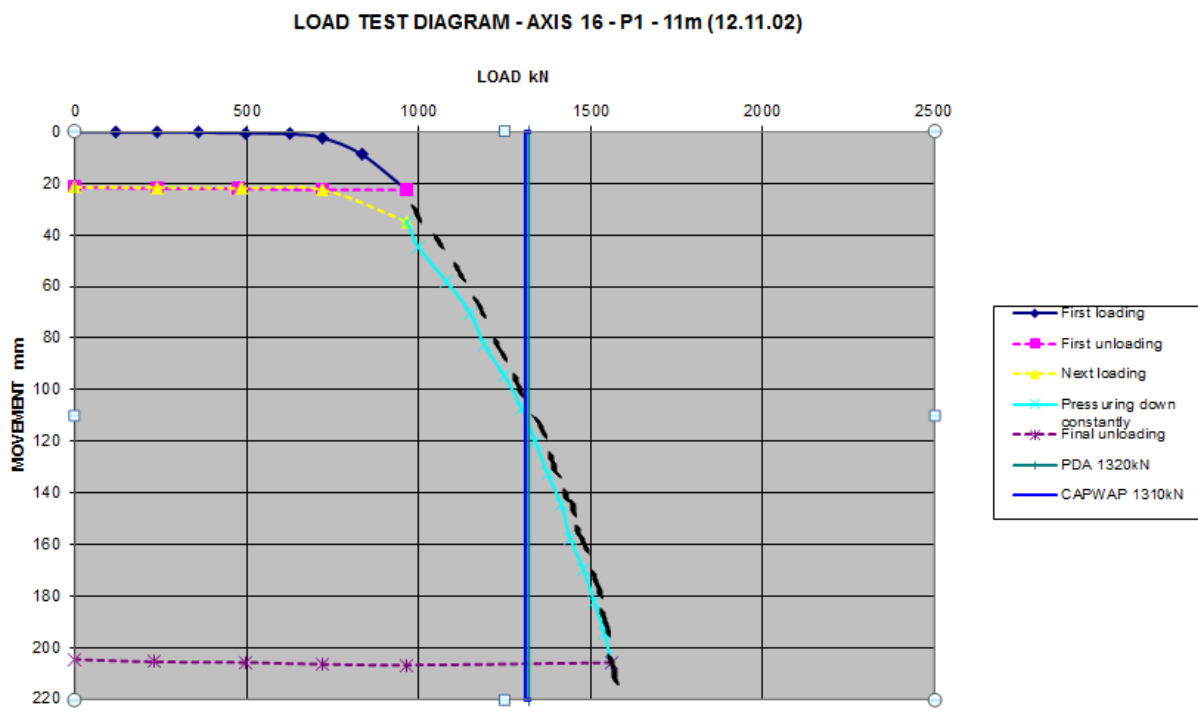

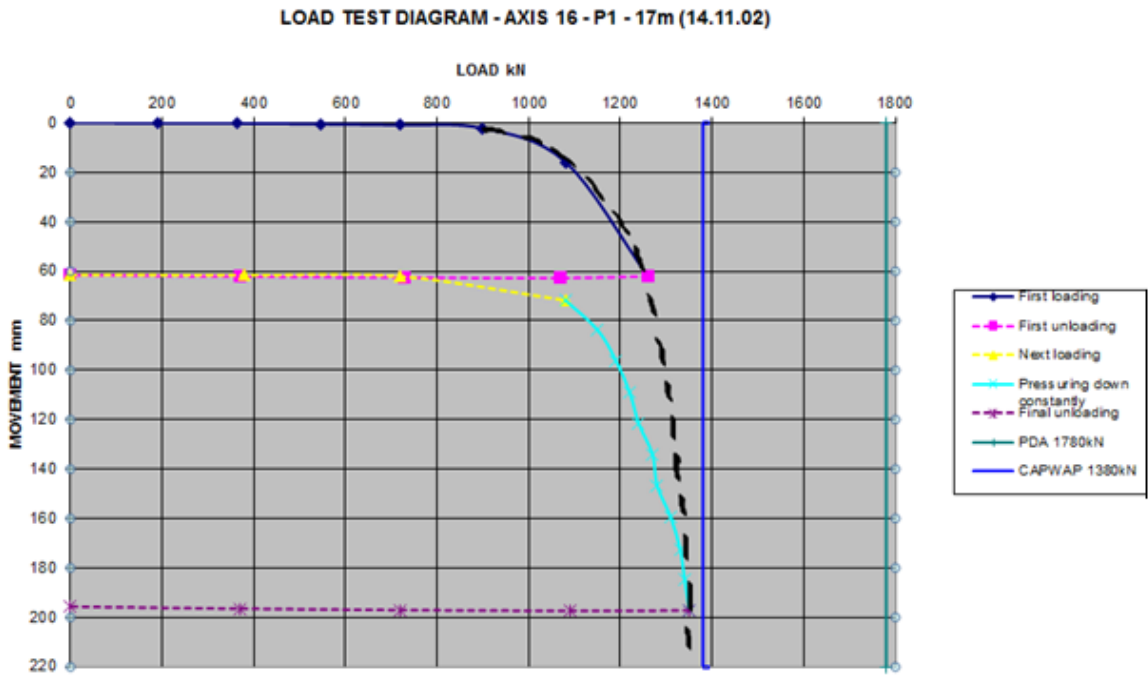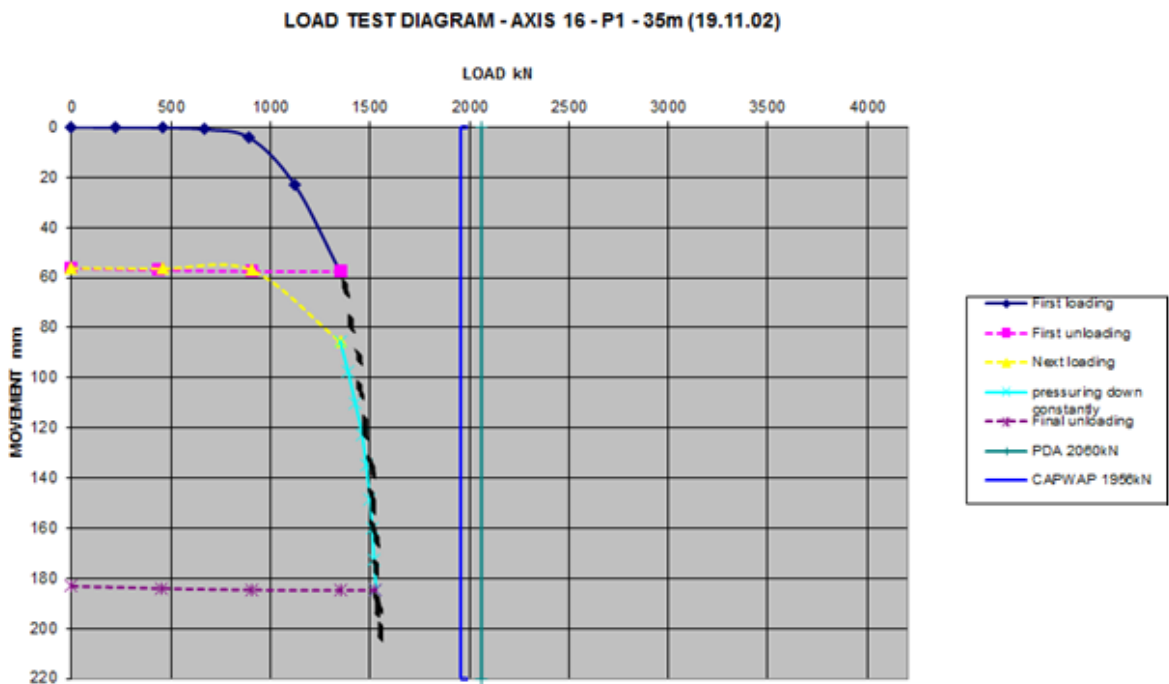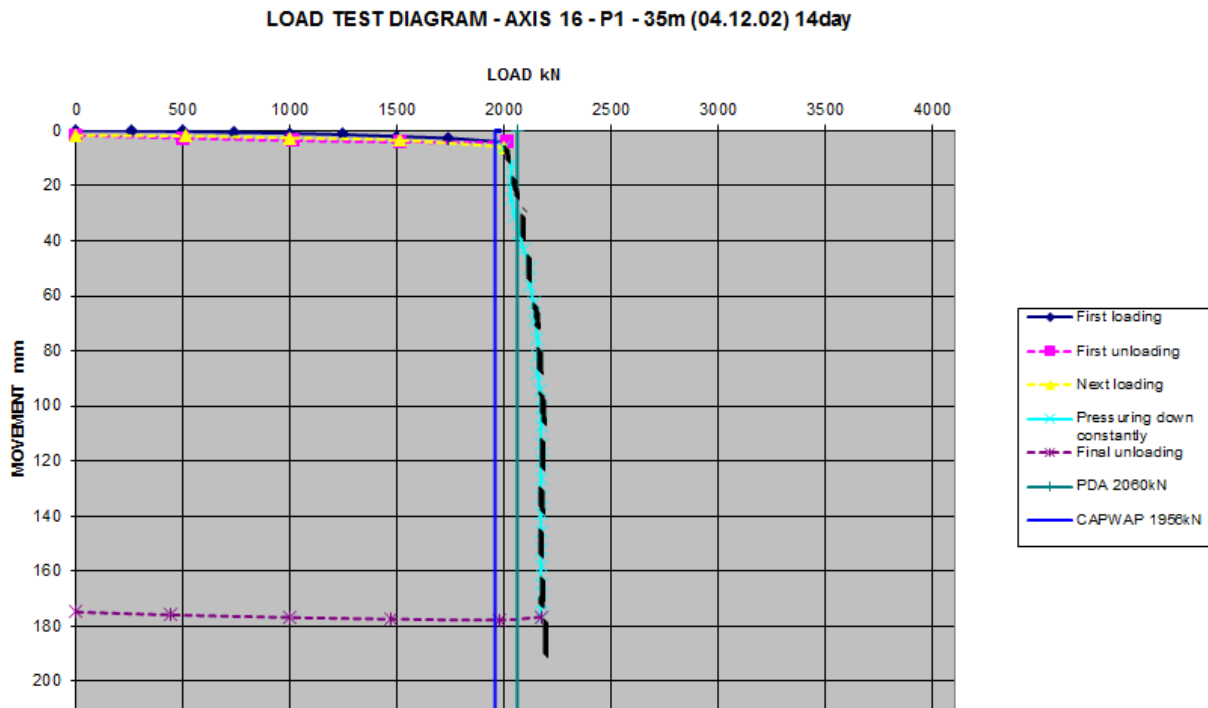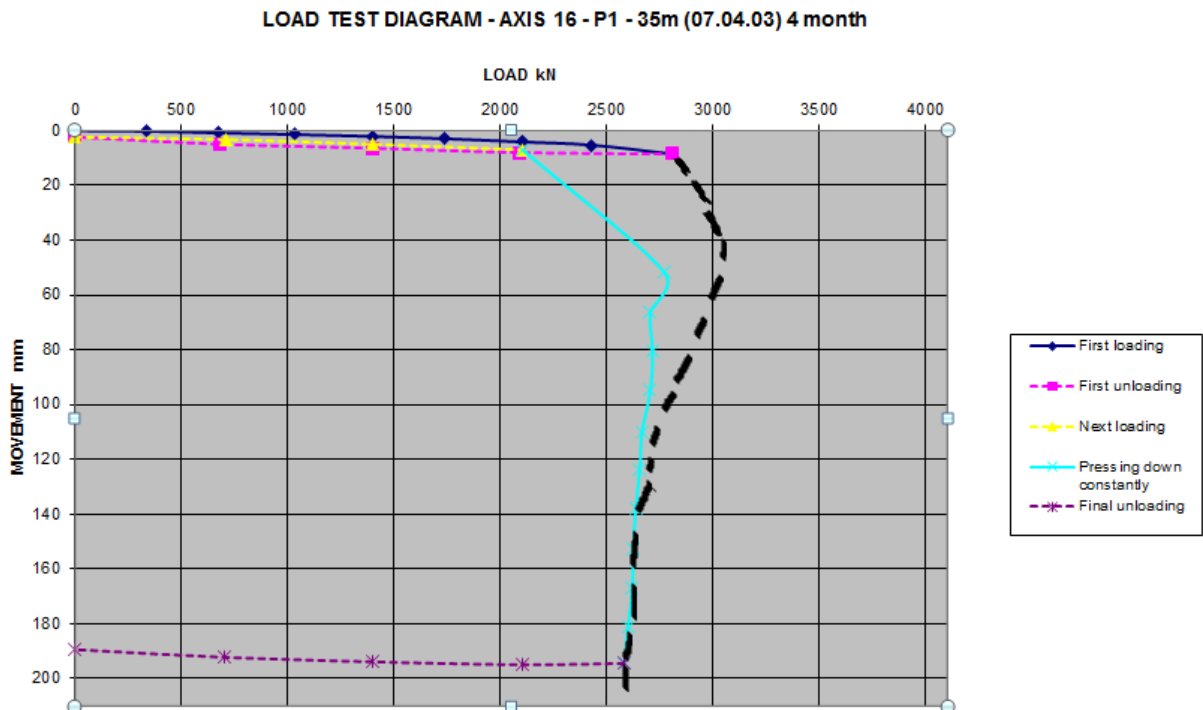*Figure 7.6 Load-movement plot at axis 16 using HP pile of 11m length measured one day after driving*

Figure 7.7 Load-movement plot at axis 16 using HP pile of 17m length measured one day after driving

Figure 7.8 Load-movement plot at axis 16 using HP pile of 35m length measured one day after driving

Figure 7.9 Load-movement plot at axis 16 using HP pile of 35m length measured 14 days after driving

Figure 7.10 Load-movement plot at axis 16 using HP pile of 35m length measured 4 months after driving

Table 7.7 Ultimate pile capacity from the static load test for axis 16P2

Length (m)	Time after driving, or the last load testing	$Q_{u, D/10}$ (KN)	$Q_{u, D/5}$ (KN)	$Q_{u, 90\%}$ (KN)	$Q_{u, 120}$ (KN)	$0.93Q_{u, failure}$ (KN)	$Q_{u, chosen}$ (KN)	Note
11	1 Day	705	710	835	760	791	710	
17	1 Day	585	590	-	620	595	590	
35	1 Day	820	810	814	750	698	814	
35	14 Days	1310	1305	-	1300	1209	1232	$Q_{u, chosen}$ $= 0.93Q_{peak}$
35	4 Months	2100	2075	-	2000	1767	2046	$Q_{u, chosen}$ $= 0.93Q_{peak}$

7.2.3 Interpretation of the load test at axis 25 P1

Static load tests, using the closed-ended steel pipe pile, were performed at axis 25 at depths 15m and 25m. At a depth of 15m, the load test was performed 1 day after driving while at a depth of 25m static load tests were performed at varying time to capture the increase in capacity due to time. The selected times were 1day, 14 days and 4 months after driving.

The following plots of diagrams were obtained from the static load tests and dynamic analyses (PDA and CAPWAP). The ultimate pile capacity obtained from the static load tests are presented in a tabular form in table 7.8.
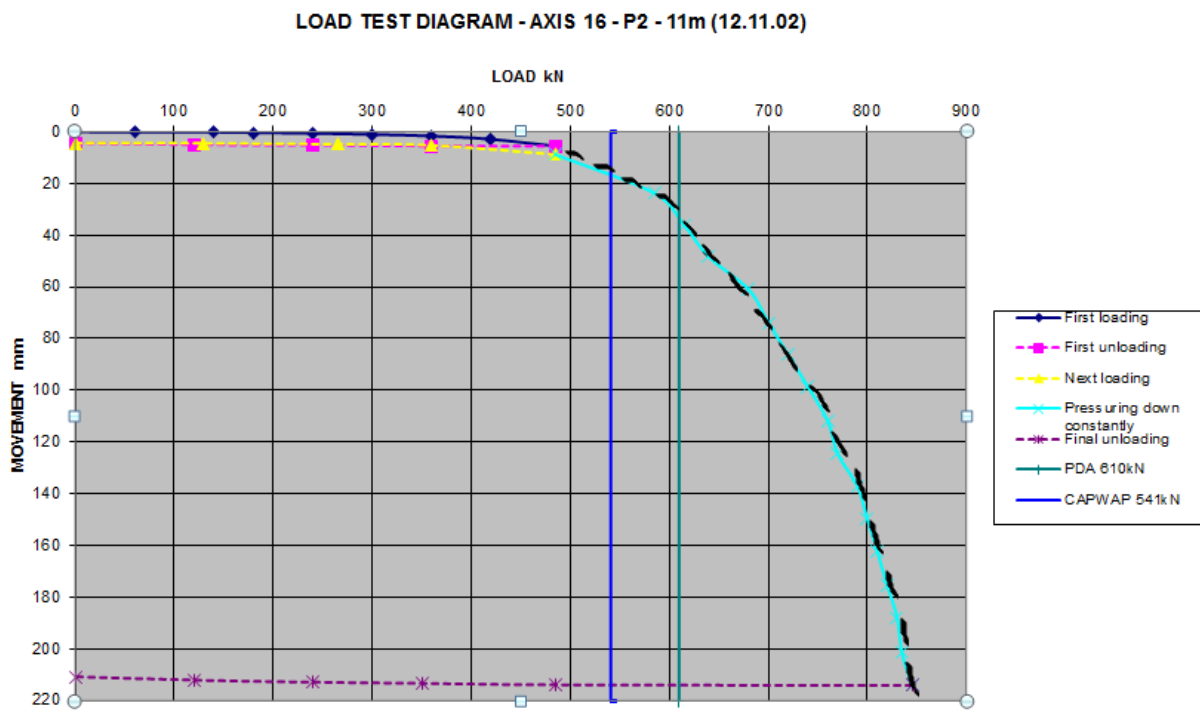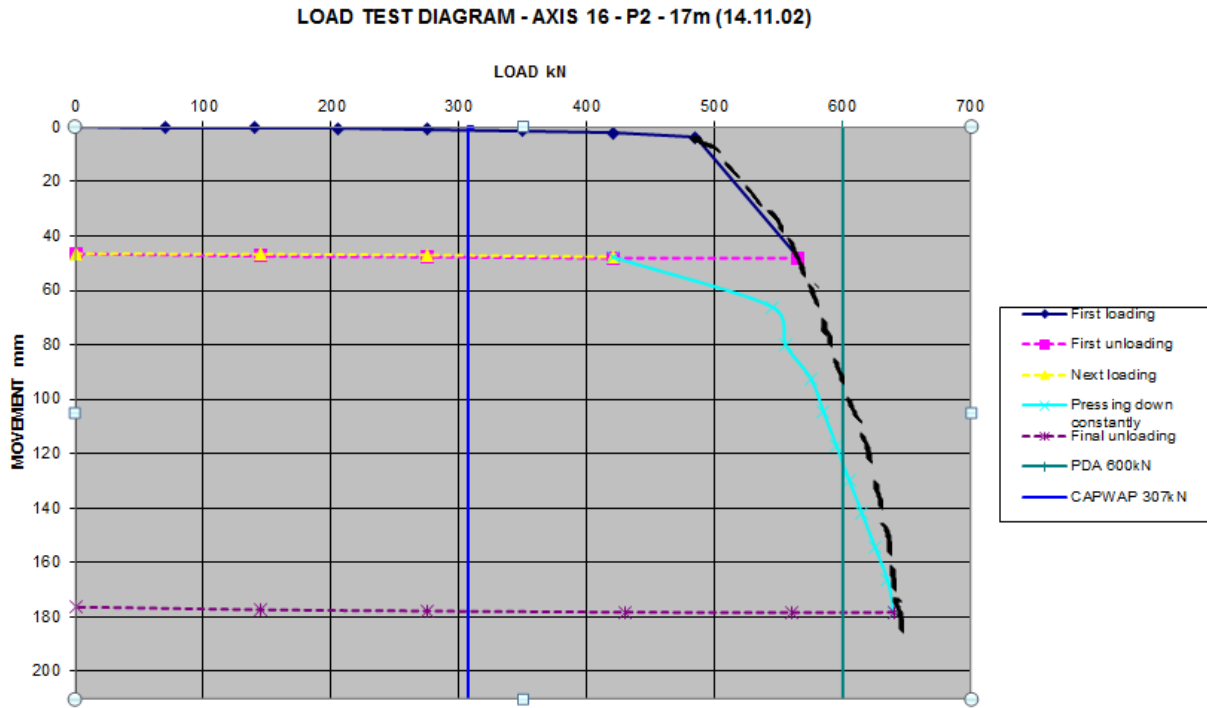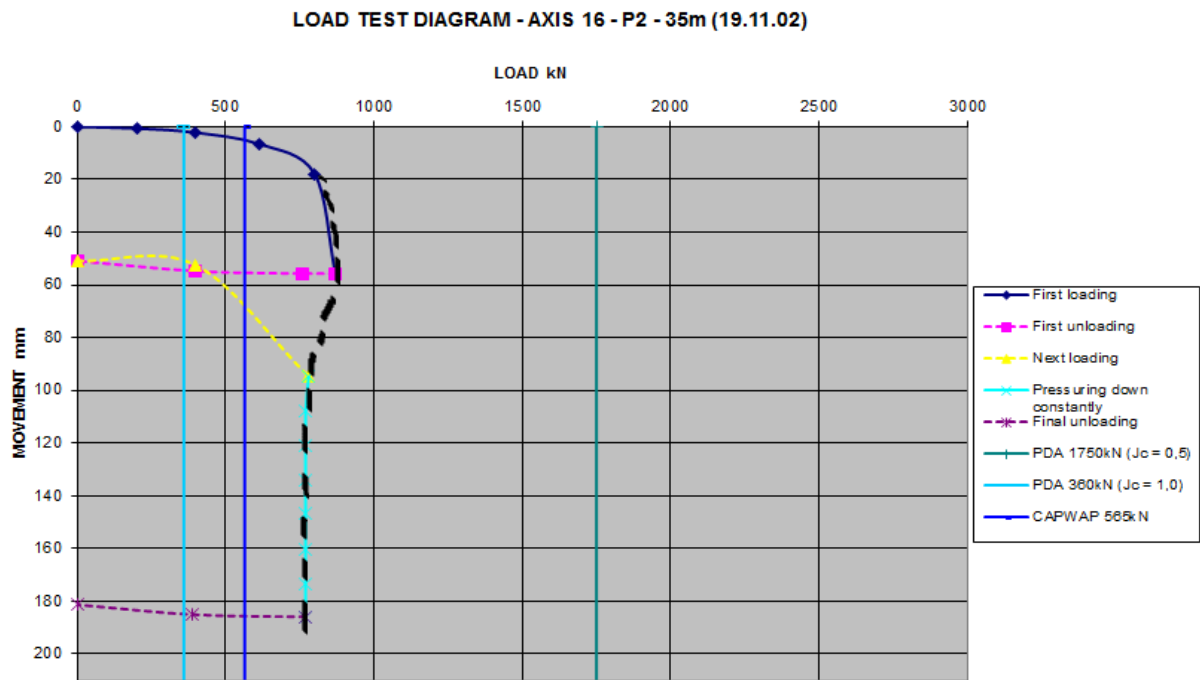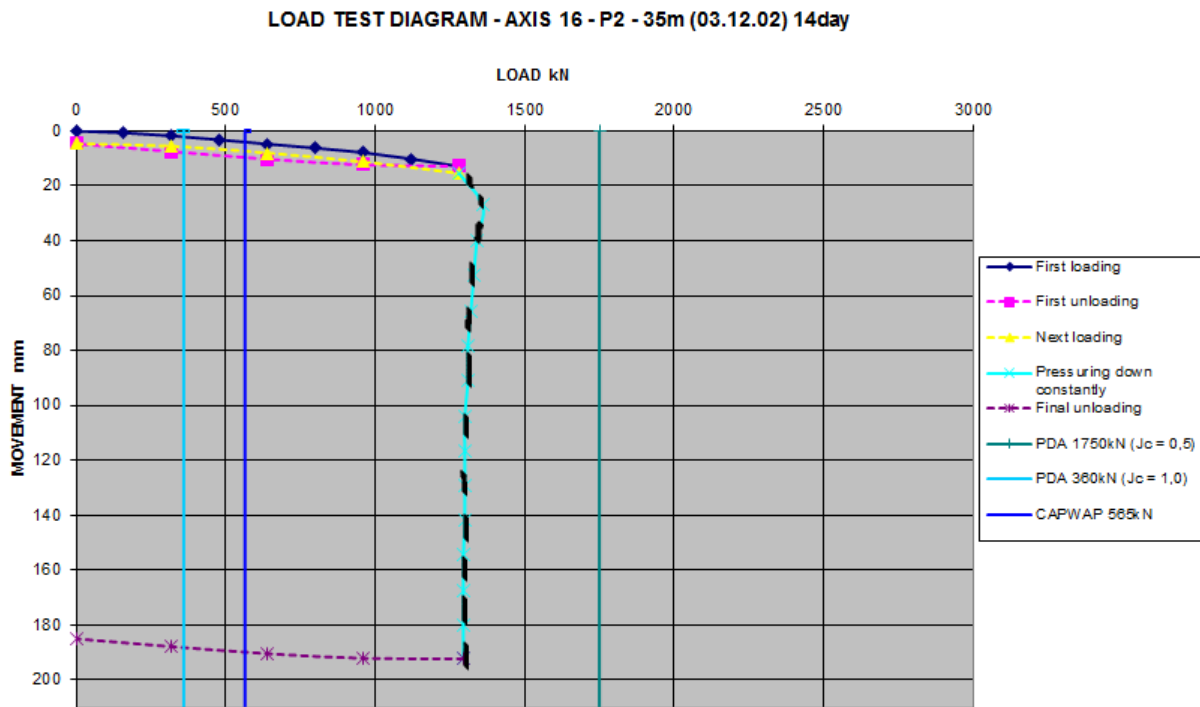

Figure 7.11 Load-movement plot at axis 25 using steel pipe pile of 15m length measured one day after driving

Figure 7.12 Load-movement plot at axis 25 using steel pipe pile of 25m length one day after driving

Figure 7.13 Load-movement plot at axis 25 using steel pipe pile of 25m length measured 14 days after driving
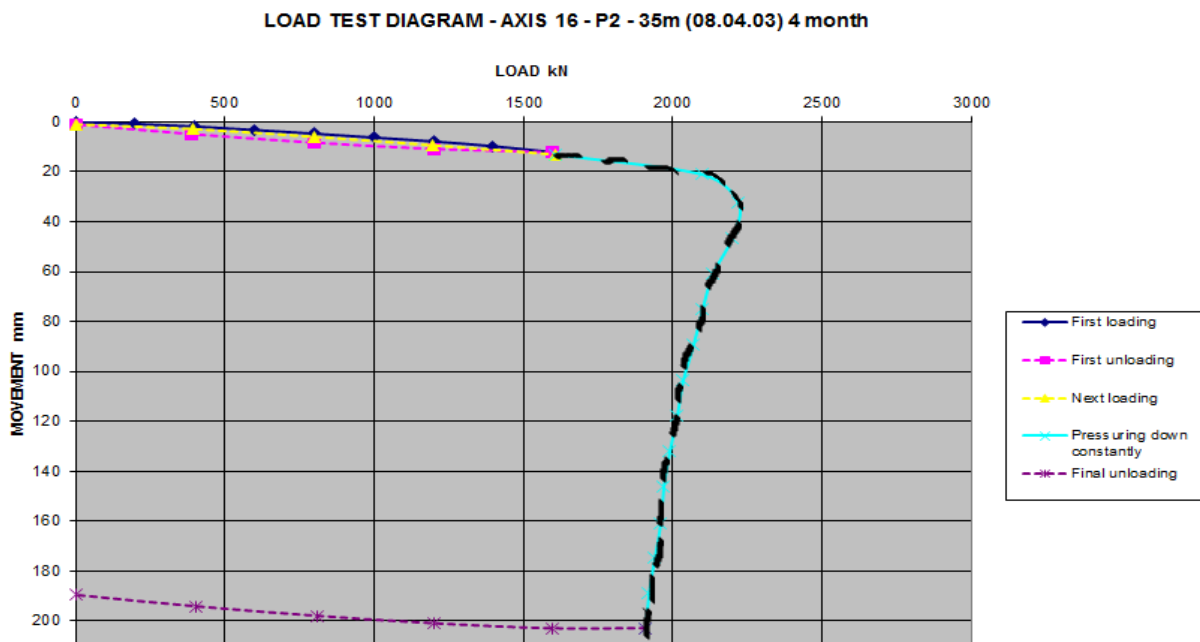
Figure 7.14 Load-movement plot at axis 25 using steel pipe pile of 25m length measured 4 months after driving

Table 7.8 Ultimate pile capacity from the static load test for axis 25P1

Length (m)	Time after driving, or the last load testing	$Q_{u,\,D/10}$ (KN)	$Q_{u,\,90\%}$ (KN)	$Q_{u,\,120}$ (KN)	$0.93Q_{u,\,failure}$ (KN)	$Q_{u,\,chosen}$ (KN)
15	2 Days	1875	2035	2000	1953	1875
25	2 Days	2640	3290	3000	3162	2640
25	14 Days	3300	3660	3500	3488	3300
25	5 Months	3500	3445	3750	3720	3445

7.2.4 Interpretation of the load test at axis 25 P2

In the case of HP pile, the static load tests were performed at depths 15 and 25m from the ground surface. In a similar manner to that of axis 25P1, the static load test at a depth of 15m was performed one day after installation of the pile while at a depth of 25m load tests were performed 1 day, 14 days and 4 months after installation.

The following plots of diagrams were obtained from the static load tests and dynamic analyses (PDA and CAPWAP). The ultimate pile capacity obtained from the static load tests are presented in a tabular form in table 7.9.
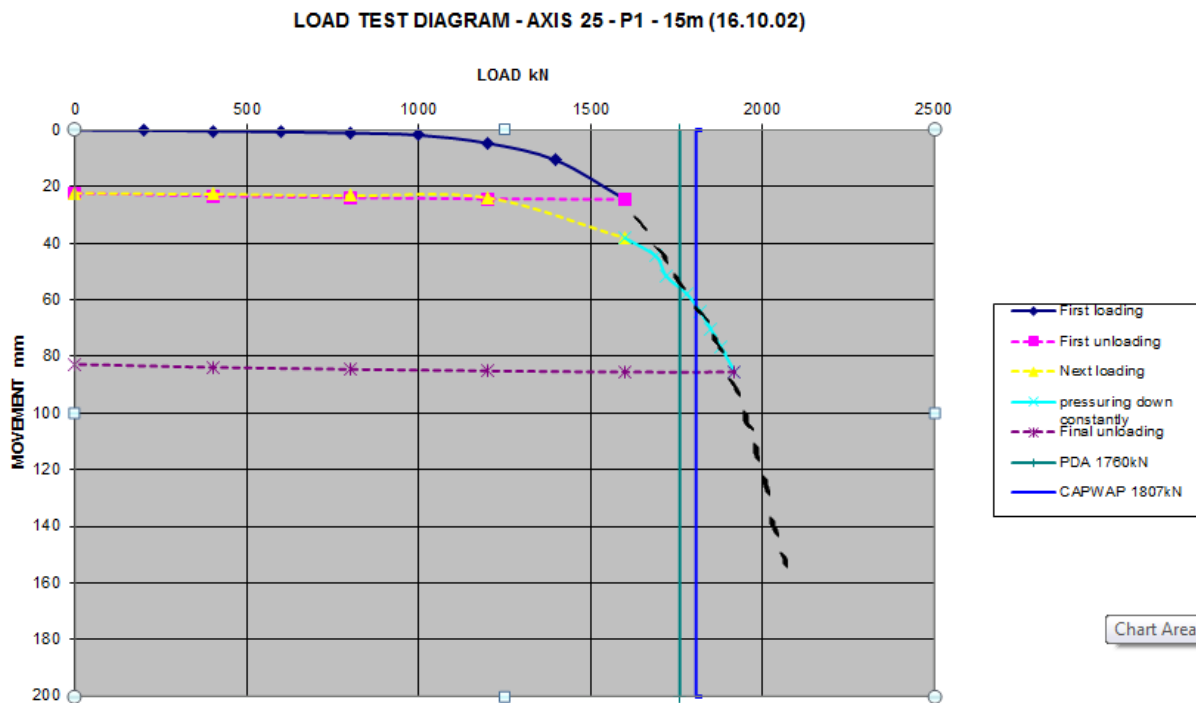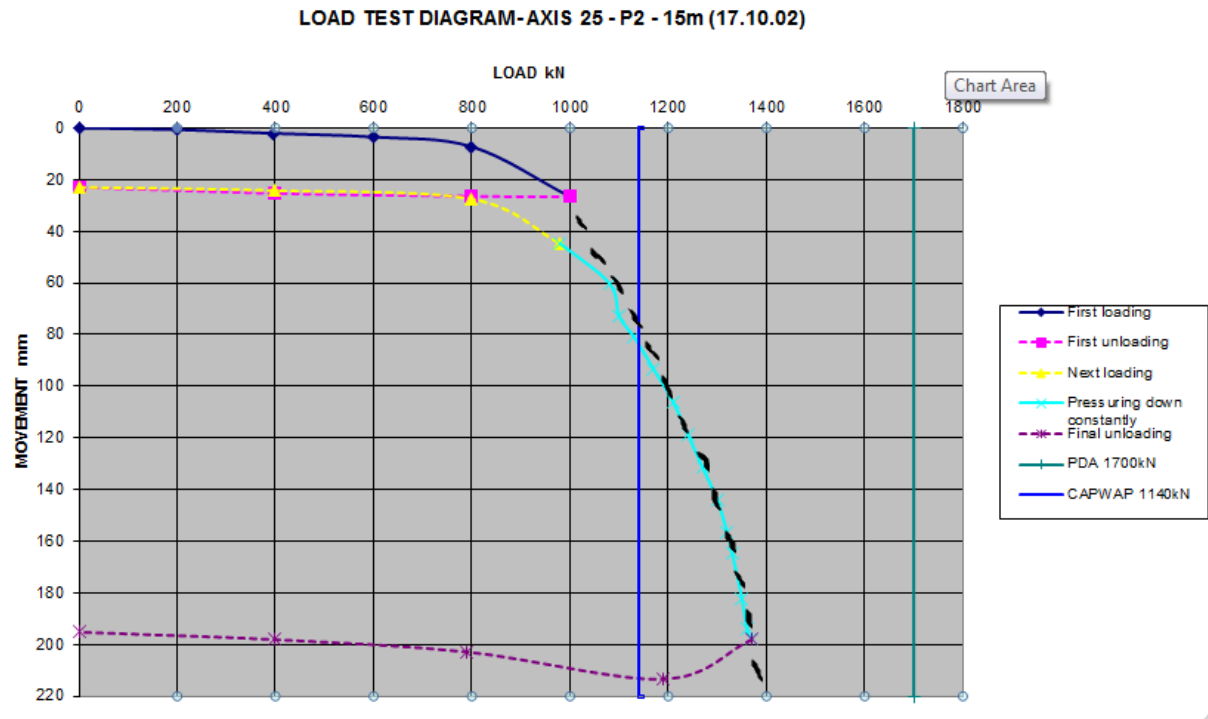
Figure 7.15 Load-movement plot at axis 25 using HP pile of 15m length measured one day after driving
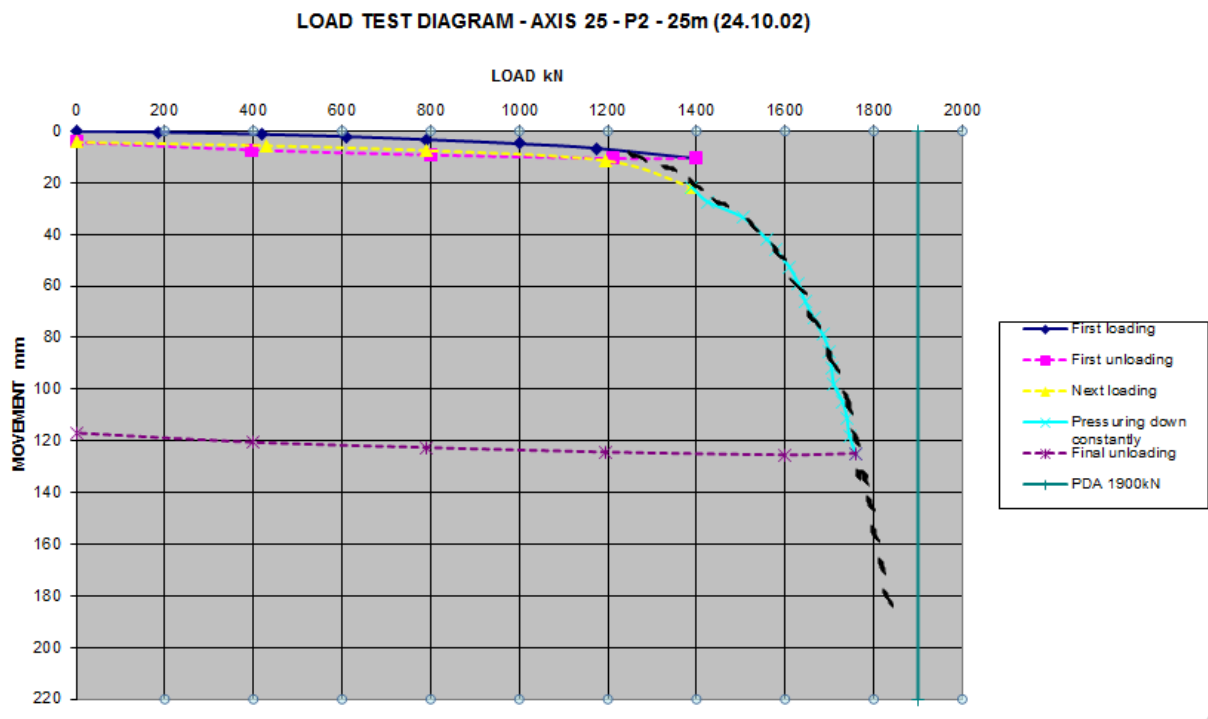
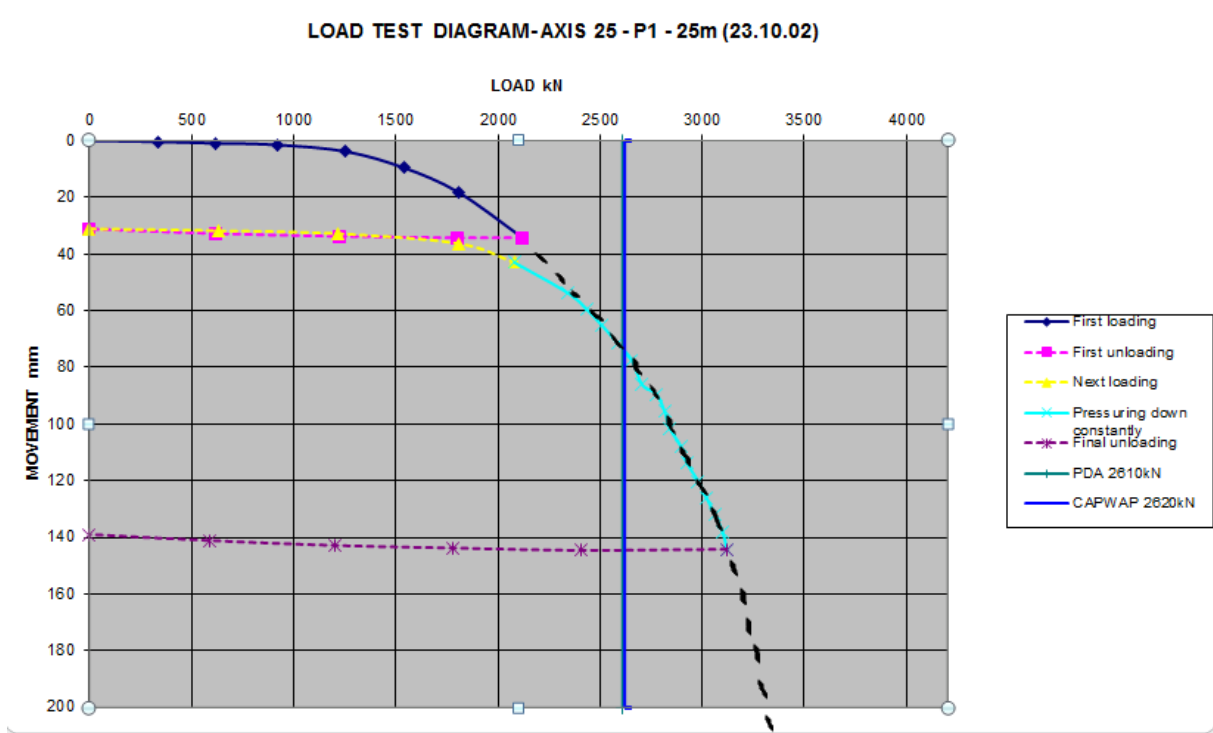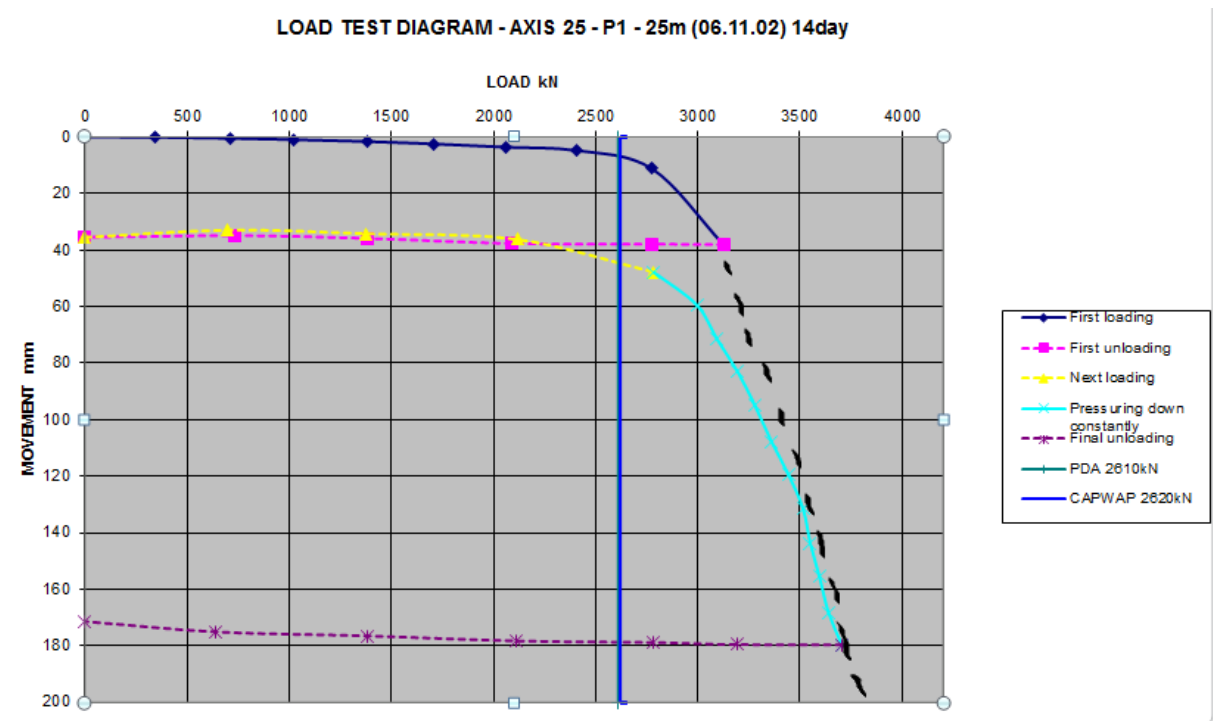*Figure 7.16 Load-movement plot at axis 25 using HP pile of 25m length measured one day after driving*
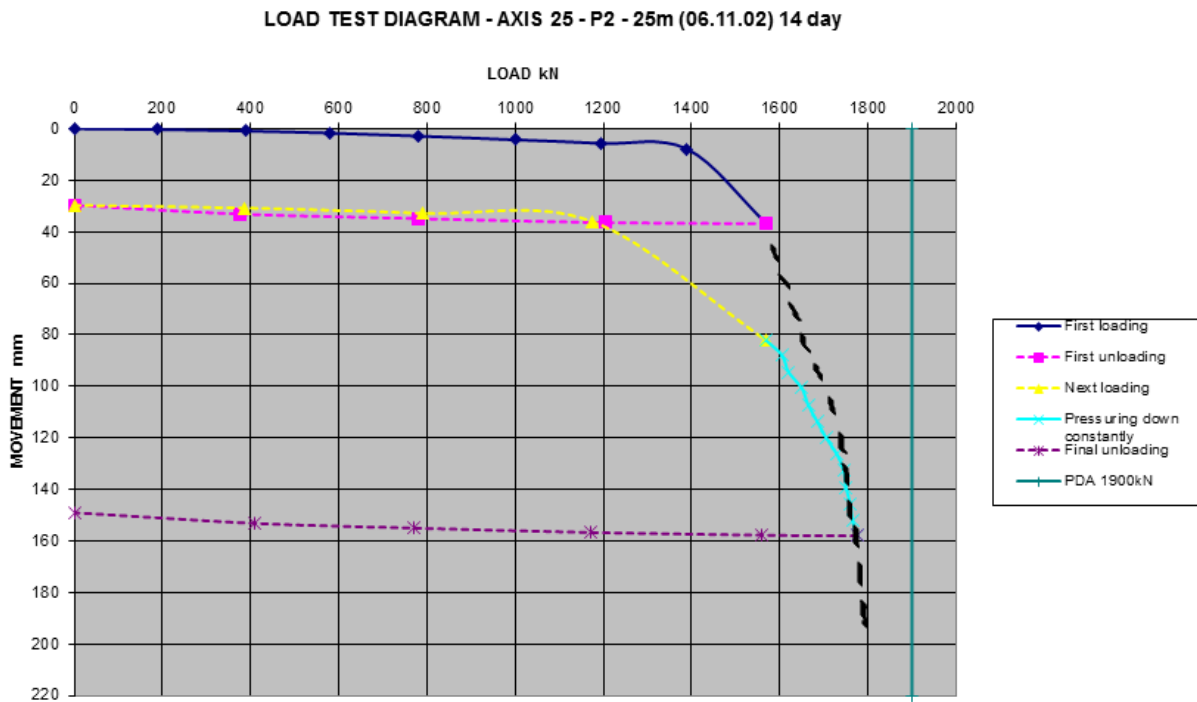
Figure 7.17 Load-movement plot at axis 25 using HP pile of 25m length measured 14 days after driving

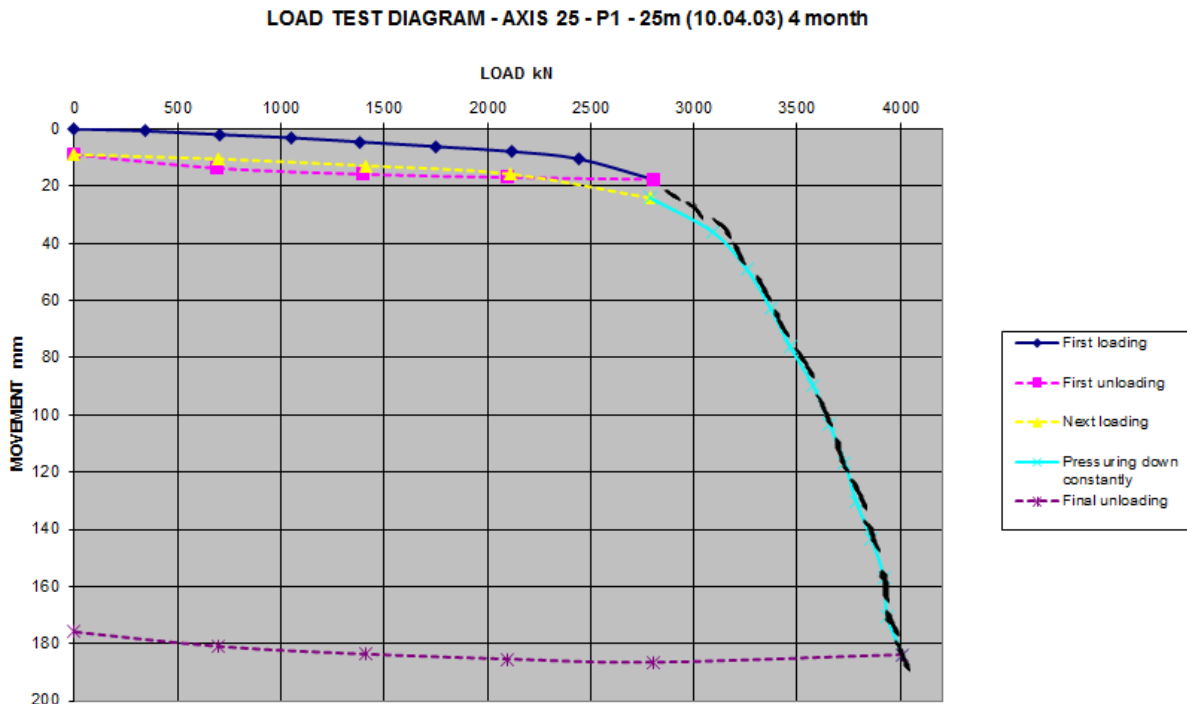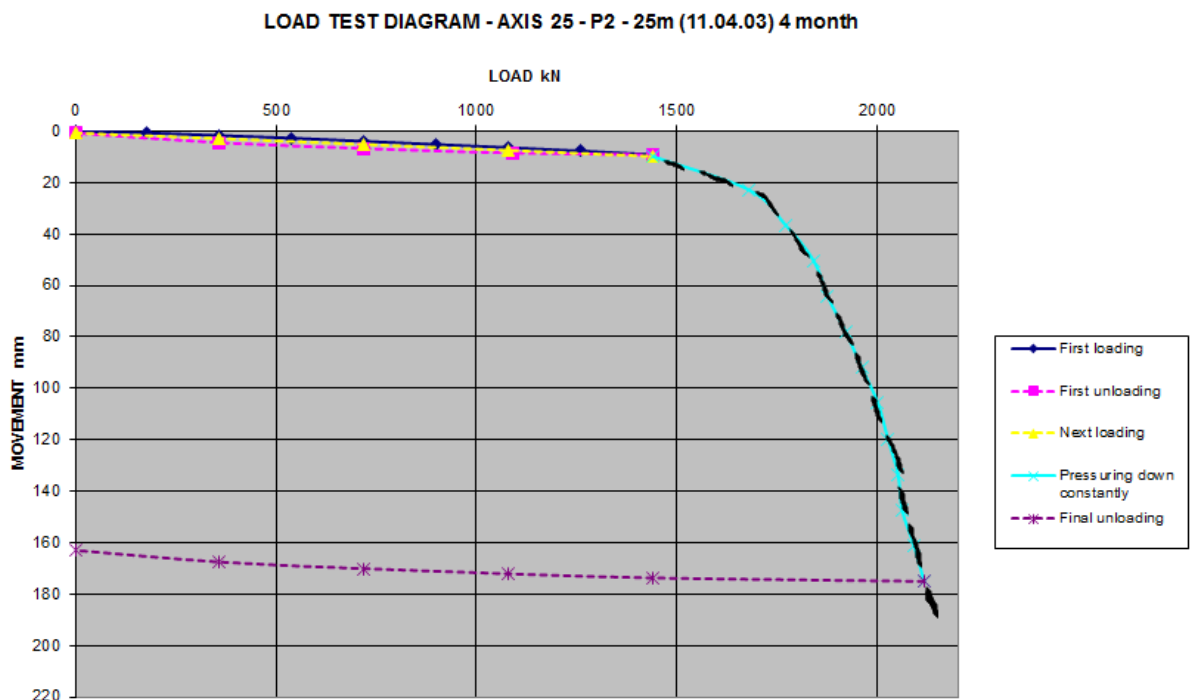*Figure 7.18 Load-movement plot at axis 25 using HP pile of 25m length measured 4 months after driving*

Table 7.9 Ultimate pile capacity from the static load test for axis 25P2

Length (m)	Time after driving, or the last load testing	$Q_{u, D/10}$ (KN)	$Q_{u, D/5}$ (KN)	$Q_{u, 90\%}$ (KN)	$Q_{u, 120}$ (KN)	$0.93 Q_{u, failure}$ (KN)	$Q_{u, chosen}$ (KN)
15	3 Days	1140	1160	1245	1250	1302	1160
25	3 Days	1680	1695	1540	1760	1693	1540
25	13 Days	1640	1650	_	1720	1665	1540
25	5 Months	1885	1890	1800	2040	2000	1800

7.3 Comparison of the ultimate pile bearing capacity from the various empirical and theoretical methods with that of the static load test result

In this section, graphs were used to compare the results obtained using the static loads test with that of empirical and theoretical models. In the next section, i.e. section 7.4, comparisons were also done between the static load test, PDA and CAPWAP results.

7.3.1 Comparison of the various empirical and theoretical methods with the static load test result at axis 16P1

Figure 7.19 Comparison of the various empirical and theoretical methods with the static load test result at axis 16P1

From figure 7.19, we can see that the Norwegian Pile Guideline (2005) fits pretty well with the ultimate pile capacity obtained from the static load test measured 1day after driving in the sand layer and with the ultimate pile capacity obtained from the static load test measured 4 months after driving in the clay layer. The Janbu method overestimates the ultimate pile capacity slightly as compared with the Norwegian Pile Guideline (2005). The NGI-99 method overestimates the ultimate pile capacity at shallow depths specifically, in the sand layer, but fits pretty well with the capacity obtained from the static load test measured 4 months after driving in the clay layer. The API RP 2A LRFD (2007) method overestimates the capacity all way in both sand and clay layers. For instance, the API RP 2A LRFD (2007) overestimates the ultimate pile capacity at a depth of 35m by 92.2%.

From figure 7.19 we can also see that the full capacity at the sand –clay interface overestimate the ultimate pile capacity, so we can see that the punching through effect has a reality.

Generally, the Norwegian Pile Guideline (2005) captures the ultimate pile capacity obtained from the static load test pretty well as compared with the other methods.

7.3.2 Comparison of the various empirical and theoretical methods with the static load test result at axis 16P2
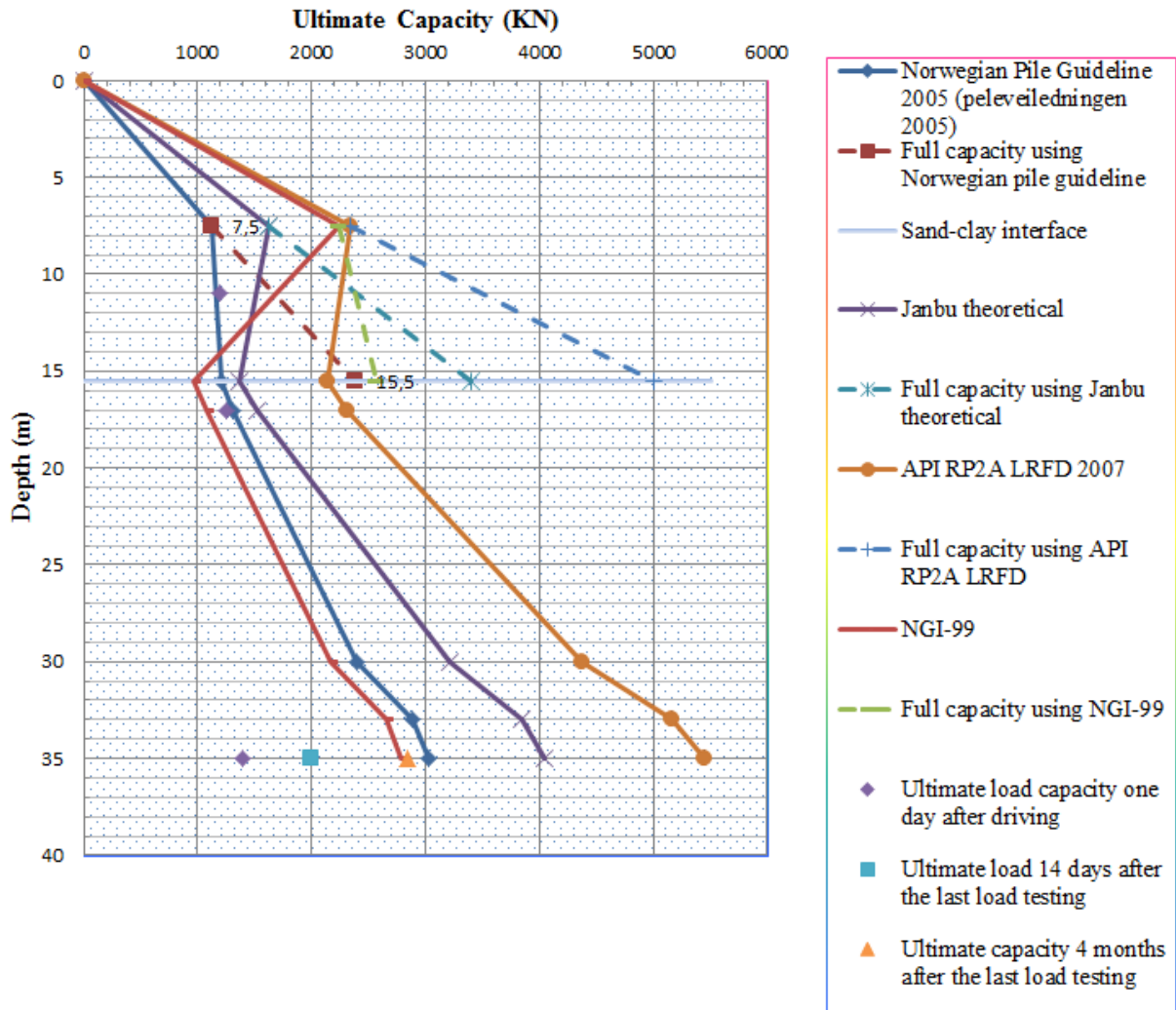

Figure 7.20 Comparison of the various empirical and theoretical methods with the static load test result at axis 16P2

From figure 7.20, we can see that the Norwegian Pile Guideline (2005) fits pretty well with the ultimate pile capacity obtained from the static load test measured 1 day after driving at shallow depths (sand layer) and with the ultimate pile capacity obtained from the static load test measured 4 months after driving in the clay layer. The Janbu and the API RP 2A LRFD

(2007) overestimates the ultimate pile capacity. For instance, the API RP 2A LRFD (2007) and Janbu overestimates the ultimate pile capacity at a depth of 35m by 34% and 24% respectively.

Generally, the Norwegian Pile Guideline (2005) captures the ultimate pile capacity obtained from the static load test pretty well as compared with the other methods.

7.3.3 Comparison of the various empirical and theoretical methods with the static load test result at axis 25P1

Figure 7.21 Comparison of the various empirical and theoretical methods with the static load test result at axis 25P1

From figure 7.21, we can observe that the Norwegian Pile Guideline (2005) captures pretty well the ultimate pile capacity obtained from the static load test measured 2 days after driving at shallow depth (at 15m) and the ultimate pile capacity obtained from the static load test measured 4 months after driving at deeper depth (at 25m). The Janbu method overestimates the ultimate pile capacity slightly. The NGI-99 and API RP 2A LRFD (2007) overestimates the ultimate pile capacity by considerable amount. For instance, at a depth of 25m the NGI-99 and API RP 2A LRFD (2007) overestimates the ultimate capacity by 33% and 145% respectively.

Generally, the Norwegian Pile Guideline (2005) captures the ultimate pile capacity obtained from the static load test pretty well as compared with the other methods.

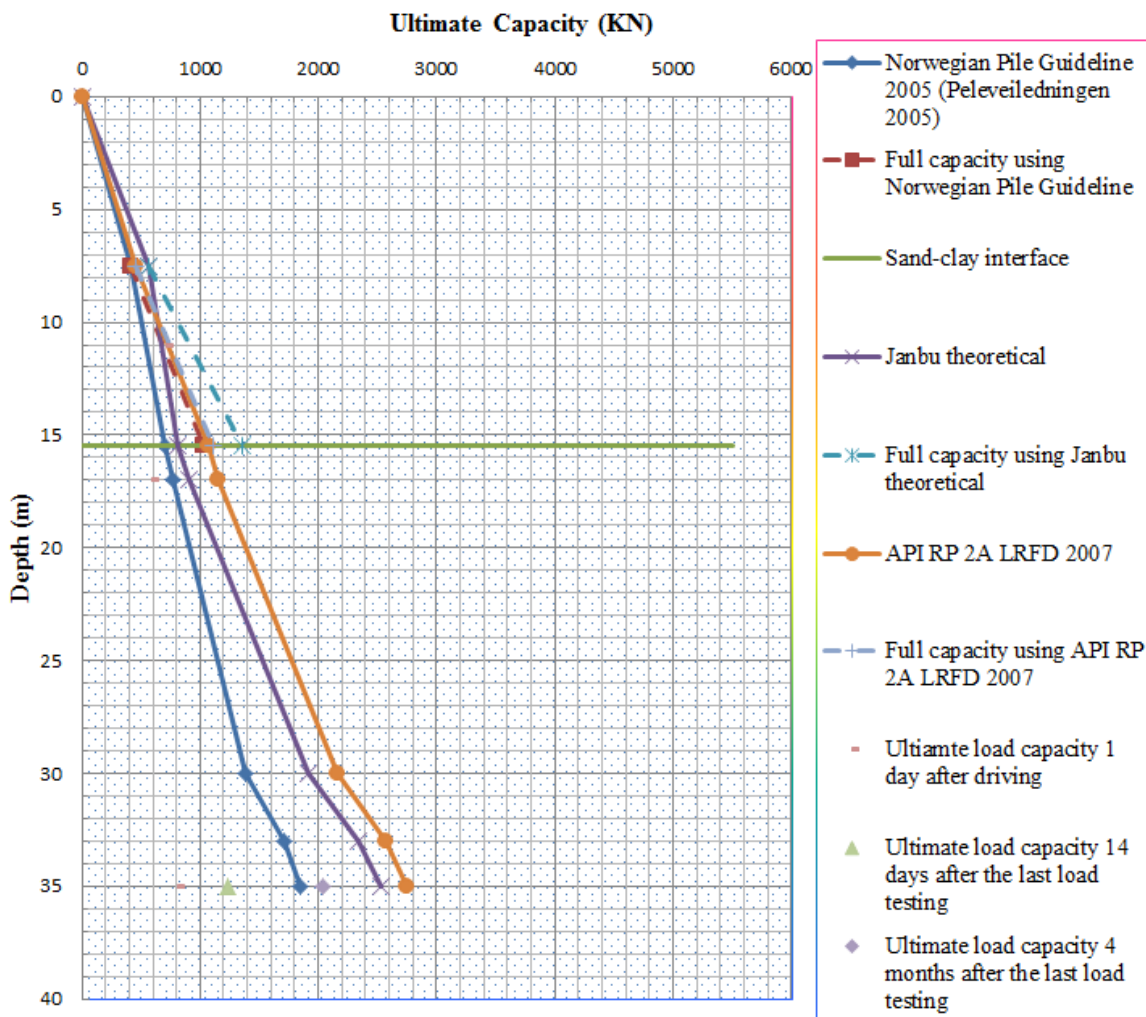### 7.4.4 Comparison of the various empirical and theoretical methods with the static load test result at axis 25P2
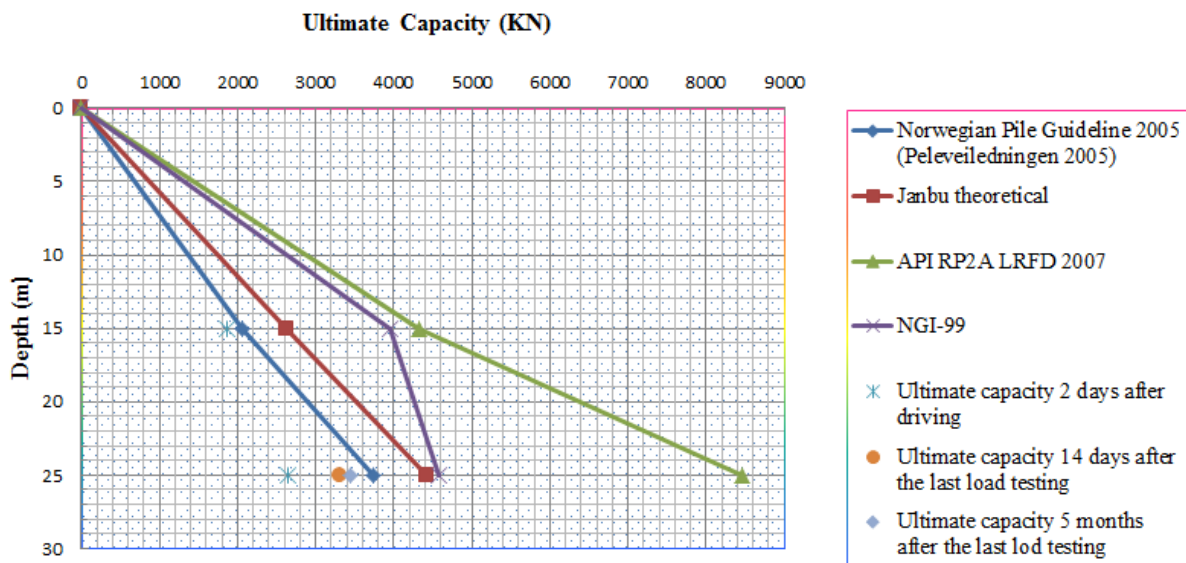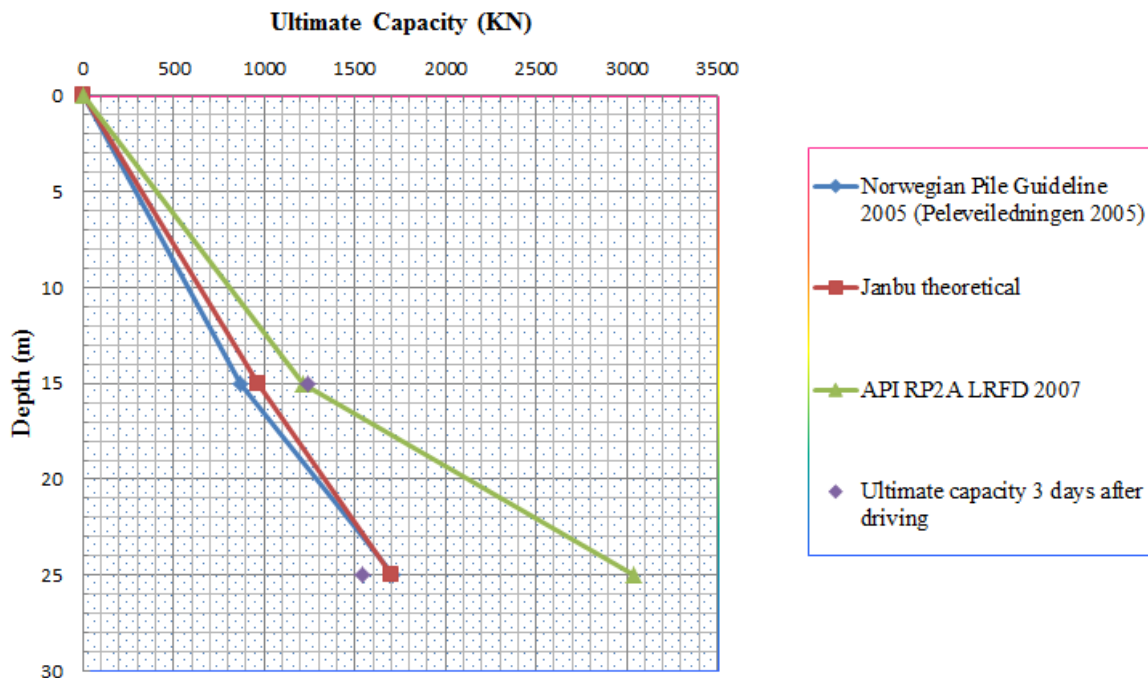

Figure 7.22 Comparison of the various empirical and theoretical methods with the static load test result at axis 25P2

From figure 7.22, we can observe that both the Norwegian Pile Guideline (2005) and Janbu methods capture the ultimate pile capacity obtained from the static load test measured 3 days after driving at deeper depth (at depth 25m) and both underestimate the ultimate pile capacity slightly at shallow depth (at depth 15m). The API RP 2A LRFD (2007) captures pretty well ultimate pile capacity obtained from the static load test measured 3 days after driving at shallow depth (at 15m), but over estimates at deeper depths. For instance at a depth of 25m the API RP 2A LRFD (2007) overestimates the ultimate load by 69%.

Generally, the Norwegian Pile Guideline (2005) and Janbu methods capture the ultimate pile capacity obtained from the static load test pretty well as compared with the API RP 2A LRFD (2007).

7.4 Comparison of ultimate pile bearing capacity determined by PDA, CAPWAP and static load test

In this section, tables were used to compare the results obtained from the static load test with that of the PDA and CAPWAP. The PDA and CAPWAP were measured with the same length of pile and the same date and static load tests were measured at most 2 days difference and their lengths vary at most 2m as compared with the PDA or CAPWAP. Therefore, these data are suitable for us to make a comparison among them.

Axis 16 – Pile P1 steel pipe pile

Table 7.10 Comparison of the PDA, CAPWAP and static load test results for pile length 9-11m for axis 16P1

Condition	PDA capacity	CAPWAP Capacity	Static load test capacity
Pile length (m)	9	9	11
Time of measurement	11.11.2002	11.11.2002	12.11.2002
Ultimate capacity (KN)	1320	1310	1200
Tip resistance, CAPWAP		753 (57%)	

Table 7.10 presents comparison of the capacity obtained from the PDA, CAPWAP and static load test for axis 16 using steel pipe pile. The PDA, CAPWAP and static load test were measured at a depth of 9m, 9m and 11m respectively. From this table we can clearly see that there is pretty good agreement between the three measured values.

Table 7.11 Comparison of the PDA, CAPWAP and static load test results for pile length 16.1-17m for axis 16P1

Condition	PDA capacity	CAPWAP Capacity	Static load test capacity
Pile length (m)	16.1	16.1	17
Time of measurement	13.11.2002	13.11.2002	14.11.2002
Ultimate capacity (KN)	1780	1380	1255
Tip resistance, CAPWAP		992 (72%)	

Table 7.11 presents comparison of the capacity obtained from the PDA, CAPWAP and static load test for axis 16 using steel pipe pile. The PDA, CAPWAP and static load test were measured at a depth of 16.1m, 16.1m and 17m respectively. From this table we can clearly see that there is pretty good agreement between the CAPWAP and static load test capacity and the PDA capacity estimates a little higher.

Table 7.12 Comparison of the PDA, CAPWAP and static load test results for pile length 33-35m for axis 16P1

Condition	PDA capacity	CAPWAP Capacity	Static load test capacity
Pile length (m)	33	33	35
Time of measurement	18.11.2002	18.11.2002	19.11.2002
Ultimate capacity (KN)	2060	1956	1400
Tip resistance, CAPWAP		292 (15%)	

Table 7.12 presents comparison of the capacity obtained from the PDA, CAPWAP and static load test for axis 16 using steel pipe pile. The PDA, CAPWAP, and static load test were measured at a depth of 33m, 33m and 35m respectively. From this table we can observe that the PDA and CAPWAP capacity estimates a higher capacity than the static load test result.

Axis 16 – Pile P2 steel HP pile

Table 7.13 Comparison of the PDA, CAPWAP and static load test results for pile length 9-11m for axis 16P2

Condition	PDA capacity	CAPWAP Capacity	Static load test capacity
Pile length (m)	9	9	11
Time of measurement	11.11.2002	11.11.2002	12.11.2002
Ultimate capacity (KN)	610	541	710
Tip resistance, CAPWAP		153 (28%)	

Table 7.13 presents comparison of the capacity obtained from the PDA, CAPWAP and static load test for axis 16 using HP pile. The PDA, CAPWAP and static load test were measured at a depth of 9m, 9m and 11m respectively. From this table we can observe that there is a pretty good agreement between the three measured values.

Table 7.14 Comparison of the PDA, CAPWAP and static load test results for pile length 15-17m for axis 16P2

Condition	PDA capacity	CAPWAP Capacity	Static load test capacity
Pile length (m)	15	15	17
Time of measurement	13.11.2002	13.11.2002	14.11.2002
Ultimate capacity (KN)	600	307	590
Tip resistance, CAPWAP		85 (28%)	

Table 7.14 presents comparison of the capacity obtained from the PDA, CAPWAP and static load test for axis 16 using HP pile. The PDA, CAPWAP and static load test were measured at a depth of 15m, 15m and 17m respectively. From this table we can observe that the PDA and the static load test result estimate pretty the same. CAPWAP capacity is a little lower.

Table 7.15 Comparison of the PDA, CAPWAP and static load test results for pile length 34.3-35m for axis 16P2

Condition	PDA capacity	CAPWAP Capacity	Static load test capacity
Pile length (m)	34.3	34.3	35
Time of measurement	18.11.2002	18.11.2002	19.11.2002
Ultimate capacity (KN)	360	565	814
Tip resistance, CAPWAP		105 (19%)	

Table 7.15 presents comparison of the capacity obtained from the PDA, CAPWAP and static load test for axis 16 using HP pile. The PDA, CAPWAP and static load test were measured at a depth of 34.3m, 34.3m and 35m respectively. From this table we can observe that the CAPWAP capacity is pretty close to the static load test capacity as compared with the PDA capacity.

Axis 25 – Pile P1 steel pipe pile

Table 7.16 Comparison of the PDA, CAPWAP and static load test results for pile length 15m for axis 25P1

Condition	PDA capacity	CAPWAP Capacity	Static load test capacity
Pile length (m)	15	15	15
Time of measurement	14.10.2002	14.10.2002	16.10.2002
Ultimate capacity (KN)	1760	1807	1875
Tip resistance, CAPWAP		1091 (60%)	

Table 7.16 presents comparison of the capacity obtained from the PDA, CAPWAP and static load test for axis 25 using steel pipe pile. The PDA, CAPWAP and static load test were measured at a depth of 15m. From this table we can observe that there is pretty good agreement between the three values.

Table 7.17 Comparison of the PDA, CAPWAP and static load test results for pile length 23-25m for axis 25P1

Condition	PDA capacity	CAPWAP Capacity	Static load test capacity
Pile length (m)	23	23	25
Time of measurement	21.10.2002	21.10.2002	23.10.2002
Ultimate capacity (KN)	2610	2620	2640
Tip resistance, CAPWAP		244 (9%)	

Table 7.17 presents comparison of the capacity obtained from the PDA, CAPWAP and static load test for axis 25 using steel pipe pile. The PDA, CAPWAP and static load test were measured at a depth of 23m, 23m and 25m respectively. From this table we can observe that there is pretty good agreement between the three values.

Axis 25 – Pile P2 steel HP pile

Table 7.18 Comparison of the PDA, CAPWAP and static load test results for pile length 13.5-15m for axis 25P2

Condition	PDA capacity	CAPWAP Capacity	Static load test capacity
Pile length (m)	13.5	13.5	15
Time of measurement	14.10.2002	14.10.2002	17.10.2002
Ultimate capacity (KN)	1700	1140	1245
Tip resistance, CAPWAP		785 (69%)	

Table 7.18 presents comparison of the capacity obtained from the PDA, CAPWAP and static load test for axis 25 using HP pile. The PDA, CAPWAP and static load test were measured at a depth of 13.5m, 13.5m and 15m respectively. From this table we can observe that the CAPWAP capacity is pretty close to the static load test capacity as compared with the PDA capacity.

Table 7.19 Comparison of the PDA, CAPWAP and static load test results for pile length 22-25m for axis 25P2

Condition	PDA capacity	CAPWAP Capacity	Static load test capacity
Pile length (m)	22	22	25
Time of measurement	21.10.2002	21.10.2002	24.10.2002
Ultimate capacity (KN)	1900	-	1540
Tip resistance, CAPWAP		-	

Table 7.19 presents comparison of the capacity obtained from the PDA, CAPWAP and static load test for axis 25 using HP pile. The PDA, CAPWAP and static load test were measured at a depth of 22m, 22m and 25m respectively. From this table we can observe that the PDA capacity is a little higher than the static load test capacity and there is no measured data for the CAPWAP capacity.

7.5 Increase in pile bearing capacity with time

In this section, I tried to show the increase in capacity due to the two predominant causes namely, pore- pressure dissipation and aging of soil after installation of pile. Both the results from the static load test and NGI's effect of time on pile capacity prediction model were examined. For comparison the results obtained by the theoretical and empirical methods, which computed above were also put together. In this case, only axis 16 is considered for both the steel pipe pile and HP pile case. Consequently, the results of the analysis are shown in Figure 7.23 and Figure 7.24.
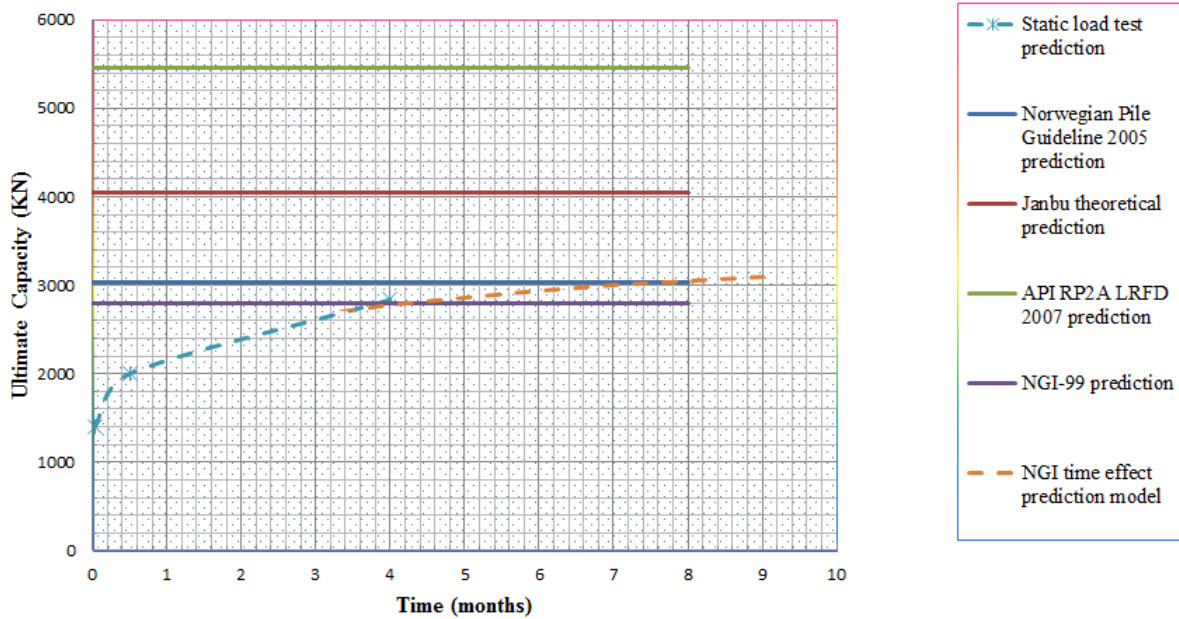
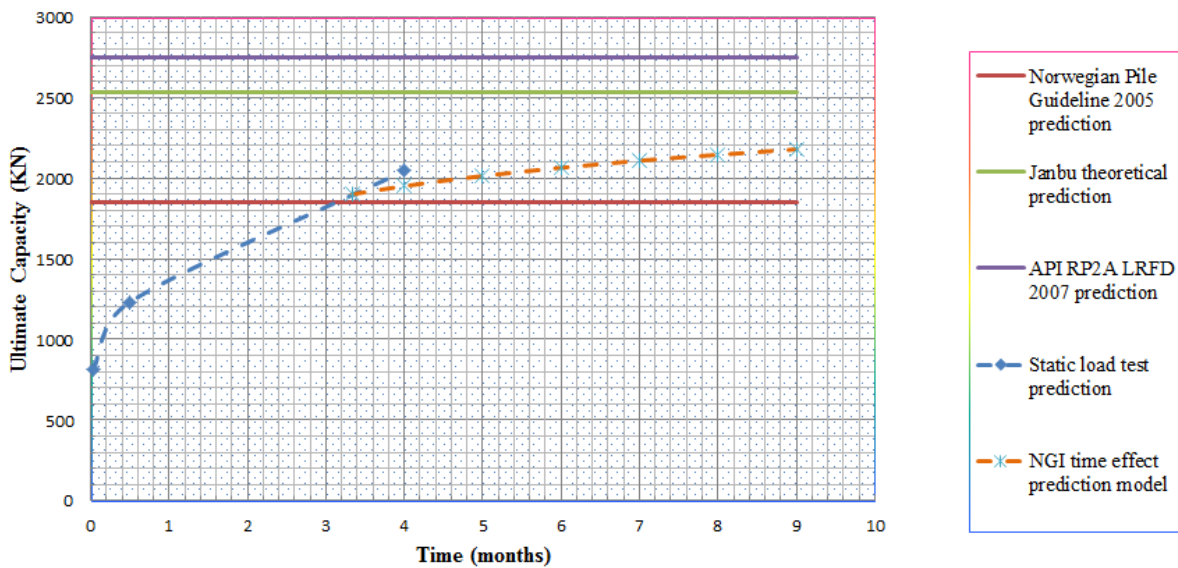*Figure 7.23 Increase in pile bearing capacity with time for axis 16P1*

Figure 7.24 Increase in pile bearing capacity with time for axis 16P2

From Figure 7.23 and Figure 7.24, we can observe that the static load test result and NGI's time effect prediction model shows an increase in pile capacity with time, on the other hand, those we compute by theoretical or empirical formulas do not really show us the development of capacity with time. We can only calculate either the short term capacity or the long term capacity. It is known that, it takes a very long time (several years) to reach to the theoretical long term capacity in clay.

7.6 Back calculation of Janbu theoretical parameters based on the static load test results

In this section, back calculation of Janbu's theoretical dimensionless bearing capacity factors S_v and N_q was done based on the static load test results.

For the Steel pipe pile (25P1)

$Q_u = 2640KN$ (Ultimate capacity 2 days after installation taken from the static load test)

Assuming CAPWAP percentage 9%

$Q_p = \frac{9}{100}(2640) = 238KN$

$Q_s = 2640 - 238 = 2402KN$

$S_v = \frac{Q_s}{(p'+a)A_p} = 0.33$

$N_q = \frac{Q_p}{(p'+a)A_p} + 1 = 3.2$

$Q_u = 3445KN$ (Ultimate capacity 5 months after installation taken from the static load test)

By looking at the load-displacement graph we can deduce that

$Q_s = 2500KN$

$Q_p = 3445 - 2500 = 945KN$ (27%)

$S_v = \frac{Q_s}{(p'+a)A_p} = 0.35$

$N_q = \frac{Q_p}{(p'+a)A_p} + 1 = 9.8$

Table 7.20 Back calculated s_v and N_q values

Time after installation	s_v	N_q	$Q_s(KN)$	$Q_p(KN)$
2 days	0.33	3.2	2402	238
5 months	0.35	9.8	2500	945

❖ From the above analyses we can see that both S_v and N_q build-up with time.

8 CONCLUSIONS AND FUTURE WORK

Based on the findings of this thesis the following can be concluded.

➢ In both axis 16 and 25, the Norwegian Pile Guideline (Peleveiledningen 2005) better approximates the pile capacity compared with the other empirical and theoretical methods mentioned in the project.

➢ In a homogeneous clay layer, NGI-99 method can give quite reliable pile capacity.

➢ The API RP 2A LRFD (2007) overestimates the pile capacity for piles installed in low plasticity clays.

➢ The API RP 2A LRFD (2007) overestimates the N_q value at higher φ subsequently will deliver higher pile capacity.

➢ NGI-99 method for sand uses either of the following parameter as an input CPT, SPT, relative density or friction angle. It can be applied especially in offshore environments where there is CPT data. However, an issue in here conversion/correlation is a controversial issue in the field of geotechnical engineering, this leads by itself some sort of uncertainty.

➢ Design of piles remained controversial over the years due to their empirical nature until recently reliable theoretical method is non-existent.

➢ The CAPWAP capacity generally predicts the pile capacity better as compared with the PDA.

➢ Static load test is the most reliable method of assessing the capacity, but as load tests are not suitable to perform on offshore environments and the expense when performed on onshore, the reliability of the method used is very important.

➢ Capacities of pile increases with time. It will be nice if future designers incorporate this effect into the pile capacity calculation.

➢ CPT based methods for sand like the NGI-99 method believed to deliver closer prediction of pile load tests, but should be applied by a qualified engineer who is experienced in the interpretation of CPT and understand the limitations and reliability of this method.

Future work

My study was limited to one specific site and it will be a lot better if the various empirical and theoretical methods were applied in different sites in different soil conditions and see the results they deliver as compared with the static load test, so future researchers can expand the work and look at this problem.

REFERENCES

[1] Tomlinson, M.J. (1998). Foundation design and construction, 6th edition Pitman, London.

[2] Bowles, J.E. (1997). Foundation analysis and design, 5th edition, McGraw Hill International editions.

[3] American petroleum Institute. (1984). Recommended practice for planning, designing and constructing fixed offshore platforms. Code RP 2A, 15 Edition, Dallas, Texas.

[4] P.M. Aas. K. Karlsrud and C.J.F.Clausen. Bearing capacity of driven piles in clay, the NGI approach. Proceedings of the international symposium on Frontiers in offshore Geotechnics (IS-FOG2005), 19-21 Sept2005, Perth, WA, Australia.

[5] P.M. Aas. K. Karlsrud and C.J.F.Clausen. Bearing capacity of driven piles in sand, the NGI approach. Proceedings of the international symposium on Frontiers in offshore Geotechnics (IS-FOG2005), 19-21 Sept2005, Perth, WA, Australia.

[6] Lacasse and Nadim (1996). Model uncertainity in pile axial capacity predictions Offshore Technology Conference, Houston, May 1996, paper OCT 7996.

[7] American Petroleum Institute 1993. Recommended practice for planning, designing and constructing fixed offshore platforms –Working Stress Design, 20th edition API RP 2A-WSD, American petroleum Institute, Washington D.C., pp. 59-61.

[8] Jardine R.J.& Chow F.C. 1996. New Design Methods for offshore Piles Jardine R.J. & Chow F.C. 1996. New Design Methods for Offshore Piles. *Marine Technology Directorate Ltd., Publication MTD 96/103*, London 1996.

[9] Fugro Engineers B.V.2004. Axial Pile Capacity Design Method for Offshore Driven Piles in Sand. Report P1003 presented to the American petroleum Institute, issue 3, 5August 2004.

[10] Chow F.C., Jardine, R.J., Brucy F. & Nauroy J.F. 1998. Effects of Time on Capacity of Pipe Piles in Dense Marine Sand. *ASCE, JGGE, Vol. 124, No. 3, March 1998.*

[11] Lehane B.M. & Gavin K. 2004. (Discussion). Determination of bearing capacity of open-ended piles in sand. *J. Geotech. & Geoenv. Engrg. ASCE,* 130 (6): 656-658.

[12] Norwegian Pile Guideline 2005. (Peleveiledningen 2005)

[13] Norsk Geoteknisk Forening/NIF. Pelefundamentering i praksis. 23-25 April 2001.

[14] William Powrie Soil. Mechanics concepts and applications, 2nd edition.

[15] Shamsher Prakash Hari D. Sharma (1990). Pile foundations in engineering practice.

[16] P. Doherty. K. Gavin. The Shaft Capacity of Displacement Piles in Clay. Journal of Geotechnical and Geoenvironmental Engineering, ASCE: 389-410

[17] Randolph, M.F. (2003) 'Science and empiricism in pile foundation design' Rankine Lecture, Geotechnique 53, No.10, pp847-875.

[18] Tomlinson, M.J. (1970). The adhesion of piles in stiff clay. Construction Industry Research and Information association Research report No. 26. London:CIRIA.

[19] Vijayvergiya, V. N. & Focht, J. A. (1972). A new way to predict the capacity of piles in clay. Proc. 4th Offshore Technology Conf. Houston 2, 865-874.

[20] Jardine, R.J., and Chow, F.C., Overy, R., and Standing, J. (2005) "ICP design methods for driven piles in sands and clays, Thomas Telford, London.

[21] White, D.J., and Lehane, B.M. (2004). "Friction fatigue on displacement piles in sand." Geotechnique, 54(10), 645-658.

[22] Randolph, M.F., Dolwin, J., and Beck, R. 1994. Design of driven piles in sand. Geotechnique, 44(3): 427-448.

[23] Kyuho Paik and Rodrigo Salgado, M.ASCE. Determination of bearing capacity of open-ended piles in sand. Jornal of geotechnical and geoenvironmental. Vol.129, No. 1, January 2003. 46p.

[24] Kjell Karlsrud (2012). Prediction of load-displacement behavior and capacity of axially loaded piles in clay based on analyses and interpretation of pile load tests. Ph.D. Thesis. Norwegian University of Science and Technology.

[25] Fellenius, B.H., 2011. "Basics of foundation design, a text book." Revised Electronic Edition, [www.Fellenius.net], 374p.

[26] American Petroleum institute (2000-2007). Recommended practice for planning, designing, and constructing fixed offshore platforms-working stress design. API RP 2A-WSD 21st ed. 2000, including Errata and Supplement Nos. 1-3, 2002-2007.

APPENDIX A

Pile capacity analyses using the various empirical and theoretical methods for axis 16

1) Axis 16(steel pipe pile) Norwegian Pile Guideline (2005)

a) Pile capacity at a depth of 7.5m below the surface

$$Q_s{}^{sand} = \beta.p_0'.A_s = 0.3\left(\frac{0KPa+50.4KPa}{2}*2.8m + \frac{50.4KPa+88KPa}{2}*4.7m\right)*2.513m$$

$$= 328KN$$

$$Q_p{}^{sand} = N_q p' A_p = 18*88KPa*0.5m^2 = 792KN$$

$$Q_{u(7.5m)} = Q_s{}^{sand} + Q_p{}^{sand} = 328KN + 792KN = 1120KN$$

b) Pile capacity at a depth of 11m below the surface

Considering the full capacity in sand we will get

$$Q_s{}^{sand} = \beta.p_0'.A_s = 0.32\left(\frac{0KPa+50.4KPa}{2}*2.8m + \frac{50.4KPa+116KPa}{2}*8.2m\right)*2.513m$$

$$= 605KN$$

$$Q_p{}^{sand} = N_q p' A_p = 18*116KPa*0.5m^2 = 1044KN$$

$$Q_{u(11m)} = Q_s{}^{sand} + Q_p{}^{sand} = 605KN + 1044KN = 1649KN$$

c) Pile capacity at a depth of 15.5m below the surface

$$Q_s{}^{sand} = \beta.p_0'.A_s = 0.3\left(\frac{0KPa+50.4KPa}{2}*2.8m + \frac{50.4KPa+152KPa}{2}*12.7m\right)*2.513m$$

$$= 1022KN$$

$$Q_p{}^{clay} = 9S_{up}A_p = 9*40KPa*0.5m^2 = 180KN$$

$$Q_{u(15.5m)} = Q_s{}^{sand} + Q_p{}^{clay} = 1022KN + 180KN = 1202KN$$

Considering full capacity in sand we will get

$$Q_p{}^{sand} = N_q p' A_p = 18*152KPa*0.5m^2 = 1368KN$$

$$Q_{u(15.5m)} = Q_s{}^{sand} + Q_p{}^{sand} = 1022KN + 1368KN = 2390KN$$

d) Pile capacity at a depth of 17m below the surface

$$Q_s{}^{sand+clay} = 1022KN + (\alpha S_u A_s) = 1022KN + (0.62 * 41KPa * 2.513m * 1.5m)$$

$$= 1118KN$$

$$Q_p{}^{clay} = 9S_{up}A_p = 9 * 43KPa * 0.5m^2 = 194KN$$

$$Q_{u(17m)} = Q_s{}^{sand+clay} + Q_p{}^{clay} = 1118KN + 194KN = 1312KN$$

e) Pile capacity at a depth of 30m below the surface

$$Q_s{}^{sand+clay} = 1022KN + (\alpha S_u A_s) = 1022KN + (0.62 * 40KPa * 2.513m * 14.5m)$$

$$= 1926KN$$

$$Q_p{}^{clay} = 9S_{up}A_p = 9 * 105KPa * 0.5m^2 = 473KN$$

$$Q_{u(30m)} = Q_s{}^{sand+clay} + Q_p{}^{clay} = 1926KN + 473KN = 2399KN$$

f) Pile capacity at a depth of 33m below the surface

$$Q_s{}^{sand+clay} = 1926KN + (\alpha S_u A_s) = 1926KN + (0.62 * 105KPa * 2.513m * 3m)$$

$$= 2417KN$$

$$Q_p{}^{clay} = 9S_{up}A_p = 9 * 105KPa * 0.5m^2 = 473KN$$

$$Q_{u(33m)} = Q_s{}^{sand+clay} + Q_p{}^{clay} = 2417KN + 473KN = 2890KN$$

g) Pile capacity at a depth of 35m below the surface

$$Q_s{}^{sand+clay} = 2417KN + (\alpha S_u A_s) = 2417KN + (0.62 * 80KPa * 2.513m * 2m)$$

$$= 2666KN$$

$$Q_p{}^{clay} = 9S_{up}A_p = 9 * 80KPa * 0.5m^2 = 360KN$$

$$Q_{u(33m)} = Q_s{}^{sand+clay} + Q_p{}^{clay} = 2666KN + 360KN = 3026KN$$

2) Axis 16 (HP pile) Norwegian Pile Guideline (2005)

a) Pile capacity at a depth of 7.5m below the surface

$$Q_s{}^{sand} = 328KN * \frac{1.476m}{2.513m} * 1.06 = 204KN$$

$$Q_p{}^{sand} = 792KN * \frac{0.136m^2}{0.5m^2} = 215KN$$

$$Q_{u(7.5m)} = Q_s{}^{sand} + Q_p{}^{sand} = 204KN + 215KN = 419KN$$

b) Pile capacity at a depth of 11m below the surface

Considering the full capacity in sand we will get:

$$Q_s{}^{sand} = 605KN * \frac{1.476m}{2.513m} * 1.07 = 380KN$$

$$Q_p{}^{sand} = 1044KN * \frac{0.136m^2}{0.5m^2} = 284KN$$

$$Q_{u(11m)} = Q_s{}^{sand} + Q_p{}^{sand} = 380KN + 284KN = 664KN$$

c) Pile capacity at a depth of 15.5m below the surface

$$Q_s{}^{sand} = 1022KN * \frac{1.476m}{2.513m} * 1.09 = 654KN$$

$$Q_p{}^{clay} = 180KN * \frac{0.136m^2}{0.5m^2} = 49KN$$

$$Q_{u(15.5m)} = Q_s{}^{sand} + Q_p{}^{clay} = 654KN + 49KN = 703KN$$

Considering the full capacity in sand we will get

$$Q_p{}^{sand} = 1368KN * \frac{0.136m^2}{0.5m^2} = 372KN$$

$$Q_{u(15.5m)} = Q_s{}^{sand} + Q_p{}^{sand} = 654KN + 372KN = 1026KN$$

d) Pile capacity at a depth of 17m below the surface

$$Q_s{}^{sand} = 654KN$$

$$Q_s{}^{clay} = 96KN * \frac{1.476m}{2.513m} * 1.1 = 62KN$$

$$Q_p{}^{clay} = 194KN * \frac{0.136m^2}{0.5m^2} = 53KN$$

$$Q_{u(17m)} = Q_s{}^{sand} + Q_s{}^{clay} + Q_p{}^{clay} = 654KN + 62KN + 53KN = 769KN$$

e) Pile capacity at a depth of 30m below the surface

$$Q_s{}^{sand} = 654KN$$

$$Q_s{}^{clay} = 904KN * \frac{1.476m}{2.513m} * 1.13 = 600KN$$

$$Q_p{}^{clay} = 473KN * \frac{0.136m^2}{0.5m^2} = 129KN$$

$$Q_{u(30m)} = Q_s{}^{sand} + Q_s{}^{clay} + Q_p{}^{clay} = 654KN + 600KN + 129KN = 1383KN$$

f) Pile capacity at a depth of 33m below the surface

$$Q_s{}^{sand} = 654KN$$

$$Q_s{}^{clay} = (904KN + 491KN) * \frac{1.476m}{2.513m} * 1.13 = 926KN$$

$$Q_p{}^{clay} = 473KN * \frac{0.136m^2}{0.5m^2} = 129KN$$

$$Q_{u(33m)} = Q_s{}^{sand} + Q_s{}^{clay} + Q_p{}^{clay} = 654KN + 926KN + 129KN = 1709KN$$

g) Pile capacity at a depth of 35m below the surface

$$Q_s{}^{sand} = 654KN$$

$$Q_s{}^{clay} = (904KN + 491KN + 249KN) * \frac{1.476m}{2.513m} * 1.14 = 1101KN$$

$$Q_p{}^{clay} = 360KN * \frac{0.136m^2}{0.5m^2} = 98KN$$

$$Q_{u(35m)} = Q_s{}^{sand} + Q_s{}^{clay} + Q_p{}^{clay} = 654KN + 1101KN + 98KN = 1853KN$$

3) Axis 16 (steel pipe pile) Janbu theoretical

a) Pile capacity at a depth of 7.5m below the surface

From chart;

$$tan\varphi = 0.7, \ r = 0.9 \rightarrow S_v = 0.35$$

$$tan\varphi = 0.7, \ \beta = 0 \rightarrow N_q = 30$$

$$Q_s{}^{sand} = Sv(p' + a)A_s = 0.35 \left(\frac{0KPa+50.4KPa}{2} * 2.8m + \frac{50.4KPa+88KPa}{2} * 4.7m \right) * 2.513$$

$$= 348KN$$

$$Q_p{}^{sand} = (N_q - 1)(p' + a)A_p = (30 - 1) * 88KPa * 0.5m^2 = 1276KN$$

$$Q_{u(7.5m)} = Q_s{}^{sand} + Q_p{}^{sand} = 348KN + 1276KN = 1624KN$$

b) Pile capacity at a depth of 11m below the surface

Considering the full capacity in sand we will get:

From chart;

$tan\varphi = 0.7, \ r = 0.9 \rightarrow S_v = 0.35$

$tan\varphi = 0.7, \ \beta = 0 \rightarrow N_q = 30$

$Q_s{}^{sand} = Sv(p' + a)A_s = 0.35 \left(\frac{0KPa+50.4KPa}{2} * 2.8m + \frac{50.4KPa+116KPa}{2} * 8.2m \right) * 2.513$

$\qquad = 662KN$

$Q_p{}^{sand} = \left(N_q - 1 \right)(p' + a)A_p = (30 - 1) * 116KPa * 0.5m^2 = 1682KN$

$Q_{u(11m)} = Q_s{}^{sand} + Q_p{}^{sand} = 662KN + 1682KN = 2344KN$

   c) Pile capacity at a depth of 15.5m below the surface

$tan\varphi = 0.7, \ r = 0.9 \rightarrow S_v = 0.35$

$tan\varphi = 0.7, \ \beta = 0 \rightarrow N_q = 30$

$Q_s{}^{sand} = Sv(p' + a)A_s = 0.35 \left(\frac{0KPa+50.4KPa}{2} * 2.8m + \frac{50.4KPa+152KPa}{2} * 12.7m \right) * 2.513$

$\qquad = 1192KN$

$Q_p{}^{clay} = 9S_{up}A_p = 9 * 40KPa * 0.5m^2 = 180KN$

$Q_{u(15.5m)} = Q_s{}^{sand} + Q_p{}^{clay} = 1192KN + 180KN = 1372KN$

Considering the full capacity in sand we will get:

$Q_p{}^{sand} = \left(N_q - 1 \right)(p' + a)A_p = (30 - 1) * 152KPa * 0.5m^2 = 2204KN$

$Q_{u(15.5m)} = Q_s{}^{sand} + Q_p{}^{sand} = 1192KN + 2204KN = 3396KN$

   d) Pile capacity at a depth of 17m below the surface

$Q_s{}^{sand+clay} = 1192KN + (rS_uA_s) = 1192KN + (0.9 * 41KPa * 2.513m * 1.5m)$

$\qquad\qquad = 1331KN$

$Q_p{}^{clay} = 9S_{up}A_p = 9 * 43KPa * 0.5m^2 = 194KN$

$Q_{u(17m)} = Q_s{}^{sand+clay} + Q_p{}^{clay} = 1331KN + 194KN = 1525KN$

   e) Pile capacity at a depth of 30m below the surface

$Q_s{}^{sand+clay} = 1192KN + (rS_uA_s) = 1192KN + (0.8 * 53KPa * 2.513m * 14.5m)$

$$= 2737KN$$

$$Q_p{}^{clay} = 9S_{up}A_p = 9 * 105KPa * 0.5m^2 = 473KN$$

$$Q_{u(30m)} = Q_s{}^{sand+clay} + Q_p{}^{clay} = 2737KN + 473KN = 3210KN$$

f) Pile capacity at a depth of 33m below the surface

$$Q_s{}^{sand+clay} = 2737KN + (rS_uA_s) = 2737KN + (0.8 * 105KPa * 2.513m * 3m)$$

$$= 3370KN$$

$$Q_p{}^{clay} = 9S_{up}A_p = 9 * 105KPa * 0.5m^2 = 473KN$$

$$Q_{u(33m)} = Q_s{}^{sand+clay} + Q_p{}^{clay} = 3370KN + 473KN = 3843KN$$

g) Pile capacity at a depth of 35m below the surface

$$Q_s{}^{sand+clay} = 3370KN + (rS_uA_s) = 3370KN + (0.8 * 80KPa * 2.513m * 2m)$$

$$= 3692KN$$

$$Q_p{}^{clay} = 9S_{up}A_p = 9 * 80KPa * 0.5m^2 = 360KN$$

$$Q_{u(35m)} = Q_s{}^{sand+clay} + Q_p{}^{clay} = 3692KN + 360KN = 4052KN$$

4) Axis 16 (HP pile) Janbu theoretical

a) Pile capacity at a depth of 7.5m below the surface

$$Q_s{}^{sand} = 348KN * \frac{1.476m}{2.513m} * 1.06 = 217KN$$

$$Q_p{}^{sand} = 1276KN * \frac{0.136m^2}{0.5m^2} = 347KN$$

$$Q_{u(7.5m)} = Q_s{}^{sand} + Q_p{}^{sand} = 217KN + 347KN = 564KN$$

b) Pile capacity at a depth of 11m below the surface

Considering the full capacity in sand we will get:

$$Q_s{}^{sand} = 662KN * \frac{1.476m}{2.513m} * 1.07 = 416KN$$

$$Q_p{}^{sand} = 1682KN * \frac{0.136m^2}{0.5m^2} = 458KN$$

$$Q_{u(11m)} = Q_s{}^{sand} + Q_p{}^{sand} = 416KN + 458KN = 874KN$$

c) Pile capacity at a depth of 15.5m below the surface

$$Q_s{}^{sand} = 1192KN * \frac{1.476m}{2.513m} * 1.09 = 763KN$$

$$Q_p{}^{clay} = 180KN * \frac{0.136m^2}{0.5m^2} = 49KN$$

$$Q_{u(15.5m)} = Q_s{}^{sand} + Q_p{}^{clay} = 763KN + 49KN = 812KN$$

Considering the full capacity in sand we will get:

$$Q_p{}^{sand} = 2204KN * \frac{0.136m^2}{0.5m^2} = 599KN$$

$$Q_{u(15.5m)} = Q_s{}^{sand} + Q_p{}^{sand} = 763KN + 599KN = 1362KN$$

    d) Pile capacity at a depth of 17m below the surface

$$Q_s{}^{sand} = 763KN$$

$$Q_s{}^{clay} = 139KN * \frac{1.476m}{2.513m} * 1.1 = 90KN$$

$$Q_p{}^{clay} = 194KN * \frac{0.136m^2}{0.5m^2} = 53KN$$

$$Q_{u(17m)} = Q_s{}^{sand} + Q_s{}^{clay} + Q_p{}^{clay} = 763KN + 90KN + 53KN = 906KN$$

    e) Pile capacity at a depth of 30m below the surface

$$Q_s{}^{sand} = 763KN$$

$$Q_s{}^{clay} = 1545KN * \frac{1.476m}{2.513m} * 1.13 = 1025KN$$

$$Q_p{}^{clay} = 473KN * \frac{0.136m^2}{0.5m^2} = 129KN$$

$$Q_{u(30m)} = Q_s{}^{sand} + Q_s{}^{clay} + Q_p{}^{clay} = 763KN + 1025KN + 129KN = 1917KN$$

    f) Pile capacity at a depth of 33m below the surface

$$Q_s{}^{sand} = 763KN$$

$$Q_s{}^{clay} = (1545KN + 633KN) * \frac{1.476m}{2.513m} * 1.13 = 1446KN$$

$$Q_p{}^{clay} = 473KN * \frac{0.136m^2}{0.5m^2} = 129KN$$

$$Q_{u(33m)} = Q_s{}^{sand} + Q_s{}^{clay} + Q_p{}^{clay} = 763KN + 1446KN + 129KN = 2338KN$$

    g) Pile capacity at a depth of 35m below the surface

$$Q_s{}^{sand} = 763KN$$

$$Q_s{}^{clay} = (1545KN + 633KN + 322KN) * \frac{1.476m}{2.513m} * 1.14 = 1674KN$$

$$Q_p{}^{clay} = 360KN * \frac{0.136m^2}{0.5m^2} = 98KN$$

$$Q_{u(35m)} = Q_s{}^{sand} + Q_s{}^{clay} + Q_p{}^{clay} = 763KN + 1674KN + 98KN = 2535KN$$

5) Axis 16 (steel pipe pile) API RP 2A (2007)

 a) Pile capacity at a depth of 7.5m below the surface

$$Q_s{}^{sand} = Kp'tan\delta A_s$$

$$= 1 * \left(\frac{0KPa + 50.4KPa}{2} * 2.8m + \frac{50.4KPa + 88KPa}{2} * 4.7m\right) * 2.513 * tan30^0 = 574KN$$

$$Q_p{}^{sand} = N_q p' A_p = 40 * 88KPa * 0.5 = 1760KN$$

$$Q_{u(7.5m)} = Q_s{}^{sand} + Q_p{}^{sand} = 574KN + 1760KN = 2334KN$$

 b) Pile capacity at a depth of 11m below the surface

Considering the full capacity in sand we will get:

$$Q_s{}^{sand} = Kp'tan\delta A_s$$

$$= 1 * \left(\frac{0KPa + 50.4KPa}{2} * 2.8m + \frac{50.4KPa + 116KPa}{2} * 8.2m\right) * 2.513 * tan30^0 = 1092KN$$

$$Q_p{}^{sand} = N_q p' A_p = 40 * 116KPa * 0.5 = 2320KN$$

$$Q_{u(11m)} = Q_s{}^{sand} + Q_p{}^{sand} = 1092KN + 2320KN = 3412KN$$

 c) Pile capacity at a depth of 15.5m below the surface

$$Q_s{}^{sand} = Kp'tan\delta A_s$$

$$= 1 * \left(\frac{0KPa + 50.4KPa}{2} * 2.8m + \frac{50.4KPa + 116KPa}{2} * 8.2m\right) * 2.513 * tan30^0 = 1967KN$$

$$Q_p{}^{clay} = 9S_{up}A_p = 9 * 40KPa * 0.5m^2 = 180KN$$

$$Q_{u(15.5m)} = Q_s{}^{sand} + Q_p{}^{clay} = 1967KN + 180KN = 2147KN$$

Considering the full capacity in sand we will get:

$$Q_p{}^{sand} = N_q p' A_p = 40 * 152 KPa * 0.5 = 3040 KN$$

$$Q_{u(15.5m)} = Q_s{}^{sand} + Q_p{}^{sand} = 1967 KN + 3040 KN = 5007 KN$$

   d) Pile capacity at a depth of 17m below the surface

$$Q_s{}^{sand+clay} = 1967 KN + (\alpha S_u A_s) = 1967 KN + (1.0 * 41 KPa * 2.513m * 1.5m)$$

$$= 2122 KN$$

$$Q_p{}^{clay} = 9 S_{up} A_p = 9 * 45 KPa * 0.5m^2 = 194 KN$$

$$Q_{u(17m)} = Q_s{}^{sand+clay} + Q_p{}^{clay} = 2122 KN + 194 KN = 2316 KN$$

   e) Pile capacity at a depth of 30m below the surface

$$Q_s{}^{sand+clay} = 1967 KN + (\alpha S_u A_s) = 1967 KN + (1.0 * 53 KPa * 2.513m * 14.5m)$$

$$= 3898 KN$$

$$Q_p{}^{clay} = 9 S_{up} A_p = 9 * 105 KPa * 0.5m^2 = 473 KN$$

$$Q_{u(30m)} = Q_s{}^{sand+clay} + Q_p{}^{clay} = 3898 KN + 473 KN = 4371 KN$$

   f) Pile capacity at a depth of 33m below the surface

$$Q_s{}^{sand+clay} = 3898 KN + (\alpha S_u A_s) = 3898 KN + (1.0 * 105 KPa * 2.513m * 3m)$$

$$= 4690 KN$$

$$Q_p{}^{clay} = 9 S_{up} A_p = 9 * 105 KPa * 0.5m^2 = 473 KN$$

$$Q_{u(33m)} = Q_s{}^{sand+clay} + Q_p{}^{clay} = 4690 KN + 473 KN = 5163 KN$$

   g) Pile capacity at a depth of 35m below the surface

$$Q_s{}^{sand+clay} = 4690 KN + (\alpha S_u A_s) = 4690 KN + (1.0 * 80 KPa * 2.513m * 2m)$$

$$= 5092 KN$$

$$Q_p{}^{clay} = 9 S_{up} A_p = 9 * 80 KPa * 0.5m^2 = 360 KN$$

$$Q_{u(35m)} = Q_s{}^{sand+clay} + Q_p{}^{clay} = 5092 KN + 360 KN = 5452 KN$$

6) Axis 16 (HP pile) API RP 2A (2007)

   a) Pile capacity at a depth of 7.5m below the surface

Condition 1)

$$Q_s{}^{sand} = Kp'tan\delta A_s$$

$$= 1 * \left(\frac{0KPa+50.4KPa}{2} * 2.8m + \frac{50.4KPa+88KPa}{2} * 4.7m\right) * 1.307 * tan30^0 = 299KN$$

$$Q_p{}^{sand} = N_q p' A_p = 40 * 88KPa * 0.136m^2 = 479KN$$

$$Q_{u(7.5m)} = Q_s{}^{sand} + Q_p{}^{sand} = 299KN + 479KN = 778KN$$

Condition 2)

$$Q_s{}^{sand} = Kp'tan\delta A_s$$

$$= 0.8 * \left(\frac{0KPa+50.4KPa}{2} * 2.8m + \frac{50.4KPa+88KPa}{2} * 4.7m\right) * 2.2 * tan30^0 = 402KN$$

$$Q_p{}^{sand} = N_q p' A_p = 40 * 88KPa * 0.0154m^2 = 54KN$$

$$Q_{u(7.5m)} = Q_s{}^{sand} + Q_p{}^{sand} = 402KN + 54KN = 456KN$$

Therefore, Condition to 2 is the governing pile capacity

   b) Pile capacity at a depth of 11m below the surface

Considering the full capacity in sand we will get:

Condition 1)

$$Q_s{}^{sand} = Kp'tan\delta A_s$$

$$= 1 * \left(\frac{0KPa+50.4KPa}{2} * 2.8m + \frac{50.4KPa+116KPa}{2} * 8.2m\right) * 1.307 * tan30^0 = 568KN$$

$$Q_p{}^{sand} = N_q p' A_p = 40 * 116KPa * 0.136m^2 = 631KN$$

$$Q_{u(11m)} = Q_s{}^{sand} + Q_p{}^{sand} = 568KN + 631KN = 1199KN$$

Condition 2)

$$Q_s{}^{sand} = Kp'tan\delta A_s$$

$$= 0.8 * \left(\frac{0KPa+50.4KPa}{2} * 2.8m + \frac{50.4KPa+116KPa}{2} * 8.2m\right) * 2.2 * tan30^0 = 765KN$$

$$Q_p{}^{sand} = N_q p' A_p = 40 * 116KPa * 0.0154m^2 = 71KN$$

$$Q_{u(11m)} = Q_s{}^{sand} + Q_p{}^{sand} = 765KN + 71KN = 836KN$$

Therefore, Condition to 2 is the governing pile capacity

c) Pile capacity at a depth of 15.5m below the surface

Condition 1)

$$Q_s{}^{sand} = Kp'tan\delta A_s$$

$$= 1 * \left(\frac{0KPa+50.4KPa}{2} * 2.8m + \frac{50.4KPa+152KPa}{2} * 12.7m\right) * 1.307 * tan30^0 = 1023KN$$

$$Q_p{}^{clay} = 9S_{up}A_p = 9 * 40KPa * 0.136m^2 = 49KN$$

$$Q_{u(15.5m)} = Q_s{}^{sand} + Q_p{}^{clay} = 1023KN + 49KN = 1072KN$$

Considering the full capacity in sand we will get:

$$Q_p{}^{sand} = N_q p' A_p = 40 * 152KPa * 0.136m^2 = 827KN$$

$$Q_{u(15.5m)} = Q_s{}^{sand} + Q_p{}^{sand} = 1023KN + 827KN = 1850KN$$

Condition 2)

$$Q_s{}^{sand} = Kp'tan\delta A_s$$

$$= 0.8 * \left(\frac{0KPa+50.4KPa}{2} * 2.8m + \frac{50.4KPa+152KPa}{2} * 12.7m\right) * 2.2 * tan30^0 = 1378KN$$

$$Q_p{}^{clay} = 9S_{up}A_p = 9 * 40KPa * 0.0154m^2 = 5.5KN$$

$$Q_{u(15.5m)} = Q_s{}^{sand} + Q_p{}^{clay} = 1378KN + 5.5KN = 1384KN$$

Considering the full capacity in sand we will get:

$$Q_p{}^{sand} = N_q p' A_p = 40 * 152KPa * 0.0154m^2 = 94KN$$

$$Q_{u(15.5m)} = Q_s{}^{sand} + Q_p{}^{sand} = 1378KN + 94KN = 1472KN$$

d) Pile capacity at a depth of 17m below the surface

$$Q_s{}^{sand+clay} = 1023KN + (\alpha S_u A_s) = 1023KN + (1.0 * 41KPa * 1.307m * 1.5m)$$

$$= 1103KN$$

$$Q_p{}^{clay} = 9S_{up}A_p = 9 * 43KPa * 0.136m^2 = 53KN$$

$$Q_{u(17m)} = Q_s{}^{sand+clay} + Q_p{}^{clay} = 1103KN + 53KN = 1156KN$$

e) Pile capacity at a depth of 30m below the surface

$$Q_s^{sand+clay} = 1023KN + (\alpha S_u A_s) = 1023KN + (1.0 * 53KPa * 1.307m * 14.5m)$$

$$= 2027KN$$

$$Q_p^{clay} = 9S_{up}A_p = 9 * 105KPa * 0.136m^2 = 129KN$$

$$Q_{u(30m)} = Q_s^{sand+clay} + Q_p^{clay} = 2027KN + 129KN = 2156KN$$

f) Pile capacity at a depth of 33m below the surface

$$Q_s^{sand+clay} = 2027KN + (\alpha S_u A_s) = 2027KN + (1.0 * 105KPa * 1.307m * 3m)$$

$$= 2439KN$$

$$Q_p^{clay} = 9S_{up}A_p = 9 * 105KPa * 0.136m^2 = 129KN$$

$$Q_{u(33m)} = Q_s^{sand+clay} + Q_p^{clay} = 2439KN + 129KN = 2568KN$$

g) Pile capacity at a depth of 35m below the surface

$$Q_s^{sand+clay} = 2439KN + (\alpha S_u A_s) = 2439KN + (1.0 * 80KPa * 1.307m * 2m)$$

$$= 2648KN$$

$$Q_p^{clay} = 9S_{up}A_p = 9 * 80KPa * 0.136m^2 = 98KN$$

$$Q_{u(35m)} = Q_s^{sand+clay} + Q_p^{clay} = 2648KN + 98KN = 2746KN$$

7) Axis 16 (steel pipe) NGI-99

a) Pile capacity at a depth of 7.5m below the surface

$$D_r = 0.4. \ln\left\{ {q_c}/{[22. (\sigma'_{v0}. \sigma_{atm})^{0.5}]} \right\} = 0.4. \ln\left\{ {5000KPa}/{[22. (100KPa. 58KPa)^{0.5}]} \right\}$$

$$D_r = 0.44$$

$$F_{Dr} = 2.1. (D_r - 0.1)^{1.7} = 2.1. (0.44 - 0.1)^{1.7} = 0.33$$

$$F_{sig} = (\frac{\sigma'_{v0}}{\sigma_{atm}})^{0.25} = \left(\frac{58KPa}{100KPa}\right)^{0.25} = 0.87$$

$$F_{tip} = 1.6 = (\text{closed ended})$$

$$F_{load} = 1.3 = (\text{compression load})$$

$$F_{mat} = 1.0 = (\text{steel})$$

$$Q_s = \frac{z}{z_{tip}} * \sigma_{atm} * F_{Dr} * F_{sig} * F_{tip} * F_{load} * F_{mat} * A_s$$

$$= \frac{3.75m}{7.5m} * 100Kpa * 0.33 * 0.87 * 1.6 * 1.3 * 1.0 * 2.513m * 7.5m = 563KN$$

$$Q_p = 0.8 \frac{q_c}{(1+Dr^2)} A_p$$

$$= 0.8 * \frac{5000KPa}{(1+0.44^2)} * 0.5m^2 = 1676KN$$

$$Q_{u(7.5m)} = Q_s + Q_p = 563KN + 1676KN = 2239KN$$

b) Pile capacity at a depth of 11m below the surface

Considering the full capacity in sand we will get:

$$D_r = 0.4. \ln\left\{ \frac{q_c}{[22. (\sigma'_{v0}. \sigma_{atm})^{0.5}]} \right\} = 0.4. \ln\left\{ \frac{5000KPa}{[22. (100KPa. 72KPa)^{0.5}]} \right\}$$

$$D_r = 0.39$$

$$F_{Dr} = 2.1. (D_r - 0.1)^{1.7} = 2.1. (0.39 - 0.1)^{1.7} = 0.26$$

$$F_{sig} = (\frac{\sigma'_{v0}}{\sigma_{atm}})^{0.25} = \left(\frac{72KPa}{100KPa} \right)^{0.25} = 0.92$$

$$F_{tip} = 1.6 = \text{(closed ended)}$$

$$F_{load} = 1.3 = \text{(compression load)}$$

$$F_{mat} = 1.0 = \text{(steel)}$$

$$Q_s = \frac{z}{z_{tip}} * \sigma_{atm} * F_{Dr} * F_{sig} * F_{tip} * F_{load} * F_{mat} * A_s$$

$$= \frac{5.5m}{11m} * 100Kpa * 0.26 * 0.92 * 1.6 * 1.3 * 1.0 * 2.513m * 11m = 688KN$$

$$Q_p = 0.8 \frac{q_c}{(1+Dr^2)} A_p$$

$$= 0.8 * \frac{5000KPa}{(1+0.39^2)} * 0.5m^2 = 1736KN$$

$$Q_{u(11m)} = Q_s + Q_p = 688KN + 1736KN = 2424KN$$

c) Pile capacity at a depth of 15.5m below the surface

$$D_r = 0.4. \ln\left\{ \frac{q_c}{[22. (\sigma'_{v0}. \sigma_{atm})^{0.5}]} \right\} = 0.4. \ln\left\{ \frac{5000KPa}{[22. (100KPa. 90KPa)^{0.5}]} \right\}$$

$$D_r = 0.44$$

$$F_{Dr} = 2.1. (D_r - 0.1)^{1.7} = 2.1. (0.35 - 0.1)^{1.7} = 0.2$$

$$F_{sig} = (\frac{\sigma'_{vo}}{\sigma_{atm}})^{0.25} = \left(\frac{90KPa}{100KPa}\right)^{0.25} = 0.97$$

$$F_{tip} = 1.6 = \text{(closed ended)}$$

$$F_{load} = 1.3 = \text{(compression load)}$$

$$F_{mat} = 1.0 = \text{(steel)}$$

$$Q_s = \frac{z}{z_{tip}} * \sigma_{atm} * F_{Dr} * F_{sig} * F_{tip} * F_{load} * F_{mat} * A_s$$

$$= \frac{7.75m}{15.5m} * 100Kpa * 0.2 * 0.97 * 1.6 * 1.3 * 1.0 * 2.513m * 15.5m = 786KN$$

$$Q_p = 0.8\frac{q_c}{(1+Dr^2)} A_p$$

$$= 0.8 * \frac{5000KPa}{(1+0.35^2)} * 0.5m^2 = 1782KN$$

$$Q_{u(15.5m)} = Q_s + Q_p = 786KN + 1782KN = 2568KN$$

Case 2: Considering the tip resistance of the clay

$$Q_p{}^{clay} = 9S_{up}A_p = 9 * 40KPa * 0.5m^2 = 180KN$$

$$Q_{u(15.5m)} = Q_s{}^{sand} + Q_p{}^{clay} = 786KN + 180KN = 966KN$$

d) Pile capacity at a depth of 17m below the surface

$$Q_s{}^{sand+clay} = 786KN + (\alpha S_u A_s) = 786KN + (0.62 * 41KPa * 2.513m * 1.5m)$$

$$= 882KN$$

$$Q_p{}^{clay} = 9S_{up}A_p = 9 * 43KPa * 0.5m^2 = 194KN$$

$$Q_{u(17m)} = Q_s{}^{sand+clay} + Q_p{}^{clay} = 882KN + 194KN = 1076KN$$

e) Pile capacity at a depth of 30m below the surface

$$Q_s{}^{sand+clay} = 786KN + (\alpha S_u A_s) = 786KN + (0.62 * 40KPa * 2.513m * 14.5m)$$

$$= 1690KN$$

$$Q_p{}^{clay} = 9S_{up}A_p = 9 * 105KPa * 0.5m^2 = 473KN$$

$$Q_{u(30m)} = Q_s{}^{sand+clay} + Q_p{}^{clay} = 1690KN + 473KN = 2163KN$$

f) Pile capacity at a depth of 33m below the surface

$$Q_s{}^{sand+clay} = 1690KN + (\alpha S_u A_s) = 1690KN + (0.62 * 105KPa * 2.513m * 3m)$$

$$= 2181KN$$

$$Q_p{}^{clay} = 9S_{up}A_p = 9 * 105KPa * 0.5m^2 = 473KN$$

$$Q_{u(33m)} = Q_s{}^{sand+clay} + Q_p{}^{clay} = 2181KN + 473KN = 2654KN$$

g) Pile capacity at a depth of 35m below the surface

$$Q_s{}^{sand+clay} = 2181KN + (\alpha S_u A_s) = 2181KN + (0.62 * 80KPa * 2.513m * 2m)$$

$$= 2430KN$$

$$Q_p{}^{clay} = 9S_{up}A_p = 9 * 80KPa * 0.5m^2 = 360KN$$

$$Q_{u(35m)} = Q_s{}^{sand+clay} + Q_p{}^{clay} = 2430KN + 360KN = 2790KN$$

APPENDIX B

Pile capacity analyses using the various empirical and theoretical methods for axis 25

1) Axis 25 (steel pipe pile) Norwegian Pile Guideline (2005)

$$Q_u = Q_s + Q_p$$

$$= \beta . p'_0 . A_s + N_q p' A_p$$

a) Pile capacity at a depth of 15m below the surface

$$Q_s = \beta . p'_0 . A_s = 0.3 \left(\frac{0 KPa + 27 KPa}{2} * 1.5m + \frac{27 KPa + 135 KPa}{2} * 13.5m \right) * 2.513m = 840 KN$$

$$Q_p = N_q p' A_p = 18 * 135 KPa * 0.5m^2 = 1215 KN$$

$$Q_{u(15m)} = Q_s + Q_p = 840 KN + 1215 KN = 2055 KN$$

b) Pile capacity at a depth of 25m below the surface

$$Q_s = \beta . p'_0 . A_s$$

$$= 0.25 \left(\frac{0 KPa + 27 KPa}{2} * 1.5m + \frac{27 KPa + 135 KPa}{2} * 13.5m + \frac{135 KPa + 215 KPa}{2} * 10m \right) * 2.513$$

$$= 1799 KN$$

$$Q_p = N_q p'^{A_p} = 18 * 215 KPa * 0.5m^2 = 1935 KN$$

$$Q_{u(25m)} = Q_s + Q_p = 1799 KN + 1935 KN = 3734 KN$$

2) Axis 25 (HP pile) Norwegian Pile Guideline (2005)

HP 400*122

Depth(m)	Roughness(r)	$1/rm$
15	0.8	1.13
30	0.7	1.21
45	0.6	1.29

a) Pile capacity at a depth of 15m below the surface

$$Q_s = 840KN * \frac{1.476m}{2.513m} * 1.1 = 543KN$$

$$Q_p = N_q p' A_p = 18 * 135KPa * 0.136m^2 = 330KN$$

$$Q_{u(15m)} = Q_s + Q_p = 543KN + 330KN = 873KN$$

b) Pile capacity at a depth of 25m below the surface

$$Q_s = 1799KN * \frac{1.476m}{2.513m} * 1.12 = 1183KN$$

$$Q_p = N_q p'^{A_p} = 18 * 215KPa * 0.136m^2 = 526KN$$

$$Q_{u(25m)} = Q_s + Q_p = 1183KN + 526KN = 1709KN$$

3) Axis 25 (steel pipe pile) API RP 2A (2007)

a) Pile capacity at a depth of 15m below the surface

$$Q_s = Kp' tan\delta A_s$$

$$= 1 * \left(\frac{0KPa+27KPa}{2} * 1.5m + \frac{27KPa+135KPa}{2} * 13.5m\right) * 2.513m * tan30^0$$

$$= 1616KN$$

$$Q_p = N_q p' A_p = 40 * 135KPa * 0.5m^2 = 2700KN$$

$$Q_{u(15m)} = Q_s + Q_p = 1616KN + 2700KN = 4316KN$$

b) Pile capacity at a depth of 25m below the surface

$$Q_s = Kp' tan\delta A_s$$

$$= 1 * \left(\frac{0KPa+27KPa}{2} * 1.5m + \frac{27KPa+135KPa}{2} * 13.5m + \frac{135KPa+215KPa}{2} * 10m\right) * 2.513m * tan30^0$$

$$= 4155KN$$

$$Q_p = N_q p' A_p = 40 * 215KPa * 0.5m^2 = 4300KN$$

$$Q_{u(25m)} = Q_s + Q_p = 4155KN + 4300KN = 8455KN$$

4) Axis 25 (HP pile) API RP 2A (2007)
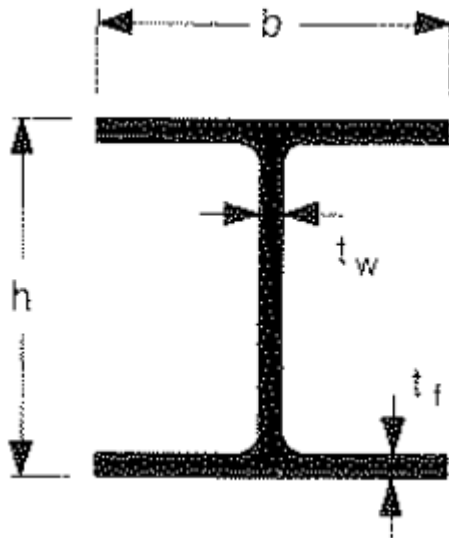
$$t_w = t_f = 14mm \qquad\qquad A_s = 0.0154mm^2$$

$$b = 390mm$$

$$h = 348mm$$

Condition 1

The soil in between the flanges sticks to the H-pile: In this case the H pile is modeled as a closed pipe pile with the same cross-section at the toe as the H pile. Defining the equivalent diameter (D_e).

$$D_e = \sqrt{\frac{4A}{\pi}} =$$

Where

$$A = \text{the total pile section} = 0.390m * 0.348m = 0.136m^2$$

$$D_e = \sqrt{\frac{4*0.136}{\pi}} = 0.416$$

Condition 2

The soil in between the flanges does not stick to the H pile: In this case the h pile is modeled as a pipe pile of the same steel cross-section with the same frictional surface (per linear meter). Defining the equivalent diameter (D_e)

$$p = \pi D_e + \pi(D_e - 2t)$$

$$A = \frac{\pi D_e^2}{4} - \pi.(\frac{D_e - 2t}{4})^2$$

Where

$$t = \text{wall thickness}$$

$$p = \left((390 - (2 * 14)) * 2\right) + (2 * 390) + (2 * 348) = 2200mm = 2.2m$$

$$A_s = \left(14 * \left(348 - (2 * 14)\right)\right) + (2 * 390 * 14) = 15400mm^2 = 0.0154m^2$$

$$2.2 = \pi D_e + \pi(D_e - 2t)\dots\dots\dots\dots\dots\dots \text{ (1)}$$

$$0.0154 = \frac{\pi D_e{}^2}{4} - \pi.\left(\frac{D_e - 2t}{4}\right)^2 \dots\dots\dots\dots\dots \text{ (2)}$$

Solving equation 1) and 2) simultaneously we obtain

$$D_e = 0.3654m$$

$$t = 0.0153m$$

a) Pile capacity at a depth of 15m below the surface

Condition 1)

$$Q_s = Kp'tan\delta A_s$$

$$= 1 * \left(\frac{0KPa + 27KPa}{2} * 1.5m + \frac{27KPa + 135KPa}{2} * 13.5m\right) * 1.307m * tan30^0$$

$$= 840KN$$

$$Q_p = N_q p' A_p = 40 * 135KPa * 0.136m^2 = 734KN$$

$$Q_{u(15m)} = Q_s + Q_p = 840KN + 734KN = 1574KN$$

Condition 2)

$$Q_s = Kp'tan\delta A_s$$

$$= 0.8 * \left(\frac{0KPa + 27KPa}{2} * 1.5m + \frac{27KPa + 135KPa}{2} * 13.5m\right) * 2.2m * tan30^0$$

$$= 1132KN$$

$$Q_p = N_q p' A_p = 40 * 135KPa * 0.0154m^2 = 83KN$$

$$Q_{u(15m)} = Q_s + Q_p = 1132KN + 83KN = 1215KN$$

Therefore, Condition to 2 is the governing pile capacity

b) Pile capacity at a depth of 25m below the surface

Condition 1)

$$Q_s = Kp'tan\delta A_s$$

$$= 1 * \left(\frac{0KPa+27KPa}{2} * 1.5m + \frac{27KPa+135KPa}{2} * 13.5m + \frac{135KPa+215KPa}{2} * 10m\right) * 1.307m * tan30^0$$

$$= 2161KN$$

$$Q_p = N_q p' A_p = 40 * 215KPa * 0.136m^2 = 1170KN$$

$$Q_{u(25m)} = Q_s + Q_p = 2161KN + 1170KN = 3331KN$$

Condition 2)

$$Q_s = Kp'tan\delta A_s$$

$$= 0.8 * \left(\frac{0KPa+27KPa}{2} * 1.5m + \frac{27KPa+135KPa}{2} * 13.5m + \frac{135KPa+215KPa}{2} * 10m\right) * 2.2m * tan30^0$$

$$= 2910KN$$

$$Q_p = N_q p' A_p = 40 * 215KPa * 0.0154m^2 = 132KN$$

$$Q_{u(25m)} = Q_s + Q_p = 2910KN + 132KN = 3042KN$$

Therefore, Condition to 2 is the governing capacity

5) Axis 25 (steel pipe) Janbu Theoretical

   a) Pile capacity at a depth of 15m below the surface

From chart;

$$tan\varphi = 0.7, \ r = 0.8 \rightarrow S_v = 0.24$$

$$tan\varphi = 0.7, \ \beta = 0 \rightarrow N_q = 30$$

$$Q_s = Sv(p' + a)A_s$$

$$= 0.24 \left(\frac{0KPa+27KPa}{2} * 1.5m + \frac{27KPa+135KPa}{2} * 13.5m\right) * 2.513m = 672KN$$

$$Q_p = (N_q - 1)(p' + a)A_p = (30 - 1) * 135KPa * 0.5m^2 = 1958KN$$

$$Q_{u(15m)} = Q_s + Q_p = 672KN + 1958KN = 2630KN$$

   b) Pile capacity at a depth of 25m below the surface

$tan\varphi = 0.7, \ r = 0.7 \rightarrow S_v = 0.18$

$tan\varphi = 0.7, \ \beta = 0 \rightarrow N_q = 30$

$Q_s = Sv(p' + a)A_s$

$$= 0.24 \left(\frac{0KPa+27KPa}{2} * 1.5m + \frac{27KPa+135KPa}{2} * 13.5m + \frac{135KPa+215KPa}{2} * 10m \right) * 2.513m$$

$$= 1295KN$$

$Q_p = (N_q - 1)(p' + a)A_p = (30 - 1) * 215KPa * 0.5m^2 = 3118KN$

$Q_{u(25m)} = Q_s + Q_p = 1295KN + 3118KN = 4412KN$

6) Axis 25 (HP pile) Janbu theoretical

a) Pile capacity at a depth of 15m below the surface

$Q_s = 672KN * \frac{1.476m}{2.513m} * 1.1 = 434KN$

$Q_p = (30 - 1) * 135KPa * 0.136m^2 = 532KN$

$Q_{u(15m)} = Q_s + Q_p = 434KN + 532KN = 966KN$

b) Pile capacity at a depth of 25m below the surface

$Q_s = 1295KN * \frac{1.476m}{2.513m} * 1.12 = 852KN$

$Q_p = (30 - 1) * 215KPa * 0.136m^2 = 848KN$

$Q_{u(25m)} = Q_s + Q_p = 852KN + 848KN = 1700KN$

7) Axis 25 (steel pipe) NGI-99

a) Pile capacity at a depth of 15m below the surface

$D_r = 0.4. \ln\left\{ q_c \Big/ [22. (\sigma'_{v0}. \sigma_{atm})^{0.5}] \right\} = 0.4. \ln\left\{ 7100KPa \Big/ [22. (100KPa. 75KPa)^{0.5}] \right\}$

$D_r = 0.52$

$F_{Dr} = 2.1. (D_r - 0.1)^{1.7} = 2.1. (0.52 - 0.1)^{1.7} = 0.48$

$F_{sig} = (\frac{\sigma'_{v0}}{\sigma_{atm}})^{0.25} = \left(\frac{75KPa}{100KPa} \right)^{0.25} = 0.93$

$F_{tip} = 1.6 = \text{(closed ended)}$

$F_{load} = 1.3 = $ (compression load)

$F_{mat} = 1.0 = $ (steel)

$Q_s = \dfrac{z}{z_{tip}} * \sigma_{atm} * F_{Dr} * F_{sig} * F_{tip} * F_{load} * F_{mat} * A_s$

$\quad = \dfrac{7.5m}{15m} * 100Kpa * 0.48 * 0.93 * 1.6 * 1.3 * 1.0 * 2.513m * 15m = 1750KN$

$Q_p = 0.8 \dfrac{q_c}{(1+Dr^2)} A_p$

$\quad = 0.8 * \dfrac{7100KPa}{(1+0.52^2)} * 0.5m^2 = 2204KN$

$Q_{u(15m)} = Q_s + Q_p = 1750KN + 2204KN = 3954KN$

b) Pile capacity at a depth of 25m below the surface

$D_r = 0.4. \ln \left\{ 7100KPa \middle/ [22.(100KPa.115KPa)^{0.5}] \right\} = 0.44$

$F_{Dr} = 2.1.(D_r - 0.1)^{1.7} = 2.1.(0.44 - 0.1)^{1.7} = 0.33$

$F_{sig} = (\dfrac{\sigma'_{v0}}{\sigma_{atm}})^{0.25} = \left(\dfrac{115KPa}{100KPa} \right)^{0.25} = 1.035$

$Q_s = \dfrac{12.5m}{25m} * 100Kpa * 0.33 * 1.035 * 1.6 * 1.3 * 1.0 * 2.513m * 25m = 2232KN$

$Q_p = 0.8 * \dfrac{7100KPa}{(1+0.44^2)} * 0.5m^2 = 2346KN$

$Q_{u(25m)} = Q_s + Q_p = 2232KN + 2346KN = 4578KN$

APPENDIX C

Figures
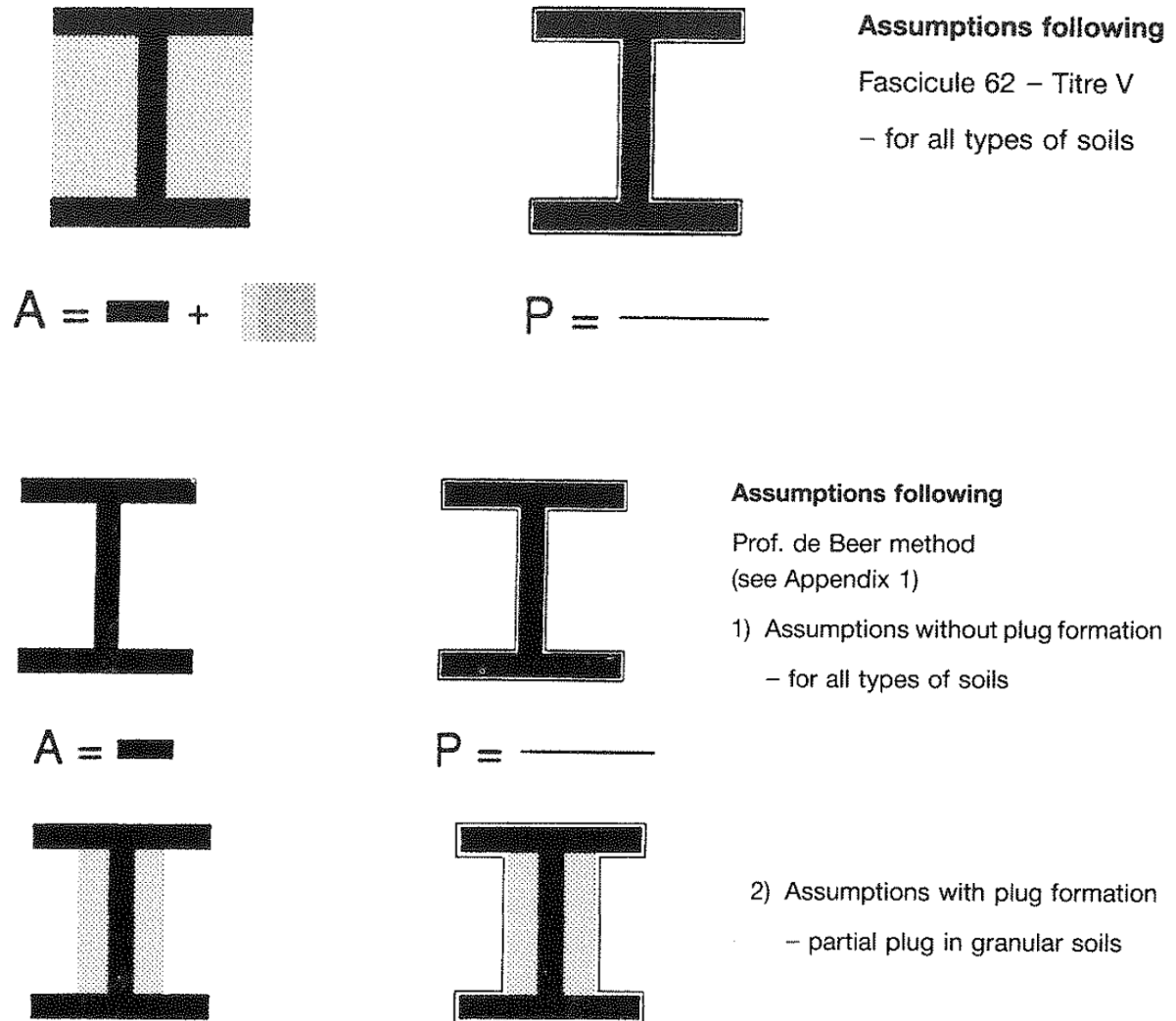
Figure C1- Plugging in HP piles[7]

C P T - sondering

Projekt		Plats	Fundament nr. 16
Drammensbrua		Borrhål	1602
1375 (GeoVita as prosjektnummer)		Datum	19990413

Förborrningsdjup	1.70 m	Förborrat material	Sand/Tørrskorpe
Startdjup	1.70 m	Geometri	Alternativ
Stoppdjup	66.67 m	Vätska i filter	
Grundvattenyta	2.80 m	Operatör	
Referens	Terreng	Utrustning	ENVI-sonde
Nivå vid referens	2.80 m	[X] Portryck registrerat vid sondering	

Kalibreringsdata

Spets	9556	Inre friktion O_c	0.0 kPa
Datum		Inre friktion O_f	0.0 kPa
Areafaktor a	0.700	Cross talk c_1	0.000
Areafaktor b	0.000	Cross talk c_2	0.000

Skalfaktorer

Portryck		Friktion		Spetstryck	
Område	Faktor	Område	Faktor	Område	Faktor

☐ Använd skalfaktorer vid beräkning

Inmatade nollvärden

	Portryck	Friktion	Spetstryck
Före	100	0	0
Efter	100	0	0

Beräknade nollvärden (kPa)

	Portryck	Friktion	Spetstryck
Före	100.00	0.00	0.00
Efter	100.00	0.00	0.00
Diff	0.00	0.00	0.00

Korrigering

Portryck	(ingen)
Friktion	(ingen)
Spetstryck	(ingen)

Portrycksobservationer

Djup (m)	Portryck (kPa)
2.80	0.00

Skiktgränser

Djup (m)
1.70
15.50

Klassificering

Djup (m)		Densitet	Flytgräns	Jordart
Från	Till	(ton/m³)		
0.00	1.70	1.80		Sand/Tørrskorpe
1.70	15.50	1.80		Sa M
15.50	30.00	1.90		Le M NC
30.00	67.00	1.90		Le F NC

Anmärkning

D:\lank-privat\GeoVita-hjemmearbeid\CPTU-Drammen\Hull16.cpw

Statens geotekniska institut
58 l 93 Linköping, telefon 0 l3-20 18 00, fax 0 l3-20 19 l4

Figure C2- CPT data at axis 16
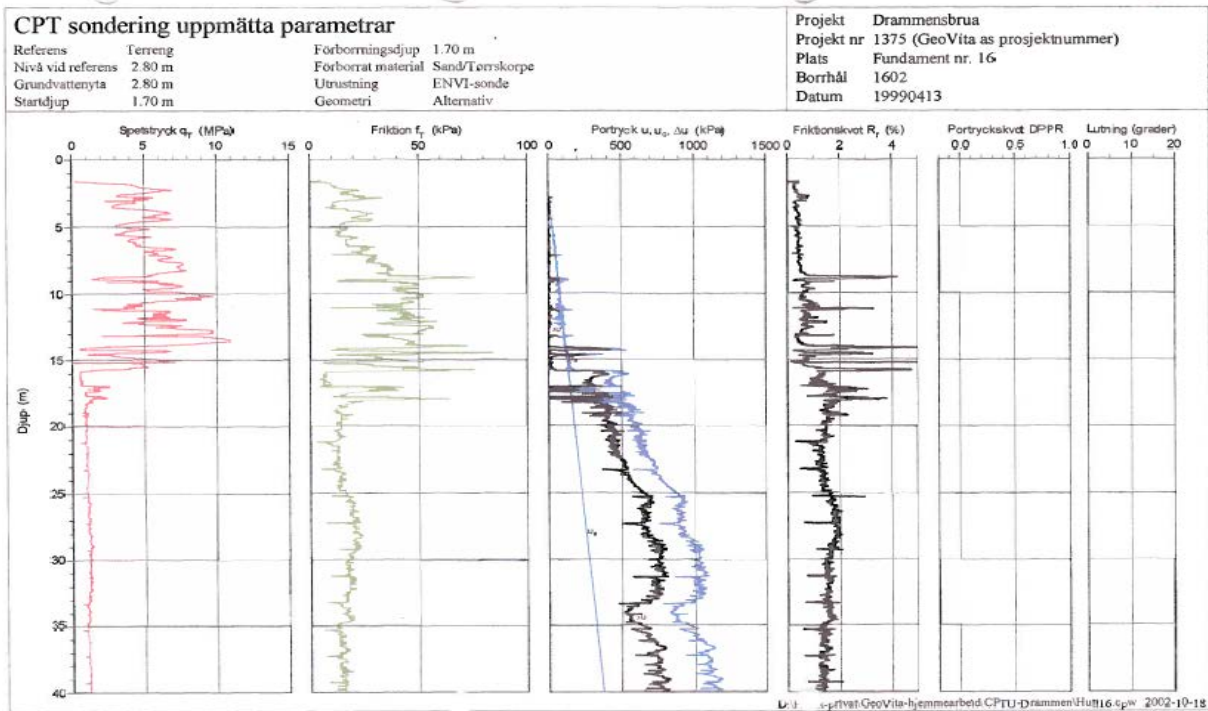
Figure C3- CPT tip resistance, sleeve friction, pore pressure and frictional ratio plots at axis 16
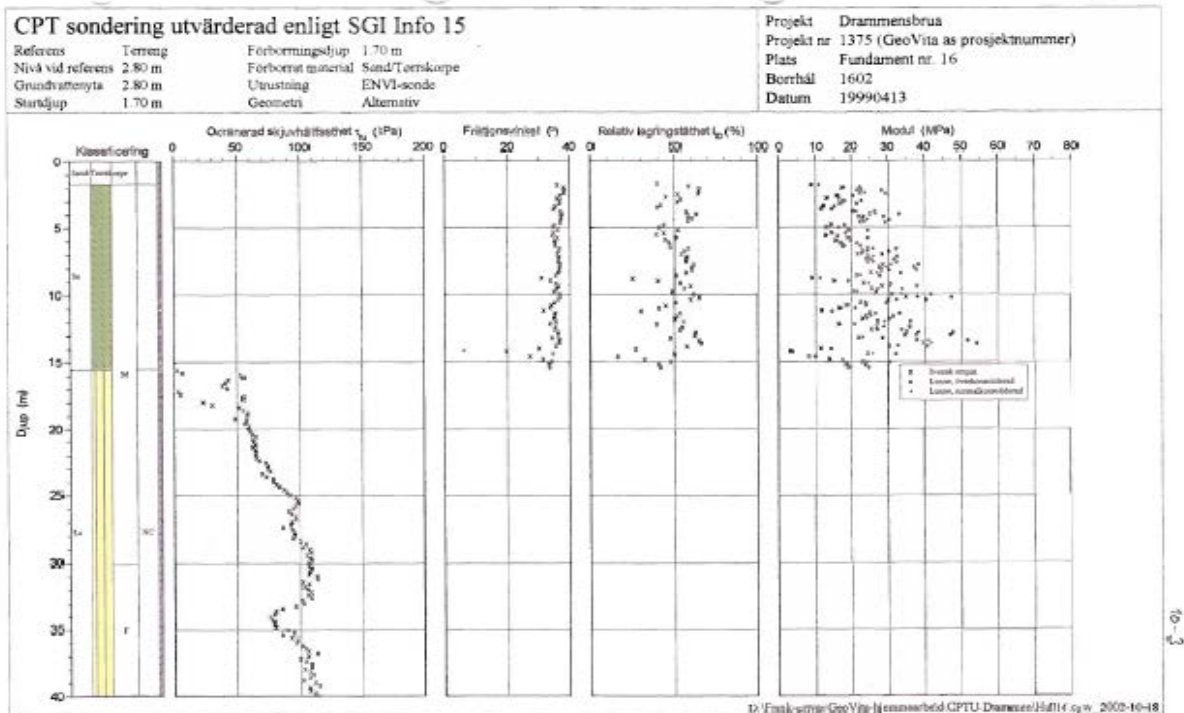
Figure C4- Shear strength, friction angle, relative density and modulus interpreted from the CPT at axis 16

C P T - sondering

Projekt		Plats	Fundament nr. 25
Drammensbrua		Borrhål	2502
1375 (GeoVita as prosjektnummer)		Datum	19990420

Förborrningsdjup	3.00 m	Förborrat material	
Startdjup	3.00 m	Geometri	Normal
Stoppdjup	27.36 m	Vätska i filter	
Grundvattenyta	1.50 m	Operatör	
Referens	Terreng	Utrustning	ENVI-sonde
Nivå vid referens	1.50 m	[X] Portryck registrerat vid sondering	

Kalibreringsdata

Spets	9556	Inre friktion O_c	0.0 kPa
Datum		Inre friktion O_f	0.0 kPa
Areafaktor a	0.700	Cross talk c_1	0.000
Areafaktor b	0.000	Cross talk c_2	0.000

Inmatade nollvärden

	Portryck	Friktion	Spetstryck
Före	100	0	0
Efter	100	0	0

Skalfaktorer

Portryck Område Faktor	Friktion Område Faktor	Spetstryck Område Faktor

☐ Använd skalfaktorer vid beräkning

Beräknade nollvärden (kPa)

	Portryck	Friktion	Spetstryck
Före	100.00	0.00	0.00
Efter	100.00	0.00	0.00
Diff	0.00	0.00	0.00

Korrigering

Portryck	(ingen)
Friktion	(ingen)
Spetstryck	(ingen)

Portrycksobservationer

Djup (m)	Portryck (kPa)
1.50	0.00

Skiktgränser

Djup (m)

Klassificering

Djup (m) Från	Till	Densitet (ton/m³)	Flytgräns	Jordart
0.00	3.00	1.80		Forboret
3.00	11.00	1.75		Sa L
11.00	15.00	1.80		Sa M
15.00	17.00	1.90		Sa F
17.00	27.40	1.80		Sa M

Anmärkning

D:\Frank-privat\GeoVita-hjemmearbeid CPTU-Drammen Hull25.cpw

Statens geotekniska institut
581 93 Linköping, telefon 013-20 18 00, fax 013-20 19 14
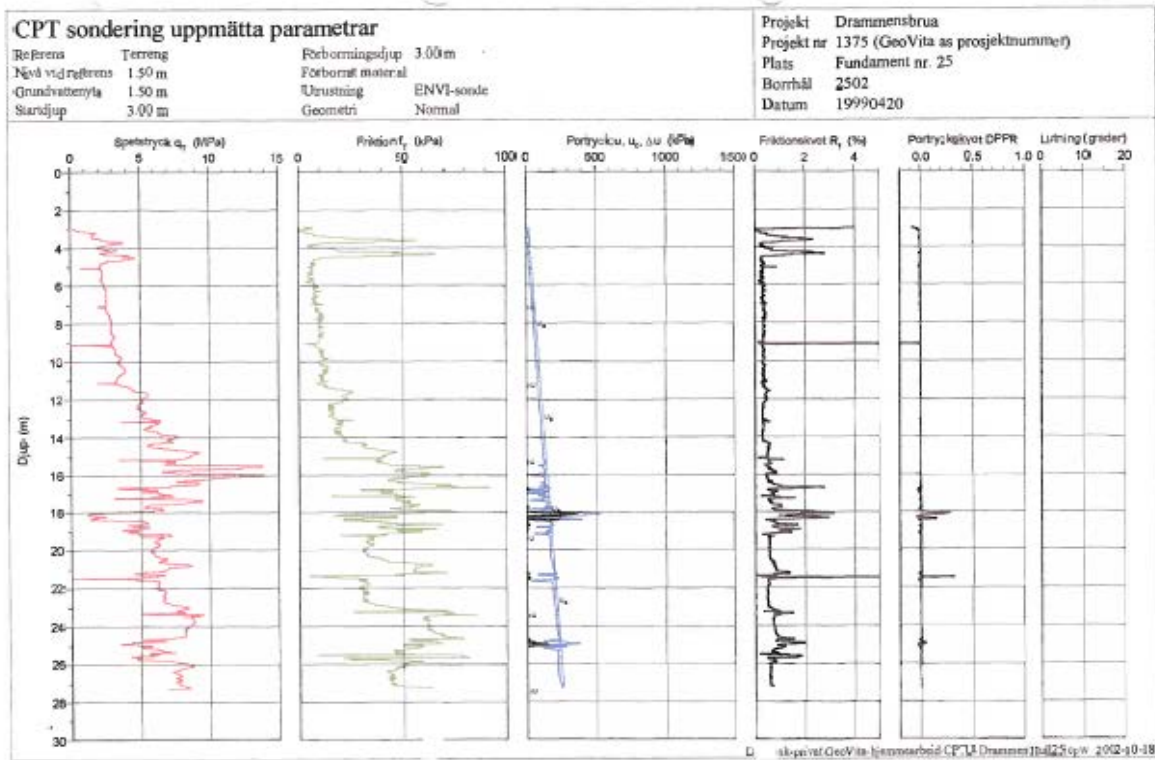
Figure C5- CPT data at axis 25

Figure C6- CPT tip resistance, sleeve friction, pore pressure, friction ratio and pore pressure ratio plots at axis 25
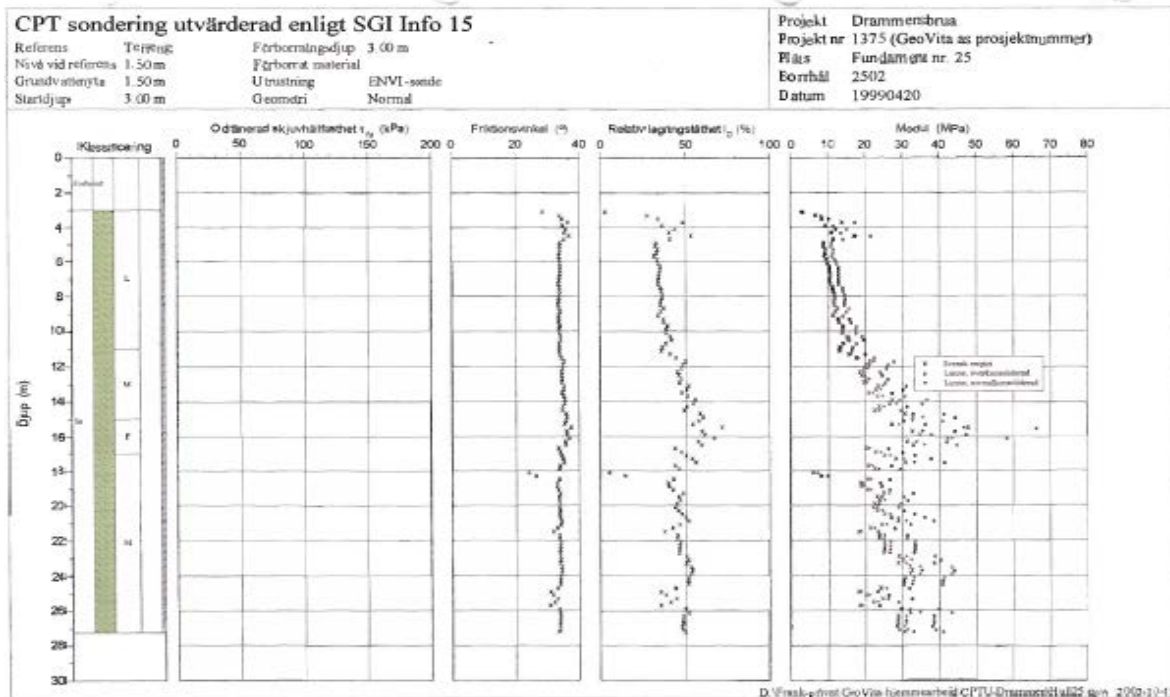

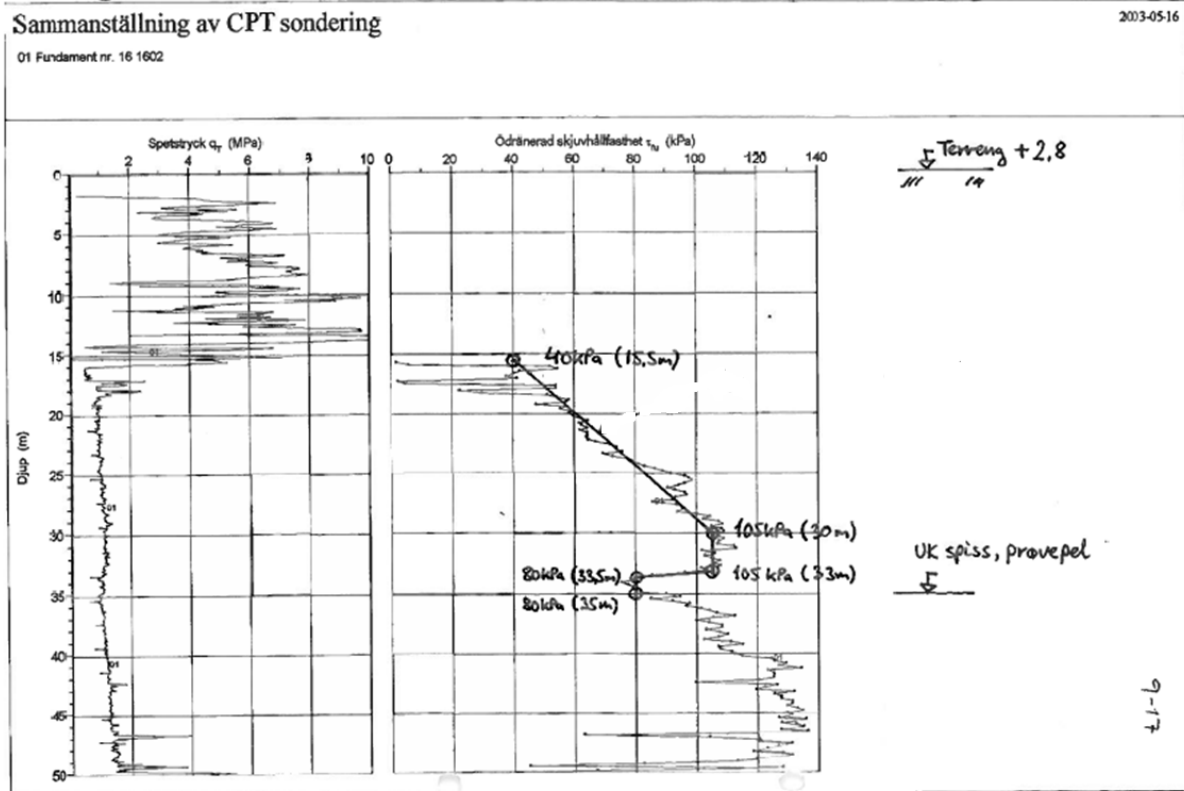*Figure C7- Shear strength, friction angle, relative density and modulus interpreted from the CPT for axis 25*

Figure C8- Shear strength interpreted from the CPT for axis 16